Genetic Analysis of F1 Cluster Phages that Infect *Mycobacterium smegmatis* Identifies Two Distinct Holin-Like Proteins that Regulate the Host Lysis Event

Running Title: Two Distinct Phage Holin Proteins Regulate the Host Lysis Event in *M. smegmatis*

Richard S. Pollenz[a#], Kira Ruiz-Houston[b], Wynter Dean[a] and Loc Nguyen[a]

[a]Department of Molecular Bioscience, University of South Florida, Tampa, FL

[b]Department of Microbiology, University of Wisconsin, Madison, WI

[#]Corresponding Author:

Richard S Pollenz

Department of Molecular Biosciences

University of South Florida

4202 E Fowler Ave ISA2015

Tampa, FL 33620

pollenz@usf.edu

813-767-3984

ABSTRACT

Phages Girr and NormanBulbieJr (NBJ) infect Gram-positive *Mycobacterium smegmatis* mc^2 155. Both phages contain conserved lysis cassettes that harbor two endolysin genes (*lysin A* and *lysin B*) and two genes encoding transmembrane domain (TMD) holin-like proteins. The first holin-like protein, termed LysF1a is 88 amino acids, has two TMDs and a predicted N-in-C-in membrane topology. The second, termed LysF1b, has a single N-terminal TMD and a predicted N-out-C-in topology making it distinct from the 1TMD type III holins or spanins in size and membrane topology. Deletion of either *lysF1a* or *lysF1b* results in lysis defect phenotypes manifest by reduced plaque size and changes to lysis timing in liquid culture. Deletion of both *lysF1a* and *lysF1b* genes is lethal to phage propagation supporting holin function. Phages expressing only the LysF1b protein trigger lysis prematurely when exposed to energy poisons while phages expressing only LysF1a do not show early triggering. Lysis recovery mutants were isolated from phages lacking the *lysF1b* gene and these mutants generated wild type plaque size but triggered lysis prematurely and showed ~65% reductions in burst size. Genome sequencing identified different point mutations that mapped to TMD1 or the C-terminal region of the *lysF1a* gene. Finally, infection of an *M. smegmatis* strain that does not produce lipomannan and lipoarabinomannan by either wild type phages or phages carrying the *lysF1b* deletion showed modest plaque size increases and did not fully complement the lysis defect of phages lacking the *lysF1b* gene. Collectively, the findings show that both LysF1a and LysF1b function as holins and are required for efficient bacterial lysis. LysF1a does not function as an antiholin but requires the expression of the LysF1b protein for efficient lysis functioning. The requirement of two holins with distinct membrane topologies for host lysis has not been described previously.

INTRODUCTION

With an estimated 10^{31} different bacteriophage particles in the world, the pathway whereby dsDNA phages lyse their bacterial hosts after infection and replication is one of the most common cell fates on earth [1]. Extensive biochemical and genetic work with dsDNA phages that infect Gram-negative hosts has established a general three-step model for the triggering of the lysis pathway that involves three distinct sets of proteins. The first are endolysin/s that have defined catalytic activity to lyse the peptidoglycan (PG) layer [2]. The second are holin or antiholin proteins that have between 1-4 transmembrane domain helices (TMD). These proteins work together to, 1) control the timing of the lysis event following phage infection [3, 4], 2) assist with the destabilization of the membrane proton motive force (PMF) [3, 4] and 3) in the canonical holin models, generate large 1μm "pores" in the inner membrane (IM) to allow the exit of the endolysin enzymes to the periplasmic space where they can access and cleave the PG layer [5, 6]. Finally, there are secreted membrane proteins and lipoproteins termed spanins that are associated with the IM and outer membrane (OM). There proteins interact after the PG layer is cleaved to generates the lesion across the IM and OM that allows for the efficient release of the phage progeny [7-9].

dsDNA phages such as lambda, P2, and phage 21 all have genomes < 50,00bp and have a clustered lysis cassette that contain all the genes necessary to mediate the bacterial lysis event [10-12]. Phage lambda encodes the canonical type I holin protein that has 3TMDs and forms large oligomers that create 1μm holes in the IM to allow exit of the endolysin from the cytoplasm to the periplasmic space [12]. Phage 21 defines the type II pinholin lysis pathway and utilizes a 2TMD holin protein that forms ~1,000 heptamers in the IM. The pinholins create only nanometer size holes that are not big enough to allow exit of the endolysin, and they function to disrupt the PMF and trigger lysis. Thus, phages that encode pinholins also encode endolysins that carry secretion-arrest-release (SAR) signals and the SAR-endolysin is held in an inactive

state in the IM prior to triggering. The disruption of the PMF causes the release of the IM tethered SAR-endolysin to the periplasmic space where it cleaves the PG [4, 13, 14]. In both lambda and phage 21, a single open reading frame with two in-frame start codons (dual start motif) encodes two holin proteins that only differ by the addition of 1-2 N-terminal amino acids [10, 11, 14, 15]. The longer version of each holin functions as the inactive antiholin and in both cases a percentage of the holin forms dimers with the antiholin that holds that holin in an inactive state prior to triggering. Upon triggering, the antiholin assumes active holin function greatly increasing the amount of active holin protein available for hole formation. In phages with large genomes, such as P1 and T4, the holin, antiholin, endolysin and spanin genes can be bioinformatically characterized throughout the genome and are not in a defined cassette. The type III holin from phage T4 has a single N-terminal TMD with an N-in-C-out topology with the bulk of the sequence oriented in the periplasmic space [16, 17]. T4 phage encodes two different antiholin proteins that modulate the holin lysis timing and participate in the lysis inhibition activity of phage T4 [16, 17]. Thus, a common theme in the phage-mediated lysis pathway of lambda, P1, P2 and T4 is the utilization of holins and antiholins to regulate the lysis event. However, another variation of the lysis pathway has recently been shown for the Enterococcal phage Mu [18]. Mu does not utilize canonical holins and antiholins in the bacterial lysis pathway and instead uses a novel 1TMD protein termed a releasin protein to release the SAR-endolysin from the IM so it can cleave the PG [18]. As with lambda and phage 21, Mu contains canonical spanins to create the final lesion for progeny release once the PG has been cleaved. It is speculated that Mu does not utilize the holin/antiholin regulated lysis mechanism because it copies its genome via replicative transposition during the lytic cycle and has less selective pressure due to transposition immunity [18]. This pathway adds yet another variation in phage-mediated bacterial lysis and it is striking that all the *E. coli* phages that have been rigorously studied utilize a similar set of tools to complete the lysis pathway through distinct molecular mechanisms.

There are 1000s of annotated dsDNA phages that infect Gram-positive hosts, yet the molecular mechanism that these pages use to lyse their hosts is not resolved to the level of the *E. coli* phages. Although it is hypothesized that the lysis mechanism in these phages will utilize a similar set of proteins as described for phages that infect Gram-negative bacteria, the bulk of biochemical and genetic work has focused more on the enzymes that target the cell wall than on the holins, possibly because these enzymes may be employed as antibiotic agents [19-21]. Gram-positive bacteria lack a formal OM and instead have a much more complex PG layer and an extended structural cell wall components beyond the PG such as arabinogalactans and mycolic acids [22-25]. Thus, addition of an endolysin to Gram-positive bacteria can result in cell death. Bioinformatic, biochemical and genetic analysis has identified several types of phage-encoded endolysins that target different regions of the cell wall. The first type of endolysin is termed lysin A and targets distinct domains of the peptidoglycan [20, 26]. These enzymes are highly modular, do not contain canonical SAR domains, and deletion studies show that the lysin A is essential to phage propagation [27, 28]. It is unknown if the lysin A is released to the peptidoglycan layer through holins since some studies show that exogenous expression of selected lysin A enzymes can be cytotoxic to *M. smegmatis* [20, 29-32]. Many phages that infect Gram-positive hosts also contain a second endolysin termed lysin B that targets the linkages in the mycolic acid layer of the cell wall [27, 30, 33, 34]. It has been hypothesized that lysin B provides a fitness advantage for optimal bacterial lysis and phage release since deletion of lysin B results in viable phages with reduced plaque and burst size [27].

In phages that infect Gram-positive hosts the presence of genes that encode holin-like proteins has primarily been characterized by bioinformatic analysis and many of the phages contain more than one gene encoding a TMD protein that could serve as a holin or antiholin. Currently there are reports on host lysis by phages that infect *Staphylococcus aureus* [35-37], *Bacillus sp*. [38], *Lactococcal sp*. [39], *Oenococcus oeni* [40, 41], *Streptococcus sp* [42], *Gordonia rubripertincta* [43-45] and *Mycobacterium sp*. [46-53]. The holin function for the

encoded TMD proteins in most of these reports is based primarily on the proximity of the TMD gene/s near an endolysin. Where biochemical work is reported, the majority has been carried out using exogenous expression of the TMD genes in *E. coli*. However, there are several reports on phages that infect *Mycobacterium smegmatis* where gene deletion has been utilized to evaluate lysis function of the predicted holin proteins.

The first study evaluated two genes encoding TMD proteins that are found directly downstream of the *lysin A* and *lysin B* in the F1 cluster phage Ms6 [48-50]. Ms6 gene *26* encodes an 88 amino acid protein with 2TMDs while gene *27* encodes a 124 amino acid protein with 1TMD. Deletion of gene *26* resulted in reduced lysis timing, reduced plaque size but wild type burst size, while deletion of gene *27* resulted in delayed lysis timing, increased plaque size and increased burst size. However, there are limitations to these findings because holin function was not verified using energy poisons and the mutant phages were not tested in liquid lysis assays in the *M. smegmatis* host versus *E. coli*. In addition, the experiments to assess function and interaction of the two proteins were carried out using recombinant *E. coli* expression systems that are not physiologic. Thus, while it appears that both proteins are needed for the lysis event, it is unclear how each is contributing to the lysis of the *M. smegmatis* host.

The second set of studies evaluated phage D29, a cluster A2 phage that also infects *M. smegmatis* [51-54]. D29 has a lysis cassette with a *lysin A* (gene *10*), 2TMD holin (gene *11*) and a *lysin B* (gene *12*). It is important to note that the 2TMD holin of D29 is not an ortholog to the 2TMD protein in Ms6 and differs significantly in amino acid sequence and size. The lysis cassette that is also distinct from most other actinobacteriophages in that it has no other genes encoding holin-like TMD proteins within or near the putative lysis cassette. Deletion of gene *11* results in a viable phage with a different phenotype that the 2TMD deletion in Ms6 [51]. D29_Δ*11* phage shows a modest 30% reduced plaque size, slightly delayed lysis timing and reduced burst size [51]. The lack of a more severe lysis phenotype is surprising given that gp11 is the only defined holin, especially since the D29 lysin A does not have a defined signal peptide

or SAR-like domain for export [31, 32]. However, it has been reported that the D29 lysin A may be exported prior to lysis in a yet to be defined pathway that appears to be independent of the holin [31, 32]. Alternatively, the modest lysis phenotype could also indicate that D29 has additional holin-like genes that are not located within the defined “lysis cassette” region. Such a scenario has recently been described in a bioinformatic study of the lysis cassettes of 77 phages that infect the Gram-positive *Gordonia rubripertincta* strain [44]. This study showed that there was a high level of diversity of the lysis cassette gene organization and that putative holin-like genes could be identified in genomic regions distal to the endolysin containing lysis cassettes [44]. This study also showed that most of the phages evaluated had at least two holin-like genes.

In summary, there is limited biochemical and genetic analysis of host lysis pathways by phages that infect Gram-positive hosts, especially within the host bacteria. Consistent findings suggest: 1) the putative holin genes do not appear to have dual start motifs like those identified in lambda and phage 21; 2) that most annotated phages have multiple genes predicted to encode holin-like TMD proteins; 3) that the TMD proteins are predicted to have 1, 2, or 4 TMDs; and 4) that the putative holin-like genes can be bioinformatically identified outside of lysis cassettes even in phages that have compact genomes of < 60,000bp. Of these findings, one of the most intriguing is the presence of multiple genes that encode predicted holin-like TMD proteins. Since antiholins have not been experimentally identified in phages that infect Gram-positive hosts, one interpretation of these data are that holins and antiholins are expressed from distinct genes as shown for *E. coli* phages P2 and T4 [16, 17, 55, 56]. It is also possible that some of the TMD genes encode proteins with spanin-like functions that interact with the complex cell wall of the Gram-positive bacteria. This hypothesis is supported by a report that identified a 177 amino acid protein termed LysZ, that is encoded by phages that infect *Corynebacterium glutamicum* and may function to disrupt the integrity of the bacterial cell wall [57]. The current study aims to evaluate how two predicted holin-like TMD proteins encoded by

phages Girr and NormanBulbieJr (NBJ) function in the lysis pathway of *Mycobacterium smegmatis* mc^2 155 by utilizing recombineered phages and multiple lysis assays under physiological growth conditions. The findings show that both proteins termed, LysF1a and LysF1b function as holins and are required for efficient bacterial lysis. The results also show that the expression of the LysF1b protein is required for efficient functioning of the LysF1a protein and that the LysF1a is not an antiholin. These results suggest a novel model for host lysis that requires two holins with distinct membrane topologies.

MATERIALS AND METHODS

Bioinformatic analysis of transmembrane domains and AlphaFold3 analysis

The identification of transmembrane domains (TMD) and protein topologies was carried out essentially as described by Pollenz et al., 2024 [44] utilizing Deep TMHMM (v1.0.24) [58, TOPCONS (v2.0) [59], SignalP-5.0 and SignalP-6.0 [60], LipoP 1.0 [61] and HHpred (databases: PDB_mmCIF70_30_Mar; Pfam-A_v37) [62]. All membrane proteins described in this report had 100% consensus predictions of TMD domain location, number and protein topology in all programs. Structural predictions of proteins and protein-protein interactions were determined using AlphFold3 [63]. For single proteins, pTM scores >50% indicate high confidence in the model predictions. For protein-protein interactions, ipTM scores <90% are considered low confidence and should be used with caution [63]. All amino acid alignments were performed using Clustal Omega [64].

Bacterial strains, growth and plaque assay

The list of bacterial strains, phage and plasmids utilized in this study is presented in Table 1. *Mycobacterium smegmatis* mc^{2}155 [65] was used as wild type host for all phage related experiments. *M. smegmatis* ∆mtpA and *M. smegmatis* ∆mtpA-comp are described in [66]. *M. smegmatis* strains were propagated on Middlebrook 7H10 agar supplemented with 10% Albumen Dextrose Complex (ADC; 5% albumen, 2% dextrose, 154mM NaCl) at 37°C. To

generate saturated stock cultures, a single colony of *M. smegmatis* was propagated in 25ml of Middlebrook 7H9 media supplemented with 10% ADC, 1mM $CaCl_2$, 0.5% glycerol and 0.05%

Table 1. Bacterial Strains, Phage and Plasmids

Bacterial Strains	**Genotype/Features**	**Reference/Source**
M. smegmatis	*Mycobacterium smegmatis* mc^2 155	65
M. smegmatis ΔmptA	*Mycobacterium smegmatis* mc^2 155 lacking the mptA enzyme	66
M. smegmatis ΔmptA-comp	*ΔmptA* strain carrying complementing mtpA expression plasmid	66
E. coli	*Escherichia coli* NEB5α $F'I^Q$	New England Biolabs
Bacteriophage	**Genotype/Features**	**Source**
Phage Girr_WT	Mycobacteriophage Girr	68. PhagesDB: https://phagesdb.org/phages/Girr
Phage Girr_*Δ29*-20	Girr_WT with deletion of gene *29*	This study
Phage Girr_*Δ29*-25	Girr_WT with deletion of gene *29*	This study
Phage Girr_*ΔlysF1a*	Girr_WT with deletion of gene *34*	This study
Phage Girr_*ΔlysF1b*	Girr_WT with deletion of gene *35*	This study
Phage NBJ_WT	Mycobacteriophage NormanBulbieJr	69. PhagesDB: https://phagesdb.org/phages/NormanBulbieJr
Phage NBJ_*Δ29*	NBJ_WT with deletion of gene *29*	This study
Phage NBJ_*ΔlysF1a*	NBJ_WT with deletion of gene *33*	69
Phage NBJ_*ΔlysF1b*	NBJ_WT with deletion of gene *34*	This study
Plasmids	**Features**	**Source**
pExTra-Girr_*29*	pExTra01::(Ptet-Girr_*34*-mcherry); Kan^R	68
pExTra-Girr_*34*	pExTra01::(Ptet-Girr_*34*-mcherry); Kan^R	68
pExTra-Girr_*35*	pExTra01::(Ptet-Girr_*35*-mcherry); Kan^R	68
pExTra-NBJ_*29*	pExTra01::(Ptet-NBJ_*29*-mcherry); Kan^R	69
pExTra-NBJ_*32*	pExTra01::(Ptet-NBJ_*32*-mcherry); Kan^R	69
pExTra-NBJ_*33*	pExTra01::(Ptet-NBJ_*33*-mcherry); Kan^R	69
pExTra-Waterfoul_*32*	pExTra01::(Ptet-Waterfoul_*32*-mcherry);	67

	Kan^R	
pExTra-Waterfoul_*32*ΔN	pExTra01::(Ptet-Waterfoul_*32(truncation of N-terminal TMD)*-mcherry); Kan^R	This study
pExTra-Waterfoul_*32*ΔC-40	pExTra0 ::(Ptet-Waterfoul_*32(truncation of C-terminal 40aa)*-mcherry); Kan^R	This study
pJV53	Acetamide inducible plasmid with Ched9c gene *60-61*. Kan^R	70

Tween-80 with shaking (225rpm) at 37°C. For all liquid lysis and one-step experiments, 100ul of saturated stock was added to 250ml baffled flasks containing 55ml of supplemented 7H9 without Tween. Cultures were shaken (225rpm) overnight at 37°C and utilized in experiments the next day while in log phase growth (OD_{600} <0.8). Titering experiments showed that an *M. smegmatis* culture at an OD_{600} of 1.0 was equal to ~6.5 x 10^7 CFU/ml. This value was utilized when phages were infected at different MOIs. Plaque assays were completed by mixing the appropriate amount of phage with 250ul of saturated *M. smegmatis* in Middlebrook 7H9 media supplemented with 10% ADC, 1mM $CaCl_2$ and 0.5% glycerol. The mixture was vortexed and incubated at 22°C for 10 minutes. Following the infection, the sample was mixed with 4-5ml of top agar (Middlebrook 7H9, 1mM $CaCl_2$, 0.5% agar) and plated immediately onto 7H10 agar plates. Plates were allowed to harden and placed in a 37°C bacterial incubator for 16-48 hrs. Competent *M. smegmatis* cells for recombineering or for plasmid transfection and complementation studies were prepared as described previously [28, 67-69]. *Escherichia coli* NEB5α $F'I^Q$ (New England Biolabs) was used for plasmid amplification and purification and grown in LB broth or on LB agar supplemented with 50ug/ml kanamycin sulfate and.

Plasmid constructs, *M. smegmatis* transformation and complementation analysis

All PCR primers utilized in this study are shown in Table S1. To generate the inducible expression plasmids pExTra_Waterfoul_*32ΔN*, pExTra_Waterfoul_*32ΔC40*, pExTra_Waterfoul_32 was PCR amplified with Q5 DNA polymerase (New England Biolabs)

using Waterfoul specific primers containing with pExTra homology regions (Table S1). Purified PCR products (were ligated into linearized pExTra01 using isothermal assembly (NEB HiFi 2x Master Mix) as described [65-67]. Recombinant plasmids were recovered by transformation of *E. coli* NEB5α $F'I^Q$ and colonies selected on LB agar supplemented with 50µg/µl kanamycin sulfate. Plasmid DNA was purified using the GeneJet kit (Fisher) and all plasmids were sequence-verified by Sanger sequencing using the pExTra Seq primer (Azenta). For generating complementing strains, competent *M. smegmatis* cells were prepared as described [67-69] and 40µl mixed with 100ng plasmid DNA in a 1mm electroporation cuvette. The sample was electroporated with 1800V and the time constant set to 5.0 msec. Following electroporation, the sample was mixed with 950µl of supplemented 7H9 media without Tween and shaken (225rpm) at 37°C for 120 minutes. Following the recovery period, 10µl-100µl aliquots were spread on 7H10 agar plates supplemented with 10µg/µl kanamycin sulfate and incubated at 37°C for 3-5 days. To generate cultures for plaque assay, single colonies of *M. smegmatis* carrying the appropriate plasmid were harvested into 25ml of supplemented 7H9 media containing 10µg/µl kanamycin sulfate. Cultures were shaken (225rpm) at 37°C for 24-48 hours. Saturated cultures at OD_{600} > 1.5 were centrifuged at 6200rpm for 10 minutes and the pellets resuspended in supplemented 7H9 media (without Tween) to a final OD_{600} of 2.0. These cells were utilized for phage infection and then mixed with 4.5ml top agar supplemented with 10ng/µl kanamycin sulfate with or without 100ng/µl anhydrotetracycline (aTc). The mixture was added to 7H10 agar containing 10µg/µl kanamycin sulfate supplemented with or without 100ng/µl aTc and incubated at 37°C for the times indicated in the results section.

Bacteriophage recombineering and genome sequencing

All gblocks and PCR primers utilized in this study are shown in Table S1. The deletion of genes in phage Girr and NBJ were carried out using the Bacteriophage Recombineering of Electroporated DNA (BRED) procedure as described [28, 70], with the following modifications.

Phage genomic DNA was purified using the Wizard DNA Clean up kit (Promega). dsDNA recombineering substrates were synthesized as gblocks (Integrated DNA Technologies). To generate µg quantities of dsDNA substrates, gblocks were solubilized in water to 10ng/µl and PCR amplified with gblock specific primers using 2X Q5 master mix (New England Biolabs). PCR products were purified using Zymoclean DNA recovery (Zymoresearch). To generate recombinant phage, 200-400ng dsDNA substrate was mixed with 100ng phage genomic DNA and incubated on ice for 10min. The DNA mixture was added to 100µl of recombineering *M. smegmatis* in a 2mm electroporation cuvette and electroporated at 2500V with the time constant set to 20.0 msec. Following electroporation, 900µl of supplemented 7H9 media was added to the cells and they were shaken (225rpm) at 37°C for 90 minutes. Following the recovery period, the sample was mixed with 250µl of saturated *M. smegmatis* and plated with 5ml 7H9 top agar onto 7H10 agar plates. Plates were incubated at 37°C for 18-24 hours to recover primary plaques. Primary plaques were picked into 120µl of phage buffer (10 mM Tris-HCl, pH 7.5; 10 mM $MgSO_4$, 68.5 mM NaCl; 1mM $CaCl_2$), vortexed, and incubated at 22°C for 2-8 hrs. The presence of mutant phage genomes was determined by Deletion Amplification Detection Assay (DADA) PCR [28] using a 20µl reaction with: 1µl of plaque sample, 2µl of 0.2 µM DADA primer mix (1:1 mix of For and Rev primers), 5µl glycerol (40%), 2µl water and 10µl OneTaq 2x Master Mix (New England Biolabs). PCR conditions were: 94°C for 1 minute followed by 35 cycles of 94°C-1min/66°C 1min and a final 66°C step for 5 minutes. Positive primary plaque samples were serially diluted and plated on wild type or complementing *M. smegmatis* as indicated. Secondary plaques were picked as above and screened by standard PCR using gene specific flanking primers. Pure populations of mutant phage were evaluated by full genome sequencing as described [71, 72]. Briefly, Genomic DNA was used to create sequencing libraries with the NEB XLEP-P1 kit. Sequencing was performed by the Pittsburgh Bacteriophage Institute and the library run on an Illumina NextSeq 1000 instrument. Raw reads were trimmed with cutadapt 4.7 (using the option: –nextseq-trim 30) and filtered with skewer 0.2.2 (using the options: -q 20 -Q

30 -n -l 50) prior to assembly. The resulting sequences were assembled using Consed (v29.0) with Unicycler (v5.0) and contigs checked for completeness, accuracy, and genome termini. Final phage contigs were aligned to wild type phage to identify deletions and point mutations.

Plaque size analysis

Plaques were generated using the plaque assay procedure described above. For experiments where plaque size would be evaluated between several different phages, identical bacterial samples, incubation times, phage concentrations and top agar amounts were utilized. Plaque size was evaluated using ImageJ software [73] and by manual measurement using photos embedded in PowerPoint and custom rulers. In most experiments, results are presented for an average of 50 plaques and the statistical significance of measurements determined by unpaired t-test (https://www.graphpad.com/quickcalcs/ttest1/). Plaque volume was calculated by the formula $\pi r^2 h$ where r is the radius of the plaque and h was set to 1mm for the top agar thickness.

Liquid lysis assay

Liquid lysis assays were carried out essentially as described by Payne et al., 2009 [27] with the following modifications. Briefly, overnight cultures of *M. smegmatis* in log phase growth were diluted to an OD_{600} of 0.25-0.30 in supplemented 7H9 without Tween and 40ml of culture was added to 250ml baffled flasks. High titer phage lysate was added to the cultures to create an MOI of 10 and the mixture set at 37°C for 30 minutes without shaking. T_0 for all experiments was the time of phage addition. After 30 minutes (T_{30}), the cultures were constantly shaken a 225rpm and aliquots of cells removed with a syringe and sterile needle from the shaking culture without stopping the incubator. The OD_{600} of the sample was immediately recorded for each aliquot using a GENESYS spectrophotometer (Fisher Scientific). In some experiments, KCN (1M in water), or $CHCl_3$ (100%) was added directly to the shaking culture to produce a final concentration of 10mM or 1%, respectively. All liquid lysis experiments were repeated at least five separate times and representative experiments are presented.

ATP assay

The presence of ATP in culture supernatants was determined utilizing the ENLIGHTEN kit (Promega). Briefly, liquid lysis assays were carried out as described above. A 500ul aliquot of culture was removed at indicated time points and immediately passed through a 0.2µ syringe filter to remove bacteria. The sample was frozen at -20°C prior to analysis. The presence of ATP in culture supernatants was determined by mixing 5µl with 50µl ENLIGHTEN reagent (Promega), mixing for 5 seconds and then reading the integrated luminescence over 10 seconds using a GloMax luminometer (Promega). To assure that the readings were within the linear range of the instrument an ATP standard curve was utilized.

One-step growth curves and burst size determination

Several experimental procedures have been utilized for one-step growth curves with Gram-positive bacteria [32, 47, 49, 51]. In our hands, none of these procedures generated consistent results or provided the ability to directly measure burst size. Thus, we developed a one-step protocol that is illustrated in Figure S1 and described below. To prepare the cells, the OD_{600} of fresh overnight cultures of *M. smegmatis* in log growth were determined and 10ml centrifuged at 3,000rpm for 10 minutes. The cells were resuspended in supplemented 7H9 to a final concentration equal to an OD_{600} of 3.2/ml. 250µl of cells (~5 x 10^7 cfu) were added to microfuge tubes and ~5 x 10^7 phage added to the cells to create an MOI of 1. The same amount of phage were also added to 250µl of supplemented 7H9 media without cells to verify the titer and determine the level of phage adsorption. The mixture was vortexed and set at 37°C for 30 minutes without shaking. T_0 for all experiments was the time of phage addition to the cells. After 30 minutes, 750µl of supplemented 7H9 was added to all samples. Samples were vortexed and centrifuged at 6,200rpm for 4 minutes to separate unabsorbed phage. The supernatant was saved for analysis of titer and adsorption, and the cell pellet immediately resuspended in 1ml supplemented 7H9, vortexed and diluted 1:10,000 into 70ml of supplemented 7H9 in baffled 250ml flasks. An aliquot was removed and 5µl, 12.5µl and 25µl used for plaque assay to

determine the number of infectious centers to determine the precise number of infected cells. A second aliquot was removed and filtered through a 0.2μ syringe filter and 150μl utilized for plaque assay to test for unabsorbed (free) phage at T_{45} minutes (the first one-step data point). The flask was placed in a 37°C incubator and constantly shaken at 225rpm for the duration of the experiment. At specified time points, 500μl aliquots were removed from the shaking flasks and each sample immediately passed through a 0.2μ syringe filter to remove cells and collect free phage. The amount of phage in each sample was determined by performing plaque assays using 150μl of serially diluted samples (usually 10^{0} to 10^{-4} dilutions were sufficient). The phage titer in the flask, expressed as PFU/ml was determined at each time point by counting the plaques on each plate, dividing by the volume of phage used in the infection (150μl), multiplying by the dilution factor and then multiplying by 10^{3}. The number of infectious centers in the infected 70ml culture was determined by counting the plaques, dividing by the volume used for the plaque assay and multiplying by 70,000. The original phage titer and the percentage of adsorbed phage was determined by spot titers and plaque assay of the serially diluted supernatants collected from the samples of phage with and without the added cells. Since the number of cells and phage used in these experiments was held constant, this procedure consistently produced ~3.5-5.5 x 10^{7} infectious centers. This procedure also resulted in essentially zero unabsorbed phage in the culture at the start of the one-step assay. Burst size at all time points could be directly determined by dividing the total phage in the 70ml culture by the number of infectious centers. All phages were evaluated through a minimum of three separate assays. A representative data set showing the raw data for adsorption, infections centers and a one-step assay is provided in Figures S2 and S3.

RESULTS AND DISCUSSION

Topologies of Holin-like TMD Proteins Within the Lysis Cassettes of F1 Cluster Phages Girr and NormaBulbieJr.

To investigate the contribution of predicted holin-like proteins in the lysis of *M. smegmatis*, it was desirable to begin work in phages that had a defined lysis cassette and prior wet-lab data. F1 cluster phages Girr and NormanBulbieJr (NBJ) were selected since both phages have a define lysis cassette and a full genome cytotoxicity screen has been reported for both phages [68, 69]. Girr and NBJ have an average nucleotide identity of 89.86% but only share 69 of 102 genes. Both phages have a defined lysis cassette organization located downstream of the *tape measure* and *minor tail* genes and encode a Lysin A enzyme predicted to target the peptidoglycan layer and a Lysin B that targets the linkage of the arabinogalactins to the mycolic acids. The *lysin B* gene is directly followed by two genes encoding proteins that have predicted TMDs (Girr *34* and *35* and NBJ *32* and *33*).

It was first important to bioinformatically evaluate the predicted topologies of these TMD proteins and determine how they compared to previously characterized holins or other phage proteins involved in bacterial lysis. Girr *34* and NBJ *32* encode small 80aa and 77aa proteins, respectively, that have two predicted TMD regions and an N-in-C-in topology by all TMD prediction programs (Figure 2A). The proteins are 97% identical and have cytoplasmic N and C-terminal domains that each contain four charged amino acids. The presence of two TMDs and the N-in-C-in topology is like the phage 21 S^{21} type II pinholin (Figure 2BC). However, the presence of a pinholin is typically associated with a SAR-endolysin that is secreted to the periplasmic space prior to lysis triggering [10, 11, 13]. Analysis of the Girr or NBJ Lysin A proteins by the various TMD prediction programs and AlpahFold3, show no evidence of SAR domains or signal sequences (Figures S4-S6), and this is consistent with previous analysis of Lysin A proteins from phages that infect *M. smegmatis* [20]. Thus, it is critical to contrast several structural differences of gp32 and gp34 to the canonical S^{21}68 pinholin and S^{21}71 antiholin.

First, the $S^{21}68$ holin protein has only 3 N-terminal amino acids prior to the TMD1 and this feature is a critical to its function as a holin and allows the TMD1 to become cytoplasmic (Figure 2BC) [11-15]. Second, the S^{21} gene has a dual start motif that produces both the $S^{21}68$ holin protein and the $S^{21}71$ antiholin after phage infection [11-15]. The difference in the two proteins is the addition of the extra basic K residue to the N-terminal cytoplasmic domain of $S^{21}71$ that limits the TMD1 from exiting the membrane to the same degree as the $S^{21}68$ holin (Figure 2BC; [11-15]). Thus, the expression of $S^{21}71$ keeps a percentage of the $S^{21}68$ in an inactive dimer until triggering at which time the $S^{21}71$ converts to an active holin [13-15, 74, 75]. Third, the $S^{21}68_{IRS}$ protein is an engineered version of $S^{21}68$ that adds the MRYIRS motif and 4 charged residues in the N-terminal cytoplasmic domain that creates a dominant negative version of the antiholin that is poorly triggered to an active holin [74]. Neither Girr gene *34* nor NBJ gene *32* have a dual start motif that generates multiple products of the same open reading frame. Genes *34* and *32* encode a single protein product that has a predicted N-terminal cytoplasmic domain of 13-16 amino acids of which four are charged and two others are polar. Therefore, the N-terminal topology and the number of charged amino acids in Girr gp34 and NBJ gp32 are more similar with the $S^{21}71$ antiholin and $S^{21}68_{IRS}$ and would predict that TMD1 of these proteins remains embedded in the membrane. In addition, the TMDs of S^{21} both contain GxxxG motifs that are predicted to contribute to homotypic and/or heterotypic helix interactions of the monomers that facilitate the formation of the pinholes [74, 75]. While TMD1 and TMD2 of Girr and NBJ have a high percentage of GA residues (Figure 2A), they lack defined GxxxG domains found in S^{21}. Finally, Girr gp34 can't be modeled with high confidence by AlphaFold3 into either a monomer or a heptamer (Figure S7). Taken together, this data suggests that Girr gp34 or NBJ gp32 are unlikely to function as a type II holin. Based on the literature we will designate these proteins as LysF1a due to a predicted function in lysis (lys) and being first identified in F1 cluster phages.

Since there is a second gene encoding a protein with a single TMD directly downstream of the *lysF1a* gene, we hypothesized that this protein may also be involved in the lysis pathway. Girr *35* and NBJ *33* both have -4bp ATGA overlaps to the upstream *lysF1a* gene and encode 98% identical 124aa proteins with a single N-terminal TMD and a predicted N-out-C-in topology by all TMD prediction programs (Figure 3A). Both proteins have a 22 amino acid extracellular domain followed by the single TMD. There are four basic residues following the TMD and AlphaFold3 predicts an extended helical cytoplasmic C-terminal domain that contains ~50% KRDE charged residues typical of holins [10, 11]. Figure 3B shows the AlphaFold3 models and predicted topologies of representative proteins that have a single TMD and have been shown to be involved in the bacterial lysis pathway for comparison gp33 and gp35. Most pertinent is the type III holin typified by the T protein of phage T4 that forms large 1um holes like canonical type I holins [16, 17]. However, the type III holin has <20% amino acid identity to gp33 and gp35, is much larger at 221 amino acids and has the opposite membrane topology with a globular extracellular domain critical to its holin function (Figure 3B). It noteworthy that spanins also have a single TMD and model with an extended helical prediction, but like the type III holins, these proteins are also oriented in a N-in-C-out topology that has been shown experimentally and is also predicted by the TMD prediction programs (Figure 3B; [10, 11]). Interestingly, there is a recent report regarding phages that infect the Gram-positive *Corynebacterium glutamicum* strain. The authors have characterized a protein with 1 TMD that is termed LysZ and is proposed to interact with lipid-anchored glycans on the extracellular side of the IM to promote efficient lysis [57]. However, like the type III holin, LysZ is much larger than the Girr and NBJ proteins and it is proposed to have a N-in-C-out topology that allows it to interact with the lipid-anchored glycans [57]. Thus, Girr gp35 and NBJ gp33 are most similar in structure and membrane topology to the recently identified phage Mu releasin protein (Figure 3B) [18]. Releasin however, is named due to its function to release the Mu SAR-endolysin from the membrane in a holin independent manner [18]. Mu also has <20% amino acid identity to gp33

and gp35 and does not possess the highly charged cytoplasmic domain. Thus, of all the characterized proteins involved in lysis that have 1 TMD, gp35 and gp33 appear to represent a novel class of proteins and will be termed LysF1b since the gene is downstream of the *lysF1a*.

Deletion of Individual *lysF1a* and *lysF1b* Genes in Phage Girr are Viable While Deletion of Both is Lethal

To evaluate the function of the *lysF1a* and *lysF1b* genes, the BRED recombineering method was utilized to delete them in both Girr and NBJ as described in Methods. Several primary plaques were positive for each deletion and pure populations of Girr_*ΔlysF1a*, Girr_*ΔlysF1b*, NBJ_*ΔlysF1a*, and NBJ_*ΔlysF1b* were recovered from secondary plaques. Figure 4 shows the lysis cassette organizations of the Girr mutants and the PCR verification of the gene deletions from clonal high titer lysates. The data for NBJ is shown in Figure S8 and deletion of gene *33* is also presented in Wise et al. [69]. The genome structure of all deletions was confirmed by sequencing the immediate region of the deletion and by whole genome sequencing to validate that there were no point mutations outside of the targeted gene deletion region. Since deletion of either of the individual TMD genes resulted in viable phage, it was of interest to test whether a double deletion of both TMD genes was viable. For these studies Girr_*ΔlysF1a* DNA was utilized to delete *lysF1b* and a positive primary plaque was picked, resuspended in buffer and plated to recover ~250-1000 isolated plaques on complementing and non-complementing *M. smegmatis* as shown in the protocol schematic in Figure 5A. Since BRED was being used, positive primary plaques will have a mixture of the phage used for recombineering and the mutant. Lysates representing all the phage from secondary plaques were recovered and evaluated by DADA PCR to test for the presence of the double mutant. Figure 5B shows that the double mutant genotype is not recovered on wild type *M. smegmatis*, even when 800PFU were plated (gel lanes 3-6). However, when >250 phage particles are plated on the complementing *M. smegmatis* strain transfected with pExTra-Girr*34* expressing

LysF1a, a positive DADA band is observed (Figure 5B, gel lane 8). The inability to recover a phage with the deletion of both *lysF1a* and *lysF1b* is highly supportive that the expression of both Girr LysF1a and LysF1b are required for Girr viability. A lethal phenotype is observed when holin genes are deleted in *E coli.* phages that encode canonical holins required for endolysin release [10, 11].

Deletion of Individual *lysF1a* and *lysF1b* Genes in F1 Phages Result in Reduced Plaque Size

To assess the phenotypes of the mutant phage, equal concentrations of Girr_WT, Girr_*ΔlysF1a* and Girr_*ΔlysF1b* were used to infect *M. smegmatis* and the total number of recovered plaques and plaque sizes evaluated. All phages formed plaques with equivalent efficiencies under the standard assay conditions described in Methods suggesting no defects in adsorption (Figure S9). However, both Girr_*ΔlysF1a* and Girr_*ΔlysF1b* presented with significantly smaller plaques than Girr_WT (Figure 6) as did NBJ_*ΔlysF1a* and NBJr_*ΔlysF1a* (Figure S10). A summary of the plaque size data for both Girr and NBJ is presented in Table 2. Deletion of the *lysF1a* gene from Girr or NBJ results in ~40% reduction in plaque diameter and

Table 2 Plaque sizes in WT Girr and *lysF1a* and *lysF1b* deletion mutants.

PHAGE	Plaque size (mm)	% of WT (diam.)	Plaque (vol, mm^3)	% of WT (plaque vol)
NBJ_WT	3.49 +/- 0.533	100	11.479	100
NBJ_Δ*lysF1b*	1.23 +/- 0.225*	35.24*	1.425*	12.42*
NBJ_Δ*lysF1a*	2.05 +/- 0.660*	58.73*	3.96*	34.50*
Girr_WT	3.88 +/- 0.731	100	14.188	100
Girr_Δ*lysF1b*	1.28 +/- 0.376*	32.98*	1.544*	10.88*
Girr_Δ*lysF1a*	2.31 +/- 0.719*	59.53*	5.029*	35.44*

M. smegmatis was infected with identical numbers of phage and plaque size determined after 36 hrs. of growth at 37°C. Plaque diameter was measured using ImageJ. Data is presented as average +/- standard deviation for a minimum of 50 individual plaques. * = statistically significant from Girr or NBJ WT phage *p<0.0001.*

a 65% reduction in plaque volume, while deletion of the *lysF1b* is more severe showing a ~65% reduction in plaque diameter and near 90% reduction in plaque volume. To validate that these plaque size reductions were directly related to the loss of *lysF1a* or *lysF1b* genes, *M. smegmatis* containing complementing expression plasmids were infected with the mutant phages and plaque size evaluated as described in Methods. Since both Girr LysF1b and NBJ LysF1b are highly toxic when exogenously expressed in *M. smegmatis* [68, 69], complementation of the *lysF1b* deletions first utilized Waterfoul gp32. Waterfoul is a K5 cluster phage with a canonical lysis cassette and gene *32* encodes a 1TMD with the same general size and membrane topology as Girr LysF1b (Figure 3C) and is not toxic when induced by aTc in *M. smegmatis* [67]. When M*. smegmatis* transfected with Waterfoul gp32 is infected with Girr_*ΔlysF1b* in the presence of aTc, there is a significant increase in plaque size compared to untreated cells (Figure 6A). Importantly, the increase in plaque size was not observed when the N-terminal TMD domain or the highly charged C-terminal 40 amino acids of Waterfoul gp32 were truncated (Figure 6A). Thus, the complementation by Waterfoul gp32 requires the full-length protein. Recently it has been reported that the pTet promoter in pExtra is leaky and that it is possible to complete complementation analysis in the absence of aTc [68]. Thus, *M. smegmatis* was transfected with pExTra-Girr*35* and pExTra-NBJ*33* and the resulting cells infected with Girr_Δ*lys1b* as described in Methods. Figure 6B shows that there is a significant increase in plaque size when Girr_Δ*lys1b* is plated on the complementing strains expressing the LysF1b proteins compared to cells with the base pExTra01 vector. These results support that the reduced plaque size of Girr_*ΔlysF1b* is directly attributable to the loss of *lysF1b.* Similarly, the wild type plaque size is restored when *M. smegmatis* harboring the pExTra-Girr_*34* plasmid is infected with Girr_*ΔlysF1a* (Figure 8). Thus, the loss of either *lysF1* gene appears to create a lysis defect phenotype that is like the phenotype when the *lysin B* is deleted in phage Giles and the cell wall components remain a barrier to efficient phage release [27].

Deletion of Individual *lysF1* Genes Result in Distinct *M. smegmatis* Liquid Lysis Phenotypes and ATP Release.

A main function of holins is the control of the lysis timing by the destruction of the proton motive force (PMF) [10, 11]. To assess lysis timing of Girr, NBJ and the *lysF1* mutants, liquid lysis assays were performed where the optical density (OD_{600}) of infected log growth *M. smegmatis* cultures is measured over time. Importantly, in all studies, once phage had been allowed to absorb for 30 minutes, cultures were continually shaken even while samples were withdrawn so that lysis would not be prematurely triggered by changing the culture conditions [11, 76]. The data show that cultures infected with Girr_WT grow steadily until ~110 minutes post infection. Beginning at 110 minutes, there is a significant drop in the OD_{600} of the culture (triggering event) until it reaches a baseline of OD_{600} 0.10 at about 200 minutes (Figure 9A). In contrast, Girr_*ΔlysF1a* grows until ~130 minutes and then shows a reduction in OD_{600} until 300 minutes that does not reach the same OD_{600} baseline as Girr_WT even after 480 minutes of incubation (Figure 9A). Strikingly, cultures infected with Girr_*ΔlysF1b* do not show a drop in OD_{600} but appear to cease growing after ~200 minutes with only a slight decrease in OD_{600} over the remaining growth period out to 480 minutes (Figure 9A). For NBJ_WT, OD_{600} begins to drop after 130 minutes and like Girr_WT reaches a baseline of around OD_{600} 0.10 (Figure 9B). NBJ_*ΔlysF1a* shows a delay in lysis timing like Girr_*ΔlysF1a*, but the delay is more pronounced as the OD_{600} does not begin to drop until ~180 minutes post infection (Figure 9B). Just like Girr_*ΔlysF1b*, NBJ_*ΔlysF1b* ceases to grow after ~200 minutes and does not show a significant reduction in OD_{600} even after 480 minutes of growth (Figure 9B). Thus, in both phages, deletion of *lysF1a* results in a triggering delay while deletion of *lysF1b* results in no defined triggering event in this assay. It is interesting that Girr_WT and NBJ_WT show a ~20-minute difference in triggering time and that a difference is also observed between Girr_*ΔlysF1a* and NBJ_*ΔlysF1a.* These results may be due to differences in how the lysis cassette genes are expressed since

Girr has an HNH endonuclease gene between the *lysin A* and *lysin B* (Figure 1) and the intergenic region between the *lysin B* gene and the *lysF1a* is 8bp in NBJ but 38bp in Girr (Figure S11).

ATP release has been used as a measure of cell viability and membrane integrity following phage infection [27, 51]. Figure 9C shows the ATP release from the same experiment that is presented in Figure 9AB. As expected, ATP release for Girr_WT, NBJ_WT, Girr_*ΔlysF1a* and NBJ_*ΔlysF1a* generally mirrors the time at which lysis is triggered and the culture OD_{600} begin to decline. ATP levels in the media also peak when the OD_{600} baseline is reached at about 300 minutes (Figure 9C). In contrast, there is delayed but gradual increase in the amount of ATP released from the cultures infected with Girr_*ΔlysF1b* and NBJ_*ΔlysF1b* out to 300 minutes. Although the ATP level does not reach that of Girr_WT or NBJ_WT, the release of ATP confirms that cell integrity has been comprised after infection with the *lysF1b* mutants. Collectively, the important finding from this data set is that an F1 phage with only the 1TMD LysF1b protein can trigger the lysis event in the absence of the 2TMD lysF1a protein, but that the lysF1a protein does not support significant bacterial lysis as measured by a drop in OD_{600}. In fact, the liquid lysis results for Girr_*ΔlysF1b* and NBJ_*ΔlysF1b* are like those observed for the lethal *lysin A* deletion in phage Giles where the cultures stopped growing and the OD_{600} plateaued but did not decline [27]. The similarity in these results suggest that the lysis defects in the *ΔlysF1b* phage may be related to the inability of the endolysins to efficiently cleave the cell wall components because they are either not efficiently released from the infected cell or cannot be activated in some manner.

Energy Poisons Cause Early Triggering of F 1Cluster Phages with Deletion of the *lysF1a* Gene but not the *lysF1b* Gene in Liquid Lysis Assays

The results presented so far indicate that the expression of both TMD proteins are required for phage viability, but phages that express only the LysF1b protein can support

bacterial lysis while phages that express only LysF1a are viable but severely lysis compromised. The diagnostic assay for holin function is the ability to cause early triggering of an infected culture by the addition of energy poisons (e.g., cyanide or the protonophore dinitrophenol) due to the disruption of the proton motive force (PMF) [11, 76]. This type of assay has been utilized in nearly all the pioneering work on holin function of phages that infect *E. coli.* [10, 11, 18]. *M. smegmatis* was infected with Girr_WT or Girr_*ΔlysF1a* and the OD_{600} of the culture measured as described in Methods. At 110 minutes after infection, KCN (final concentration of 10mM) was added directly to one culture of Girr_*ΔlysF1a* and to a culture of uninfected cells. Figure 10A shows that Girr_WT triggers at ~110 minutes while Girr_*ΔlysF1a* triggers at 130 minutes just as in Figure 9A. However, when KCN is added to a culture infected with Girr_*ΔlysF1a*, there is a drop in OD_{600} beginning at ~120 minutes that clearly precedes the drop in the untreated Girr_*ΔlysF1a* culture. KCN addition to uninfected cells results in immediate cessation of growth, but not a significant drop in OD_{600}. To validate these results, studies were repeated with the NBJ mutants. NBJ_WT triggers later than Girr_WT at ~130 minutes and declines to OD_{600} 0.10 by 300 minutes as expected (Figure 10B). NBJ_*ΔlysF1a* shows delayed triggering just as in Figure 9B and addition of KCN to a culture infected with NBJ_*ΔlysF1a* at 120 minutes results in lysis triggering by 130 minutes with a gradual reduction in OD_{600} that mirrors the NBJ_WT. The ability of Girr_*ΔlysF1a* and NBJ_*ΔlysF1a* to trigger lysis, identifies the 1TMD LysF1b protein as a putative holin and not a releasin, since energy poisons do not trigger lysis prematurely in phage Mu [18].

The next set of studies focused on the phages with deletion of the 1TMD *lysF1b* genes to determine if they could also be triggered by the addition of KCN. Figure 10C shows the results for Girr_*ΔlysF1b*. As previously shown in Figure 9A, *M. smegmatis* infected with Girr_*ΔlysF1b* does not exhibit a defined triggering event as the cells simply cease growing with a slight reduction in OD_{600} out to 480 minutes. Addition of KCN to the Girr_*ΔlysF1b* culture at

180 minutes results in a modest 30% reduction of OD_{600} between 180-240 minutes compared to the Girr_*ΔlysF1b* untreated culture. However, following this initial decline, the level of change in OD_{600} generally mirrors that of the untreated Girr_*ΔlysF1b* culture and the KCN treated *M. smegmatis* control. In contrast, addition of 1% $CHCl_3$ to the Girr_*ΔlysF1b* culture at 180 minutes, results in an immediate precipitous drop in OD_{600} to the level of Girr_WT indicating that the endolysin enzymes are present and active in the cells. The results for NBL_*ΔlysF1b* are shown in Figure 10D and exhibit near identical results to Girr_*ΔlysF1b* in that addition of KCN cause a modest drop during the first hour after addition, and then an OD_{600} decline that mirrors the untreated NBJ_Δ*lysF1b* culture and the KCN treated *M smegmatis*. Addition of $CHCl_3$ results in the same type of sharp decline in OD_{600} to the level of the NBJ_WT baseline. Collectively, these results show that phages expressing only the 2TMD LysF1a protein are not efficiently triggered following disruption of the PMF but that the cells have the requisite enzymes for lysis since lysis occurs immediately after addition of 1% $CHCl_3$. The inability of the LysF1a proteins to be triggered by KCN is like the $S^{21}71$ or $S^{21}68_{IRS}$ antiholins [13, 74, 75].

F1 Cluster Phage Deleted for *lysF1a* have Delayed Burst Timing While Phage Deleted for *lysF1b* Deletion have Reduced Timing and Greatly Reduced Burst Size

The previous results show that infection of *M. smegmatis* with either Girr_*ΔlysF1a* or NBJ_*ΔlysF1a* results in a defined triggering (lysis) event that can be prematurely initiated by addition of KCN. However, the results do not establish if phage have been efficiently released from the lysed cells, the timing of the burst event and the burst size. Since it is not possible to utilize lysogens to study phage release in *M. smegmatis*, one-step grow curves were utilized to evaluate the various *lysF1a* and *lysF1b* mutant phages. The experimental set up for these studies is fully described in the methods and representative raw data sets are also shown in Figures S2 and S3. The one-step results from three different experiments utilizing Girr phages are presented in Figure 11. Phage release from Girr_WT shows a lag time of ~180 minutes from

the time of infection and then a gradual phage release for 90 minutes before reaching a plateau at ~300 minutes (Figure 11A). The slow release of phage over a 90-minute period is consistent with the liquid lysis assays that showed an ~60-minute timeline of OD_{600} decline after triggering. This is an important observation because there should not be a sharp, immediate lysis of all cells and accompanying phage release since the phage infections are not synchronized but carried out over a 30-minute period and the efficient release of phage from Gram-positive bacteria may also be hampered by the extensive cell wall. Girr_*ΔlysF1a* shows a delayed lag time by ~20 minutes compared to Girr_WT and a more prolonged period of phage release over 150 minutes before reaching a plateau. The overall burst size for Girr_WT over three experiments was 277 +/- 81 PFU/cell. Girr_*ΔlysF1a* showed a lower burst of 255 +/- 75 PFU/cell but this was not statistically different from the for Girr_WT. In contrast, Girr_*ΔlysF1b* shows a very small but defined burst at ~ 210 minutes that is best illustrated when the data is plotted independent of the other phages (Figure 11B). The overall burst size for Girr_*ΔlysF1b* is only ~29.2 +/- 36 PFU/cell suggesting very poor efficiency of phage release from the infected cells. Overall, this data is consistent with the plaque size and liquid lysis results and supports the hypothesis that *M. smegmatis* integrity is compromised when infected with Girr_*ΔlysF1b* but the release of phage progeny is severely impacted. In addition, the near wild type burst size observed in cells infected with Girr_*ΔlysF1a*, further support the holin function of the LysF1b protein.

Lysis Recovery Mutants Isolated from Girr_*ΔlysF1b* or NBJ_*ΔlysF1b* Show Wild Type Plaque Size and have Point Mutations in the *lysF1a* Gene

Since both Girr_*ΔlysF1b* and NBJ_*ΔlysF1b* show significant plaque size defects it was possible to screen for lysis recovery mutants (LRM) by assessing changes to the small plaque size following multiple rounds of infection and replication. Figure 12A shows the presence of a large plaque in a Girr_*ΔlysF1b* plaque assay after the second round of harvest and infection.

Table 3. Lysis Recovery Mutants (LRM) from Δ*lysF1b* Phages.

Phage	Type of mutation	Genetic location	Mutation Result
Girr_Δ*lysF1b*-LRM1	point mutation-nucleotide substitution	gene *35 (lysF1a)*	G66D
Girr_Δ*lysF1b*-LRM2	point mutation-nucleotide substitution	gene *35 (lysF1a)*	R19H
Girr_Δ*lysF1b*-LRM6	point mutation-nucleotide deletion	gene *35 (lysF1a)*	missense coding after A63 and premature stop at aa74: A63APRQPRNGFGD.STOP
Girr_Δ*lysF1b*-LRM7	point mutation-nucleotide substitution	gene *35 (lysF1a)*	G66D
Girr_Δ*lysF1b*-LRM8	point mutation-nucleotide insertion	gene *35 (lysF1a)*	stop after G66
Girr_Δ*lysF1b*-LRM11	point mutation-nucleotide insertion	gene *35 (lysF1a)*	stop after G66
Girr_Δ*lysF1b*-LRM12	point mutation-nucleotide insertion	gene *35 (lysF1a)*	stop after G66
Girr_Δ*lysF1b*-LRM14	point mutation-nucleotide substitution	gene *35 (lysF1a)*	G66D
Girr_Δ*lysF1b*-LRM15	point mutation-nucleotide insertion	gene *35 (lysF1a)*	stop after G66
Girr_Δ*lysF1b*-LRM16	point mutation-nucleotide substitution	gene *35 (lysF1a)*	A31T
NBJ_Δ*lysF1b*-LRM1	point mutation-nucleotide substitution	gene *33* (*lysF1a*)	A68E
NBJ_Δ*lysF1b*-LRM2	point mutation-nucleotide substitution	gene *33* (*lysF1a*)	A68E
NBJ_Δ*lysF1b*-LRM3	point mutation-nucleotide substitution	gene *33* (*lysF1a*)	A68E
NBJ_Δ*lysF1b*-LRM7	point mutation-nucleotide substitution	gene *33* (*lysF1a*)	D9A

When phages were recovered from the large plaque, serial diluted and replated, the wild type plaque size was recovered across the full phage population (Figure 12B). This type of experiment was repeated multiple times with Girr_Δ*lysF1b* and NBJ_Δ*lysF1b* and ten independent Girr_Δ*lysF1b*-LRMs and four independent NBJ_Δ*lysF1b*-LRMs were recovered. All Girr LRM mutants showed a large plaque phenotype compared to the parent Girr_Δ*lysF1b*

(Figure S11 and RSP, data not shown) and PCR analysis of the *lysF1a-lysF1b* genomic region confirmed that all the LRM mutants contained the expected Δ*lysF1b* deletion (Figure S12). To determine the location of any nucleotide mutations within the genome of the LRM mutants, DNA was extracted and the genomes were sequenced as detailed in Methods. In all cases, the Girr_Δ*lysF1b*-LRMs and NBJ_Δ*lysF1b*-LRMs contained the expected *lysF1b* deletion but all phage also contained either nucleotide insertions, deletions or substitutions within the *lysF1a* open reading frame that altered the amino acid sequence of the LysF1a protein. A summary of all LRM mutants is provided in Table 3 and a schematic showing the amino acid changes to the different Girr_lysF1a-LRMs is presented in Figure S13.

Six different mutations were identified in the ten Girr_Δ*lysF1b*-LRMs and two in the four NBJ_Δ*lysF1b*-LRMs.The mutations mapped to three different domains of the LysF1a protein: the N-terminal cytoplasmic domain, the first TMD or the beginning of the cytoplasmic C-terminal domain. No mutants were recovered that impacted the second TMD or distal regions of the cytoplasmic C-terminal domain. In the Girr LRM mutants, two different missense mutations were found in TMD1 of LysF1a that result in R19H and A31T while one of the NBL LRM mutants changed the charged cytoplasmic D9 to A. In addition, three G66D mutants were recovered in the Girr LRMs, and three A68E mutants were recovered in the NBJ LRMs. All of these change a small hydrophobic amino acid to a negatively charged amino acid just after the end of the TMD2 at the beginning of the cytoplasmic C-terminal domain. Finally, four mutants generate a nonsense mutation that either truncates the Girr LysF1a protein after G66 or create a frame shift after A63 that results in missense coding and a premature stop after amino acid 73. All LRM mutations result in changes to the LyF1a protein that likely alter its conformation, thus, the findings validate that the LysF1a protein can efficiently function in the lysis pathway and that the protein is not exclusively an antiholin.

Lysis Recovery Mutants Exhibit Early Lysis and Reduced Burst Size

Since the LRMs generate a wild type plaque size (Figure 12A, Figure S12), it was pertinent to evaluate the lysis timing in liquid culture and determine lag time and burst size. *M. smegmatis* was infected with Girr_WT, Girr_*ΔlysF1b* and three different Girr_*ΔlysF1b*-LRMs and the OD_{600} of the culture measured as described in Methods. Figure 13A shows that Girr_WT triggers lysis as expected at ~110-minutes while Girr_*ΔlysF1b* causes reduced culture growth but no defined triggering as also shown in Figures 9 and 10. In stark contrast, Girr_*ΔlysF1b*-LRM1*,* Girr_*ΔlysF1b*-LRM2 and Girr_*ΔlysF1b*-LRM16, all trigger lysis prematurely at ~90 minutes and ultimately reduce the OD_{600} to the same baseline as Girr_WT. When NBJ_WT, NBJ_*ΔlysF1b*, NBJ_*ΔlysF1b*-LRM1 and NBJ_*ΔlysF1b*-LRM7 were tested in the liquid lysis assay, the NBJ-LRMs also trigger lysis prematurely and reduce the OD_{600} to the same level as NBJ_WT (Figure 13B). To validate the early triggering time and assess its impact on burst size, one-step growth curves were completed as described in Methods. Figure 13C shows a representative one-step experiment with Girr_WT and two LRM mutants. Phage release from Girr_*ΔlysF1b*-LRM1 and Girr_Girr_*ΔlysF1b*-LRM2 is detected by 150 minutes and plateaus by 200-minutes, a time point at which Girr_WT has achieved <10% burst size. The two Girr LMRs average burst size is also only 95.5 +/- 12.5 PFU/cell compared to 289.6 +/- 65 PFU/cell for the Girr_WT. The reduced burst size is likely the result of lysis triggering well before all phage progeny have been full assembled and is consistent with reports that have evaluated early triggering in *E. coli* phages [11, 12, 74]. The current results also indicate that plaque size in our experimental system is not a function of burst size since a >65% reduction in burst size is still able to generate wild type-sized plaques (Figure 12A,Figure S12). These findings add further support to the hypothesis that the small plaque phenotypes of the various LysF1 mutants is the result of inefficient cell wall lysis that hampers phage release.

Analysis of *lysF1b* Phage Plaque Sizes in *M. smegmatis* Lacking the Lipoarabinomannan Layer of the Cell Wall

A recent study proposes a 1TMD protein termed LysZ may function as a spanin-like protein to disrupt the integrity of the Gram-positive *Corynebacterium glutamicum* cell wall by interacting with the lipoarabinomannan (LAM) layer [57]. In these studies, deletion of *lysZ* from phages CL31 or Cog results in a small plaque phenotype that is rescued if phage were plated on a *Corynebacteriumg glutamicum* strain that is defective in the synthesis the LAM. Since both LysZ and LysF1b have a single TMD and deletion of the genes results in small plaques, it was pertinent to determine whether an *M. smegmatis* strain lacking the mtpA enzyme required to synthesize LAM (*M. smegmatis* ΔmtpA) [66], would complement the small plaque phenotype of Girr_Δ*lysF1b*. Wild type *M. smegmatis*, *M. smegmatis* ΔmtpA, and *M. smegmatis* ΔmtpA-comp (ΔmtpA carrying complementing mtpA expression plasmid), were grown to saturation and set to OD_{600} of 2.0 prior to infection. Equal amounts of phage were used to infect and cells and plaques evaluated after incubation for 48 hrs. at 37°C. Figure 14A shows that both wild type Girr and Girr_Δ*lysF1b* exhibit a modest but significant increase in plaque size when infected into the *M. smegmatis* ΔmtpA strain compared to the wild type *M. smegmatis* or the *M. smegmatis* ΔmtpA-comp strain. Girr_WT plaques increased by 1.4-fold from 2.8mm to 3.9mm while Girr_Δ*lysF1b* increased by 1.8-fold from 0.93mm to 1.7mm (Figure 14B). To account for the possibility that the change is plaque size were caused by reduced cell growth and less *M. smegmatis* ΔmtpA bacteria growing over the courses of the experiment, studies were repeated using high density cultures at 2 x 10^8 CFU/infection. This level of bacteria will exacerbate small plaque phenotypes since the increased cells enhance absorption and reduce phage diffusion [27; 81-83]. In these studies, both Girr_WT and Girr_Δ*lysF1b* showed similar plaques size increases as the low-density experiments verifying that *M. smegmatis* lacking a formal LAM layer is generally less restrictive to lysis and phage release (RSP, data not shown). Since both

Girr_WT and Girr_Δ*lysF1b* show increased plaque size and the plaques of Girr_Δ*lysF1b* do not reach Girr_WT size, the results indicate that the lack of the LAM layer does not effectively complement the deletion of *lyF1b*. This is consistent with the proposed holin function of the LysF1b and supports the hypothesis that the LysF1b and LysZ proteins have distinct functions in the lysis pathway in their respective bacterial hosts although holin function for LysZ has not been formally evaluated.

Analysis of Additional Genes Proposed to be Involved in the Lysis Pathway of F1 Cluster Phages

It is currently unknown how the various endolysins encoded by actinobacteriophages gain access to the peptidoglycan layer following phage infection. Although exogenous expression of the lysin A from some phages is cytotoxic to *M. smegmatis*, there is no evidence of signal sequences or SAR domains in these proteins [20, 29-32]. However, *Mycobacterium sp.* appear to have several different secretion systems that do not require a signal sequence [77-80]. Additionally, it has been proposed that phage Ms6 encodes a small chaperone protein (gp23) required for the export of Lysin A because the deletion of the gene results in a small plaque phenotype [48, 50]. Since both phage Girr and NBJ encode a homolog to gp23 in the same general genomic area upstream of the Lysin A (gene *29*; Figure 15A), it was of interest to determine if deletion caused a lysis defect in Girr and NBJ. Figure 14D shows that Girr gp29 is 73 amino acids and shares 76.2% identity to Ms6 gp23 while NBJ gp29 shares 76 of 77 amino acids with gp23. BRED was utilized to delete gene *29* from Girr and two independent Girr_Δ*29* phage mutants were isolated (Figure 15B). Girr_Δ*29-20* and Girr__Δ*29-25* showed no lysis defect when compared to Girr_WT in the liquid lysis assay (Figure 15C) and showed identical plaque size to Girr_WT (Figure 15E). BRED deletion of NBJ *29* (NBJ_Δ*29*) also showed wild type plaque size (Figure 15E) and no difference in liquid lysis when compared to NBJ_WT (RSP, data not shown). To explore the possible interaction of the Lysin A and gp29 further, the

proteins were modeled using AlphaFold3. The results presented in Figures S14-16 show that all models produced data with ipTM values <0.4 indicating a very low confidence in the interactions of the proteins. Thus, these results suggest that gp29 from phage Girr or NBJ is not involved in the lysis pathway. These finding are consistent with the lethal phenotype observed when both *lysF1a* and *lysF1b* are deleted since deletion of holin genes is lethal in phages that express a cytoplasmic endolysin that must exit through the holin [10-12]. If there was another gene that was absolutely required for the lysis pathway in Girr and NBJ, especially one that could enhance the secretion of the Lysin A in a holin-independent manner, it is unlikely that deletion of *lysF1a* and *lysF1b* would be lethal. A plausible explanation for the lysis defects observed in the Ms6 studies is that the method of deletion of gene *23* somehow impacted the expression of Lysin A (gene *24*) to generate a lysis phenotype. Full genome sequencing data of the Ms6 mutants was not presented or discussed [48, 50] and the requirement of a phage encoded chaperone has not been identified in any other phage.

CONCLUSIONS AND IMPLICATIONS

The results presented in this report identify the novel LysF1a and LysF1b proteins as required holin-like components of *M. smegmatis* lysis by F1 cluster phages. The data support that LysF1a and LysF1b function together as holins to time the lysis event and disrupt the PMF, however, it appears that LysF1a requires the presence of the LysF1b protein to be active as a holin. Holin function is based on several key findings. First, the deletion of both *lysF1a* and *lysF1b* genes is lethal to phage propagation (Figure 5). This is consistent with the results from *E. coli* phages where deletion of canonical holins from phages that express cytoplasmic endolysins are lethal [10-12]. In addition, deletion of both the *lysF1a* and *lysF1b* genes in the F1 cluster phage Ms6 also appears to be lethal as no viable phage were isolated from secondary plaques [48]. Second, holin function for the LysF1b protein is directly demonstrated by the ability of energy poisons to trigger premature lysis in phages that do not express LysF1a (Figure 10). Third, holin function is supported for LysF1b instead of releasin function because there is no

defined SAR-endolysins in F1 cluster phages and the energy poisons do not trigger early lysis by releasin in phage Mu [18]. Finally, holin function is supported for LysF1a by the ability to recover LRM mutants in the Δ*lysF1b* background of both Girr and NBJ that map to the LysF1a protein and create phage that trigger lysis early but are fully lysis competent (Figure 13).

The 1TMD LysF1b proteins represent a new class of holins and appear to be found predominantly in phages that infect Gram positive hosts. HHpred analysis shows that the LysF1b proteins have a high probability hit to Pfam PF10874 (DUF2746) that contains 906 proteins. Within this Pfam are hits to phages that infect *Mycobacterium sp, Gordonia sp,* and *Streptomyces sp* and hits to *Micromonospora sp, Rothia sp, Saccharothrix sp, Nocardia terpenica, Propionicmonas paludicola, Microbacterium talmoniae, Xylanimonas oleitrophica and Actinacidiphilia glaucinigra* where the later hits are likely to proteins that are encoded by prophages within the host bacteria. To assess whether additional phages in the Actinobacteriophage Database at PhagesDB.org express a LysF1-b-like homolog [84], phages infecting *M. smegmatis* were bioinformatically evaluated as described in Methods to identify the lysis cassette and associated genes that encode proteins with 1TMD. Of the ~2,600 phages in the database, 80% encoded a LysF1b-like protein with an N-out-C-in membrane topology and the proteins were grouped to 20 different phams based on their amino acid identity [85, 86]. Representative proteins from each pham are presented in Figure S17. The proteins differ in size from 92-150 amino acids, have several basic amino acids after the TMD as highlighted in Figure 3 and have between 30%-50% DEKRH charged amino acids in the C-terminal cytoplasmic domain (Figure S17). Multiple sequence alignment indicates minimal amino acid identity between the proteins (Figure S18) and the alignment also failed to identify any small regions of high identity that might serve as functional domains. Thus, while most phages that infect *M. smegmatis* in the PhagesDB.org database express a LysF1b-like protein, it is unclear whether they all function like the LysF1b proteins from Girr and NBJ.

Since deletion of both *lysF1a* and *lysF1b* genes in F1 phages is lethal and the LysF1b protein clearly can function independent of the LysF1a, what then is the function of the 2TMD LysF1a proteins in the lysis pathway? As discussed throughout this report, a role of LysF1a as a type II pinholin is not supported by the sequence data (Figure 3), or by AlphaFold3 models (Figure S7). In fact, the amino acid sequence data and lack of lysis function in the absence of LysF1b, better supports LysF1a as an inactive antiholin. However, deletion of the *lysF1a* gene results in a lysis triggering *delay* in both Girr_Δ*lysF1b* and NBJ_ Δ*lysF1b* with the later delayed over 60 minutes compared to NBJ_WT (Figure 8). A lysis delay is not consistent with the function of LysF1a as a true antiholin to the LysF1b, since it would be expected that deletion of the antiholin would result in *early* host lysis by Girr_Δ*lysF1a* or Girr_Δ*lysF1a* since the LysF1b would not be inhibited from forming active multimers as shown for lambda S_{105} and phage 21 $S^{21}68$ [10-12]. The data also demonstrate that expression of Girr or NBJ LysF1a in the absence of the LysF1b results in cell death with release of ATP, but that actual lysis and shape change of the bacteria is not detected by changes to the OD_{600} (Figure 8). These results suggest that expression of Girr or NBJ LysF1a also will ultimately disrupt the membrane to destroy the PMF, but whatever lesion is produced cannot effectively facilitate the release of the endolysins and/or phage particles. In this context, the key findings are 1) that destabilization of the PMF alone is not sufficient to “activate” LysF1a into a lesion that supports wild type lysis or phage release (Figure 10), and 2) that LRMs can be recovered in the Δ*lysF1b* background that have point mutations LysF1a that result in a fully lysis competent LysF1a protein that happens to trigger premature (i.e. unregulated) lysis (Figure 13). These findings suggest that amino acid changes to the protein may induce conformational changes to the LysF1a that allow it to fully support bacterial lysis and phage release in the absence of the LysF1b. Thus, an attractive working model is that LysF1a is not an antiholin to LysF1b but simply is not lysis active without LysF1b. Therefore, as expression of both proteins increases following infection, they reach a

concentration at which they can formally interact, and this interaction facilitates conformational changes in the LysF1a that allow it to become active in lysis. The two proteins then function together to facilitate the release of endolysins and/or phage particles. Such a model would be like the holin/antiholin system in phage lambda and phage 21 where the phages express both active holins and inactive antiholins and triggering results in an instantaneous conversion of all proteins to active holins [10-12].

Currently, it is unclear how the LysF1a and LysF1b proteins interact and whether both proteins together actively participate in the creation a heteromeric lesion the inner membrane. Clearly, LysF1b alone can trigger lysis and facilitate significant phage release, but as stated above, lysis timing and the efficiency of phage release are still not optimal. There is also no precedent for two structurally distinct TMD proteins functioning together to make a lesion. The lysis pathway of phage P2 utilizes two distinct proteins, holin Y and antiholin LysA, but LysA protein appears to be fully regulatory to holin Y and is not converted into an active holin like the antiholins S_{107} or $S^{21}71$ [11, 55, 56]. Thus, the interaction of two distinct holin monomers that have different membrane topologies is unprecedented and will require direct study of LysF1a and LysF1b proteins within membranes to resolve the structure. Such work could also directly address whether the LysF1b also has interactions with cell wall components to facilitate phage release as suggested for the LysZ proteins of *Corynebacterium* phages [57]. Whether the other Mycobacteriophages that express different variants of the LysF1a and LysF1b proteins also utilize them in the same way as Girr and NBJ will require additional deletion and complementation studies. The current study therefore provides a framework to evaluate lysis under physiological conditions in Gram-positive hosts. It is exciting to speculate that due to the presence of *lysF1*-like and *lysZ*-like genes in so many phages, it may be that the phages that infect Gram-positive hosts use a similar set of tools to complete the lysis pathway through distinct molecular mechanisms just as observed for phages that infect *E. coli.*

DATA AVAILABILITY STATEMENT

All recombinant phage and expression plasmids used in this study are available upon request. The authors affirm that all data necessary for confirming the conclusions of this article are represented fully within the article and its tables and figures. Extended data, including plasmid Sanger sequencing data and confirmatory cytotoxicity assay data for all Girr and NBJ pExTra constructs can be found at the SEA-GENES project open access database GenesDB (https://genesdb.org). To access these data on genesDB.org, any user can register for a free account, and once logged in to this account, navigate from the home page to Cluster F1 phage Girr or NBJ. Full genome sequences of Girr and NBJ are available in GenBank through accession numbers MH669003 and MH399784, respectively.

ACKNOWLEDGMENTS

We are grateful to the members of the Science Education Alliance for their invaluable research support and for supplying phage and plasmid reagents, particularly Dainelle Heller, Viknesh Sivanathan, Graham Hatfull, Deborah Jacobs-Sera, Becky Garlena and Dan Russell. We also thank the Pittsburgh Bacteriophage Institute for genome sequencing of the phages described in this study. We want to thank A. McKitterick for helpful discussions regarding LysZ. We want to thank Y. Morita for generously sending the ΔmtpA *M. smegmatis* strains.

FUNDING

This project was funded in part by an Undergraduate Grants in Aid for Research from USF Chapter of Sigma Xi to KRH and a USF Internal Proposal Enhancement Grant to RSP.

REFERENCS

1. Mushegian AR. Are There 10(31) Virus Particles on Earth, or More, or Fewer? J Bacteriol. 2020;202(9).
2. Oliveira H, Melo LD, Santos SB, Nobrega FL, Ferreira EC, Cerca N, et al. Molecular aspects and comparative genomics of bacteriophage endolysins. J Virol. 2013;87(8):4558-70.

3. Ryan GL, Rutenberg AD. Clocking out: modeling phage-induced lysis of Escherichia coli. J Bacteriol. 2007;189(13):4749-55.

4. Pang T, Fleming TC, Pogliano K, Young R. Visualization of pinholin lesions in vivo. Proc Natl Acad Sci U S A. 2013;110(22):E2054-63.

5. Savva CG, Dewey JS, Deaton J, White RL, Struck DK, Holzenburg A, et al. The holin of bacteriophage lambda forms rings with large diameter. Mol Microbiol. 2008;69(4):784-93.

6. Savva CG, Dewey JS, Moussa SH, To KH, Holzenburg A, Young R. Stable micron-scale holes are a general feature of canonical holins. Mol Microbiol. 2014;91(1):57-65.

7. Summer EJ, Berry J, Tran TA, Niu L, Struck DK, Young R. Rz/Rz1 lysis gene equivalents in phages of Gram-negative hosts. J Mol Biol. 2007;373(5):1098-112.

8. Rajaure M, Berry J, Kongari R, Cahill J, Young R. Membrane fusion during phage lysis. Proc Natl Acad Sci U S A. 2015;112(17):5497-502.

9. Berry J, Rajaure M, Pang T, Young R. The spanin complex is essential for lambda lysis. J Bacteriol. 2012;194(20):5667-74.

10. Young R. Phage lysis: three steps, three choices, one outcome. J Microbiol. 2014;52(3):243-58.

11. Cahill J, Young R. Phage Lysis: Multiple Genes for Multiple Barriers. Adv Virus Res. 2019;103:33-70.

12. Cahill J, Holt A, Theodore M, Moreland R, O'Leary C, Martin C, et al. Spatial and temporal control of lysis by the lambda holin. mBio. 2024;15(2):e0129023.

13. Park T, Struck DK, Dankenbring CA, Young R. The pinholin of lambdoid phage 21: control of lysis by membrane depolarization. J Bacteriol. 2007;189(24):9135-9.

14. Barenboim M, Chang CY, dib Hajj F, Young R. Characterization of the dual start motif of a class II holin gene. Mol Microbiol. 1999;32(4):715-27.

15. Blasi U, Young R. Two beginnings for a single purpose: the dual-start holins in the regulation of phage lysis. Mol Microbiol. 1996;21(4):675-82.

16. Ramanculov E, Young R. An ancient player unmasked: T4 rI encodes a t-specific antiholin. Mol Microbiol. 2001;41(3):575-83.

17. Ramanculov E, Young R. Genetic analysis of the T4 holin: timing and topology. Gene. 2001;265(1-2):25-36.

18. Chamblee JS, Ramsey J, Chen Y, Maddox LT, Ross C, To KH, et al. Endolysin Regulation in Phage Mu Lysis. mBio. 2022;13(3):e0081322.

19. Raman SK, Siva Reddy DV, Jain V, Bajpai U, Misra A, Singh AK. Mycobacteriophages: therapeutic approach for mycobacterial infections. Drug Discov Today. 2024;29(7):104049.

20. Payne KM, Hatfull GF. Mycobacteriophage endolysins: diverse and modular enzymes with multiple catalytic activities. PLoS One. 2012;7(3):e34052.

21. Schmelcher M, Donovan DM, Loessner MJ. Bacteriophage endolysins as novel antimicrobials. Future Microbiol. 2012;7(10):1147-71.

22. Arenskotter M, Broker D, Steinbuchel A. Biology of the metabolically diverse genus Gordonia. Appl Environ Microbiol. 2004;70(6):3195-204.

23. Goodfellow M, Jones AL. Corynebacteriales ord. nov. Bergey's Manual of Systematics of Archaea and Bacteria. 2015. p. 1-14.

24. Brennan PJ. Structure, function, and biogenesis of the cell wall of Mycobacterium tuberculosis. Tuberculosis (Edinb). 2003;83(1-3):91-7.

25. Hart EM, Bernhardt TG. The mycomembrane. Curr Biol. 2025;35(3):R85-R6.

26. Catalao MJ, Pimentel M. Mycobacteriophage Lysis Enzymes: Targeting the Mycobacterial Cell Envelope. Viruses. 2018;10(8).

27. Payne K, Sun Q, Sacchettini J, Hatfull GF. Mycobacteriophage Lysin B is a novel mycolylarabinogalactan esterase. Mol Microbiol. 2009;73(3):367-81.

28. Marinelli LJ, Piuri M, Swigonova Z, Balachandran A, Oldfield LM, van Kessel JC, et al. BRED: a simple and powerful tool for constructing mutant and recombinant bacteriophage genomes. PLoS One. 2008;3(12):e3957.

29. Joshi H, Seniya SP, Suryanarayanan V, Patidar ND, Singh SK, Jain V. Dissecting the structure-function relationship in lysozyme domain of mycobacteriophage D29-encoded peptidoglycan hydrolase. FEBS Lett. 2017;591(20):3276-87.

30. Singh AK, Gangakhedkar R, Thakur HS, Raman SK, Patil SA, Jain V. Mycobacteriophage D29 Lysin B exhibits promising anti-mycobacterial activity against drug-resistant Mycobacterium tuberculosis. Microbiol Spectr. 2023;11(6):e0459722.

31. Pohane AA, Joshi H, Jain V. Molecular dissection of phage endolysin: an interdomain interaction confers host specificity in Lysin A of Mycobacterium phage D29. J Biol Chem. 2014;289(17):12085-95.

32. Nair G, Jain V. An intramolecular cross-talk in D29 mycobacteriophage endolysin governs the lytic cycle and phage-host population dynamics. Sci. Adv.2024;10(6):

33. Gil F, Catalao MJ, Moniz-Pereira J, Leandro P, McNeil M, Pimentel M. The lytic cassette of mycobacteriophage Ms6 encodes an enzyme with lipolytic activity. Microbiology (Reading). 2008;154(Pt 5):1364-71.

34. Gil F, Grzegorzewicz AE, Catalao MJ, Vital J, McNeil MR, Pimentel M. Mycobacteriophage Ms6 LysB specifically targets the outer membrane of Mycobacterium smegmatis. Microbiology (Reading). 2010;156(Pt 5):1497-504.

35. Loessner MJ, Gaeng S, Wendlinger G, Maier SK, Scherer S. The two-component lysis system of Staphylococcus aureus bacteriophage Twort: a large TTG-start holin and an associated amidase endolysin. FEMS Microbiol Lett. 1998;162(2):265-74.

36. Kwan T, Liu J, DuBow M, Gros P, Pelletier J. The complete genomes and proteomes of 27 Staphylococcus aureus bacteriophages. Proc Natl Acad Sci U S A. 2005;102(14):5174-9.

37. Vybiral D, Takac M, Loessner M, Witte A, von Ahsen U, Blasi U. Complete nucleotide sequence and molecular characterization of two lytic Staphylococcus aureus phages: 44AHJD and P68. FEMS Microbiol Lett. 2003;219(2):275-83.

38. Godinho LM, El Sadek Fadel M, Monniot C, Jakutyte L, Auzat I, Labarde A, et al. The Revisited Genome of Bacillus subtilis Bacteriophage SPP1. Viruses. 2018;10(12).

39. Escobedo S, Campelo AB, Wegmann U, Garcia P, Rodriguez A, Martinez B. Insight into the Lytic Functions of the Lactococcal Prophage TP712. Viruses. 2019 ;11(10).

40. Sao-Jose C, Parreira R, Vieira G, Santos MA. The N-terminal region of the Oenococcus oeni bacteriophage fOg44 lysin behaves as a bona fide signal peptide in Escherichia coli and as a cis-inhibitory element, preventing lytic activity on oenococcal cells. J Bacteriol. 2000;182(20):5823-31.

41. Gindreau E, Lonvaud-Funel A. Molecular analysis of the region encoding the lytic system from Oenococcus oeni temperate bacteriophage phi 10MC. FEMS Microbiol Lett. 1999;171(2):231-8.

42. Nelson D, Schuch R, Zhu S, Tscherne DM, Fischetti VA. Genomic sequence of C1, the first streptococcal phage. J Bacteriol. 2003;185(11):3325-32.

43. Pope WH, Mavrich TN, Garlena RA, Guerrero-Bustamante CA, Jacobs-Sera D, Montgomery MT, et al. Bacteriophages of Gordonia spp. Display a Spectrum of Diversity and Genetic Relationships. mBio. 2017;8(4).

44. Pollenz RS, Bland J, Pope WH. Bioinformatic characterization of endolysins and holin-like membrane proteins in the lysis cassette of phages that infect Gordonia rubripertincta. PLoS One. 2022;17(11):e0276603.

45. McGarrah CEE, Algarin-Martinez ED, Cavasini MED, Correa V, Danielson DF, Dean WR, et al. Isolation and Annotation of Azira, a CT Cluster Phage That Infects Gordonia rubripertincta. Microbiol Resour Announc. 2023;12(7):e0034723.

46. Dedrick RM, Marinelli LJ, Newton GL, Pogliano K, Pogliano J, Hatfull GF. Functional requirements for bacteriophage growth: gene essentiality and expression in mycobacteriophage Giles. Mol Microbiol. 2013;88(3):577-89.

47. Sandoval AM, Abram AM, Alhabib ZM, Antonyan AS, Brikho SM, Buhay SI, et al. Complete Genome Sequences of Cluster G Mycobacteriophage Darionha, Cluster A Mycobacteriophage Salz, and Cluster J Mycobacteriophage ThreeRngTarjay. Microbiol Resour Announc. 2020;9(20).

48. Catalao MJ, Gil F, Moniz-Pereira J, Pimentel M. Functional analysis of the holin-like proteins of mycobacteriophage Ms6. J Bacteriol. 2011;193(11):2793-803.

49. Garcia M, Pimentel M, Moniz-Pereira J. Expression of Mycobacteriophage Ms6 lysis genes is driven by two sigma(70)-like promoters and is dependent on a transcription termination signal present in the leader RNA. J Bacteriol. 2002;184(11):3034-43.

50. Catalao MJ, Gil F, Moniz-Pereira J, Pimentel M. The mycobacteriophage Ms6 encodes a chaperone-like protein involved in the endolysin delivery to the peptidoglycan. Mol Microbiol. 2010;77(3):672-86.

51. Bavda VR, Jain V. Deciphering the Role of Holin in Mycobacteriophage D29 Physiology. Front Microbiol. 2020;11:883.

52. Bavda VR, Yadav A, Jain V. Decoding the molecular properties of mycobacteriophage D29 Holin provides insights into Holin engineering. J Virol. 2021;95(10).

53. Kamilla S, Jain V. Mycobacteriophage D29 holin C-terminal region functionally assists in holin aggregation and bacterial cell death. FEBS J. 2016;283(1):173-90.

54. Ford ME, Sarkis GJ, Belanger AE, Hendrix RW, Hatfull GF. Genome structure of mycobacteriophage D29: implications for phage evolution. J Mol Biol. 1998;279(1):143-64.

55. To KH, Dewey J, Weaver J, Park T, Young R. Functional analysis of a class I holin, P2 Y. J Bacteriol. 2013;195(6):1346-55.

56. Christie GE, Calendar R. Bacteriophage P2. Bacteriophage. 2016;6(1):e1145782.

57. McKitterick AC, Lyerly EW, Bernhardt TG. Bacteriophages target membrane-anchored glycopolymers to promote host cell lysis and progeny release. bioRxiv. 2025:2025.06.24.661397.

58. Hallgren J, Tsirigos KD, Pedersen MD, Almagro Armenteros JJ, Marcatili P, Nielsen H, et al. DeepTMHMM predicts alpha and beta transmembrane proteins using deep neural networks. bioRxiv. 2022:2022.04.08.487609.

59. Tsirigos KD, Peters C, Shu N, Kall L, Elofsson A. The TOPCONS web server for consensus prediction of membrane protein topology and signal peptides. Nucleic Acids Res. 2015;43(W1):W401-7.

60. Almagro Armenteros JJ, Tsirigos KD, Sonderby CK, Petersen TN, Winther O, Brunak S, et al. SignalP 5.0 improves signal peptide predictions using deep neural networks. Nat Biotechnol. 2019;37(4):420-3.

61. Juncker AS, Willenbrock H, Von Heijne G, Brunak S, Nielsen H, Krogh A. Prediction of lipoprotein signal peptides in Gram-negative bacteria. Protein Sci. 2003;12(8):1652-62.

62. Soding J, Biegert A, Lupas AN. The HHpred interactive server for protein homology detection and structure prediction. Nucleic Acids Res. 2005;33(Web Server issue):W244-8.

63. Abramson J, Adler J, Dunger J, Evans R, Green T, Pritzel A, et al. Accurate structure prediction of biomolecular interactions with AlphaFold 3. Nature. 2024;630(8016):493-500.

64. Madeira F, Madhusoodanan N, Lee J, Eusebi A, Niewielska A, Tivey ARN, Lopez, R, Butcher S. The EMBL-EBI Job Dispatcher sequence analysis tools framework in 2024. Nucleic acids research. 2024;52(W1):W521–W525.

65. Snapper SB, Melton RE, Mustafa S, Kieser T, Jacobs WR, Jr. Isolation and characterization of efficient plasmid transformation mutants of Mycobacterium smegmatis. Mol Microbiol. 1990;4(11):1911-9.

66. Sparks IL, Kado T, Prithviraj M, Nijjer J, Yan J, Morita YS. Lipoarabinomannan mediates localized cell wall integrity during division in mycobacteria. Nat Commun. 2024;15(1):2191.

67. Heller D, Amaya I, Mohamed A, Ali I, Mavrodi D, Deighan P, et al. Systematic overexpression of genes encoded by mycobacteriophage Waterfoul reveals novel inhibitors of mycobacterial growth. G3 (Bethesda). 2022;12(8).

68. Pollenz RS, Barnhill K, Biggs A, Bland J, Carter V, Chase M, et al. A genome-wide cytotoxicity screen of cluster F1 mycobacteriophage Girr reveals novel inhibitors of Mycobacterium smegmatis growth. G3 (Bethesda). 2024;14(5).

69. Wise B, Edwards K, Jirsa C, [student authors], Kanther M, Payne K, Pollenz RS, Heller DM. Identification and characterization of host-modulating effectors encoded by the Cluster F1 mycobacteriophage NormanBulbieJr. bioRxiv 2025.

70. van Kessel JC, Hatfull GF. Mycobacterial recombineering. Methods Mol Biol. 2008;435:203-15.

71. Gordon D, Abajian C, Green P. Consed: a graphical tool for sequence finishing. Genome Res. 1998;8(3):195-202.

72. Russell DA. Sequencing, Assembling, and Finishing Complete Bacteriophage Genomes. Methods Mol Biol. 2018;1681:109-25.

73. Schneider CA, Rasband WS, Eliceiri KW. NIH Image to ImageJ: 25 years of image analysis. Nat Methods. 2012;9(7):671-5.

74. Pang T, Park T, Young R. Mutational analysis of the S21 pinholin. Mol Microbiol. 2010;76(1):68-77.

75. Park T, Struck DK, Deaton JF, Young R. Topological dynamics of holins in programmed bacterial lysis. Proc Natl Acad Sci U S A. 2006;103(52):19713-8.

76. Doermann AH. The intracellular growth of bacteriophages. I. Liberation of intracellular bacteriophage T4 by premature lysis with another phage or with cyanide. J Gen Physiol. 1952;35(4):645-56.

77. Rigel NW, Gibbons HS, McCann JR, McDonough JA, Kurtz S, Braunstein M. The Accessory SecA2 System of Mycobacteria Requires ATP Binding and the Canonical SecA1. J Biol Chem. 2009;284(15):9927-9936.

78. Abdallah A, Gey van Pittius N, DiGiuseppe Champion P, Cox J, Luirink J, et. al. Type VII secretion — mycobacteria show the way. Nat Rev Microbiol. 2007;5:883–891.

79. Bendtsen JD, Kiemer L, Fausbøll A, Brunak S. Non-classical protein secretion in bacteria. BMC Microbiol. 2005;5:58.

80. Zhang Z, Dong L, Li X, Deng T, Wang Q. The PE/PPE family proteins of Mycobacterium tuberculosis: evolution, function, and prospects for tuberculosis control. Front. Immunol. 2025;16:1606311.

81. Ameh EM, Tyrrel S, Harris JA, Pawlett M, Orlova EV, Ignatiou A, et al. Lysis Performance of Bacteriophages with Different Plaque Sizes and Comparison of Lysis Kinetics After Simultaneous and Sequential Phage Addition. Phage (New Rochelle). 2020;1(3):149-57.

82. Abedon ST, Yin J. Bacteriophage plaques: theory and analysis. Methods Mol Biol. 2009;501:161-74.

83. Dennehy JJ, Abedon ST, Turner PE. Host density impacts relative fitness of bacteriophage Phi6 genotypes in structured habitats. Evolution. 2007;61(11):2516-27.

84. Russell DA, Hatfull GF. PhagesDB: the actinobacteriophage database. Bioinformatics. 2017;33(5):784-6.

85. Gauthier CH, Cresawn SG, Hatfull GF. 2022. PhaMMseqs: a new pipeline for constructing phage gene phamilies using MMseqs2. G3 Genes Genomes Genetics. 2022;12(11):jkac233.

86. Gauthier CH, Hatfull GF. PhamClust: a phage genome clustering tool using proteomic equivalence. mSystems. 2023;8(5):e00443-23.

FIGURE LEGANDS

Figure 1. Lysis cassette organization of Girr and NormanBulbieJr (NBJ). Predicted protein coding genes are shown as colored boxes. The genomic location is represented by the ruler, and the numbers represent the kilobase from nucleotide 1. Both lysis cassette regions are located upstream of the *tape measure* and *minor tail* genes. Genes above the genome are transcribed in the forward direct and genes below in the reverse direction. Genes with the same color encode proteins that are grouped to the same pham. Pink shading indicated nucleotide identity >90% in the shaded region. The *lysin A, lysin B,* 2TMD *lysF1a and* 1TMD *lysF1b* genes are identified. NKF = genes with no know function; *HNH* = HNH endonuclease.

Figure 2. Amino acid sequence and topology of Girr and NBJ LysF1a proteins and comparison to phage 21 S^{21} pinholin. **A.** The amino acid sequences of Girr and NBJ LysF1a showing the location of the predicted TMDs and charged amino acids. **B.** The amino acid sequence of phage 21 S^{21}68 holin, S^{21}71 antiholin and $S^{21}68_{IRS}$ showing the location of the predicted TMDs and charged amino acids. **C.** Predicted membrane topology of Girr LysF1a, $S^{21}68_{IRS}$ and the proposed topology of the S^{21}68 holin homodimer with cytoplasmic TMD1.

Figure 3. Amino acid sequence and topology of lysis proteins with 1TMD. **A.** The amino acid sequences of Girr LysF1b, NBJ LysF1b, Waterfoul gp32 and Mu releasin showing the location of the predicted TMD and the charged amino acids. **B.** AlphaFold3 structural predictions and membrane topologies of 1TMD proteins involved in lysis. pTM values: Mu, 0.51; NBJ LysF1b, 0.40; Girr LysF1b, 0.41; Rz, 0.57; T, 0.74. **C.** Predicted topologies of Girr LysF1b and Waterfoul gp32.

Figure 4. Deletion of Girr *lysF1a* and *lysF1b*. A. Genomic structure and PCR primer set locations in Girr gene deletion mutants. Primer set 1 (P1) uses primers Girr-FL_*lysF1a* (F and R) and generates a 755bp fragment in Girr_WT and 487bp with *lysF1a* deletion. Primer set 2 (P2) uses primers Girr-FL_*lysF1b* (F and R) and generates a 933bp fragment in Girr_WT and 594bp with *lysF1b* deletion. Primer set 3 (P3) uses the forward Girr-FL_*lysF1a* and reverse Girr-FL_*lysF1b* and generates a 1189bp fragment in Girr_WT and either 921bp with *lysF1a* deletion or 818b with *lysF1b* deletion. **B.** PCR verification of high titer lysates of Girr_WT, Girr_Δ*lysF1a* and Girr_Δ*lysF1b* using the indicated primer sets. PCR band sizes are identified and show correct deletions of the indicated genes.

Figure 5. Deletion of both Girr *lysF1a* and *lysF1b*. A. Schematic showing experimental procedure. **B.** DADA PCR was carried out on the indicated samples as described in Methods. Negative control Girr_lysF1a shown in lanes 1 and 7. Positive control is the 1° plaque pick with the Girr_lysF1a/lysF1b phage and 325bp DADA band (+DADA) is shown in lanes 2 and 11. Lanes 3-6 show the DADA PCR screen of 2° lysates harvested from non-complementing *M. smegmatis* that contained the indicated number of plaques (PFU). Lanes 8-10 show DADA PCR screen of 2° lysates harvested from complementing *M. smegmatis* carrying pExTra-Girr*34*. Note the lack of a positive DADA band in all samples plated on non-complementing *M. smegmatis*.

Figure 6 Plaque sizes in Girr_WT, Girr_Δ*lysF1a* and Girr_Δ*lysF1b*. *M. smegmatis* was infected with identical numbers of phage and detailed in Methods and plaque size determined after 36 hrs. of growth at 37°C. Scale = 1cm. Plaque volume schematics are presented to illustrate the plaque size differences.

Figure 7. Complementation of plaque phenotype in Girr_Δ*lysF1b*. A. Plaque assays were completed with *M. smegmatis* using Girr_WT or Girr_Δ*lysF1b* as described in Methods. Plaque assays were completed with *M. smegmatis* complementing strains carrying the indicated pExTra-Waterfoul expression plasmids using Girr_Δ*lysF1b* as described in Methods. Plaques were evaluated following incubation at 37°C for 36 hrs. Plaques sizes were quantified using ImageJ and the average diameter +/- standard deviation for > 50 plaques is shown. * = statistically different from Girr_WT, p <*0.0001*. ** = statistically different from Girr_Δ*lysF1b* infected on *M. smegmatis* with pExTra Waterfoul_*32* with no aTc, p <*0.0001*. Scale = 1cm. B. Plaque assays were completed with *M. smegmatis* using Girr_WT or Girr_Δ*lysF1b* as described in Methods. Plaque assays were completed with *M. smegmatis* complementing strains carrying the indicated pExTra-Waterfoul expression plasmids using Girr_Δ*lysF1b* as described in Methods. Plaques were evaluated following incubation at 37°C for 48 hrs. Plaques sizes were quantified using ImageJ and the average diameter +/- standard deviation for > 50 plaques is shown * = statistically different from Girr_WT, *p <0.0001*. ** = statistically different from Girr_Δ*lysF1b* infected on *M. smegmatis* with pExTra01, *p <0.0001*. Scale = 1cm.

Figure 8. Complementation of plaque phenotype in Girr_Δ*lysF1a*. Plaque assays were completed with *M. smegmatis* using Girr_WT or Girr_Δ*lysF1a* as described in Methods. Plaque assays were completed with *M. smegmatis* complementing strains carrying pExTra-Girr_*34* expression plasmid using Girr_Δ*lysF1a*as described in Methods. Plaques were evaluated following incubation at 37°C for 48 hrs. Plaques sizes were quantified using ImageJ and the average diameter +/- standard deviation for > 50 plaques is shown. * = statistically different from Girr_WT, *p <0.0001*. ** = statistically different from Girr_Δ*lysF1a* infected on *M. smegmatis* with pExTra-Girr_*34* with no aTc, *p <0.0001*. Scale = 1cm.

Figure 9. Liquid lysis assay and ATP release from *M. smegmatis* after infection. At T_0 a log growth culture of *M. smegmatis* at an OD_{600} of ~0.25 was infected with the indicated phage at an MOI of 10:1 and incubated at 37°C for 30 minutes without shaking. Control cultures (no phage) did not receive phage. At T_{30} minutes the culture was constantly shaken a 225rpm, aliquots removed at the indicated times and bacterial growth evaluated at OD_{600}. Open white arrow shows the 30-minute infection time. **A.** Representative results following infection with Girr_WT, Girr_Δ*lysF1a* and Girr_Δ*lysF1b*. **B**. Representative results following infection with NBJ_WT, NBJ_Δ*lysF1a* and NBJ_Δ*lysF1b.* **C.** Samples of culture were removed from the cultures represented in A and B at the times indicated by the solid black triangle on the x axis. The presence of ATP was evaluated as described in Methods.

Figure 10. Energy poisons trigger early lysis in phage expressing LysF1b but not LysF1a. At T_0 a log growth culture of *M. smegmatis* at an OD_{600} of ~0.25 was infected with the indicated phage at an MOI of 10:1 and incubated at 37°C for 30 minutes without shaking. Control cultures (no phage) did not receive phage. At T_{30} minutes the culture was constantly shaken a 225rpm, aliquots removed at the indicated times and bacterial growth evaluated at OD_{600}. **A**. Representative results following infection with Girr_WT, and Girr_Δ*lysF1a*. KCN (final concentration of 10mM) was added to a culture infected with Girr_Δ*lysF1a* and an uninfected culture at 110 minutes (open arrow). **B**. Representative results following infection with NBJ_WT, and NBJ_Δ*lysF1a.* KCN (final concentration of 10mM) was added to a culture infected with NBJ_Δ*lysF1a* and uninfected culture at 120 minutes (open arrow). **C.** Representative results following infection with Girr_WT, and Girr_Δ*lysF1b*. KCN (final concentration of 10mM) or $CHCl_3$ (final concentration 1%) was added to cultures infected with Girr_Δ*lysF1b* and uninfected cultures at 180 minutes (open arrow). **D**. Representative results following infection with NBJ_WT, and NBJ_Δ*lysF1b.* KCN (final concentration of 10mM) or $CHCl_3$ (final concentration

1%) was added to cultures infected with NBJ_Δ*lysF1b* and uninfected cultures at 180 minutes (open arrow).

Figure 11. One-step growth curves of *M. smegmatis* infected with Girr_Δ*lysF1a* and Girr_Δ*lysF1b*. A. One-step growth curves using Girr_WT, Girr_Δ*lysF1a* and Girr_Δ*lysF1b* were completed as described in Methods. Each time point represents the average and standard deviation from 3 different experiments. **B**. The data for Girr_*ΔlysF1b* from panel A replotted with a different Y axis than used in A. **C**. Burst size was determined as described in Methods. The average bust size +/- standard deviation is from three different experiments and represents the average of all points once the curve reached a plateau.

Figure 12. Isolation of Girr_Δ*lysF1b*-LRM mutants. **A**. *M. smegmatis* was infected with Girr*ΔlysF1b,* plate lysates recovered from the plaque assay and *M. smegmatis* infected with the recovered phage. Panel A shows a representative plaque assay following the second round of infection. A large plaque is circled. **B**. Phage were isolated from the large plaque in A, serial diluted and used for plaque assay. Plates were incubated at 37°C for 36 hrs. **C**. Plaque assay from Girr_WT phage. Plates were incubated at 37°C for 36 hrs. Scale bar = 1cm in all images.

Figure 13. Liquid lysis and one-step assay of Girr and NBJ LRM mutants. At T_0 a log growth culture of *M. smegmatis* at an OD_{600} of ~0.25 was infected with the indicated phage at MOI 10:1 for 30 minutes at 37°C without shaking. Control cultures (no phage) did not receive phage. At T_{30} minutes the culture was constantly shaken a 225rpm and aliquots removed over time. *M. smegmatis* growth was evaluated at OD_{600}. **A**. Representative results following infection with Girr_WT and indicated LRM mutants. **B**. Representative results following infection with NBJ_WT and indicated LRM mutants **C.** One-step growth curves using Girr_WT and

Girr_Δ*lysF1b*-LRM1 and Girr_Δ*lysF1b*-LRM2 were completed as described in Methods. Each time point represents the average and standard deviation from 3 different experiments.

Figure 14. Analysis of *lysF1b* phage plaque sizes in *M. smegmatis* lacking the lipoarabinomannan layer. A. Representative plaque assays using Wild type *M. smegmatis, M. smegmatis* ΔmtpA-comp or *M. smegmatis* ΔmtpA cultures infected with the same amount of Girr_WT or Girr_Δ*lysF1b* and incubated for 48 hrs. at 37°C. Ruler = 1cm. **B**. Plaque sizes were determined as described in Methods. The average plaque diameter +/- standard deviation for 25 plaques is shown.

Figure 15. Analysis of NKF gene *29*. A. Gene organization of Girr, NBJ and Ms6 lysis cassette region. Predicted protein coding genes are shown as colored boxes. The genomic location is represented by the ruler, and the numbers represent the kilobase from nucleotide 1. Genes above the genome are transcribed in the forward direct and genes below in the reverse direction. Genes with the same color encode proteins that are grouped to the same pham. Pink shading indicated nucleotide identity >90% in the shaded region. *NKF* = Girr_*29*, NBJ_*29* and Ms6_*23*. **B**. PCR analysis of Girr_Δ*29*-20 and Girr_Δ*29*-25. **C**. Liquid lysis assay of the indicated phages was carried out as described in Methods. **D**. Amino acid alignment of Girr gp29, NBJ gp29 and Ms6 gp23 by Clustal Omega. **E**. Plaque assay of Girr_WT, Girr_Δ*29-20*, Girr Δ*29-25*, NBJ_WT, and NBJ_Δ*29.* Ruler = 1cm. Plaque sizes were determined as described in Methods. The average plaque diameter +/- standard deviation for 25 plaques is shown.

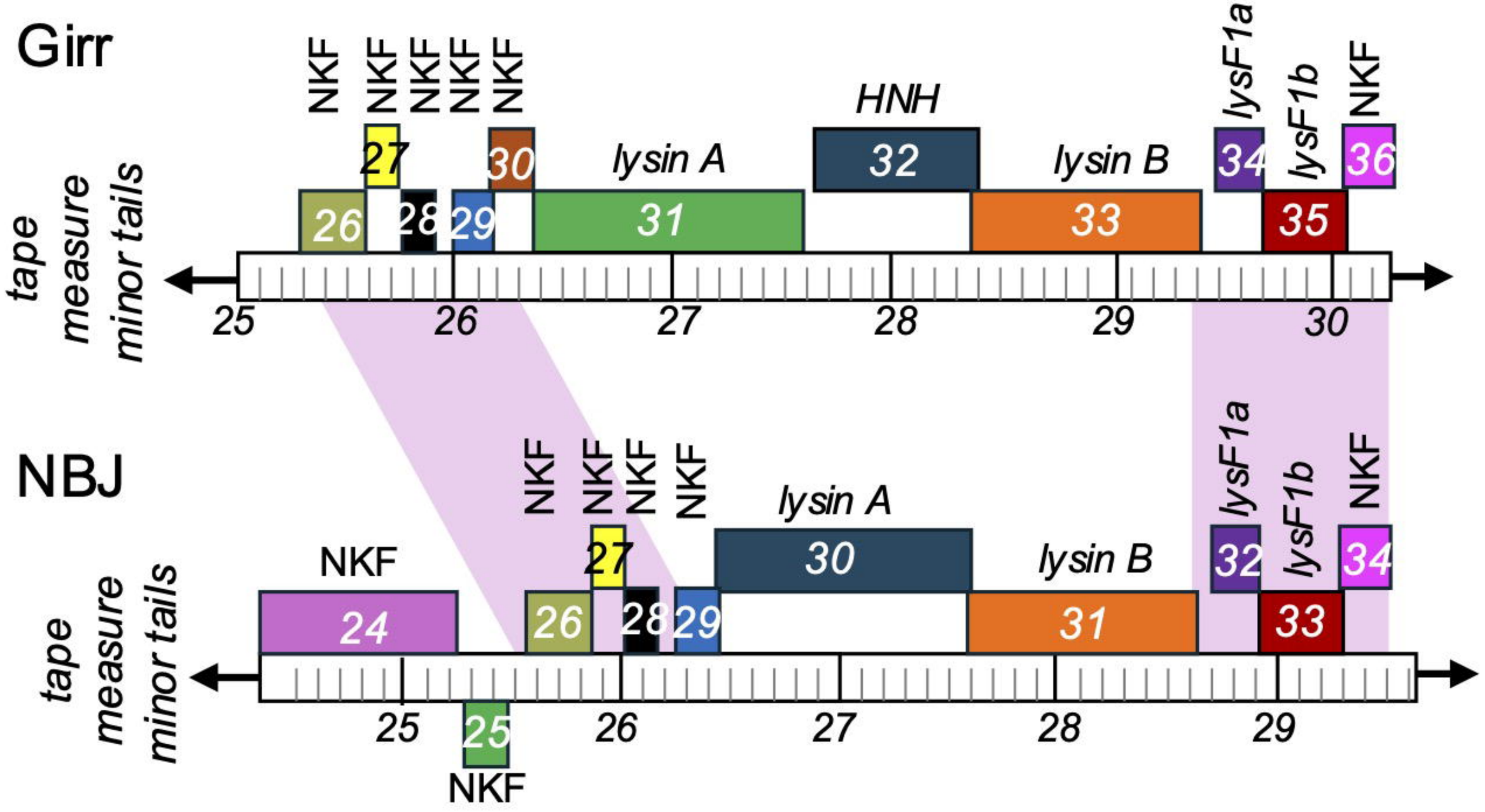
Girr
NKF
NKF
NKF
NKF
NKF
HNH
lysF1a
lysF1b
NKF
27
30
lysin A
32
lysin B
34
36
26
28
29
31
33
35
tape measure minor tails
25
26
27
28
29
30
NBJ
NKF
NKF
NKF
NKF
lysin A
lysF1a
lysF1b
NKF
NKF
27
30
lysin B
32
34
24
26
28
29
31
33
tape measure minor tails
25
25
26
27
28
29
NKF

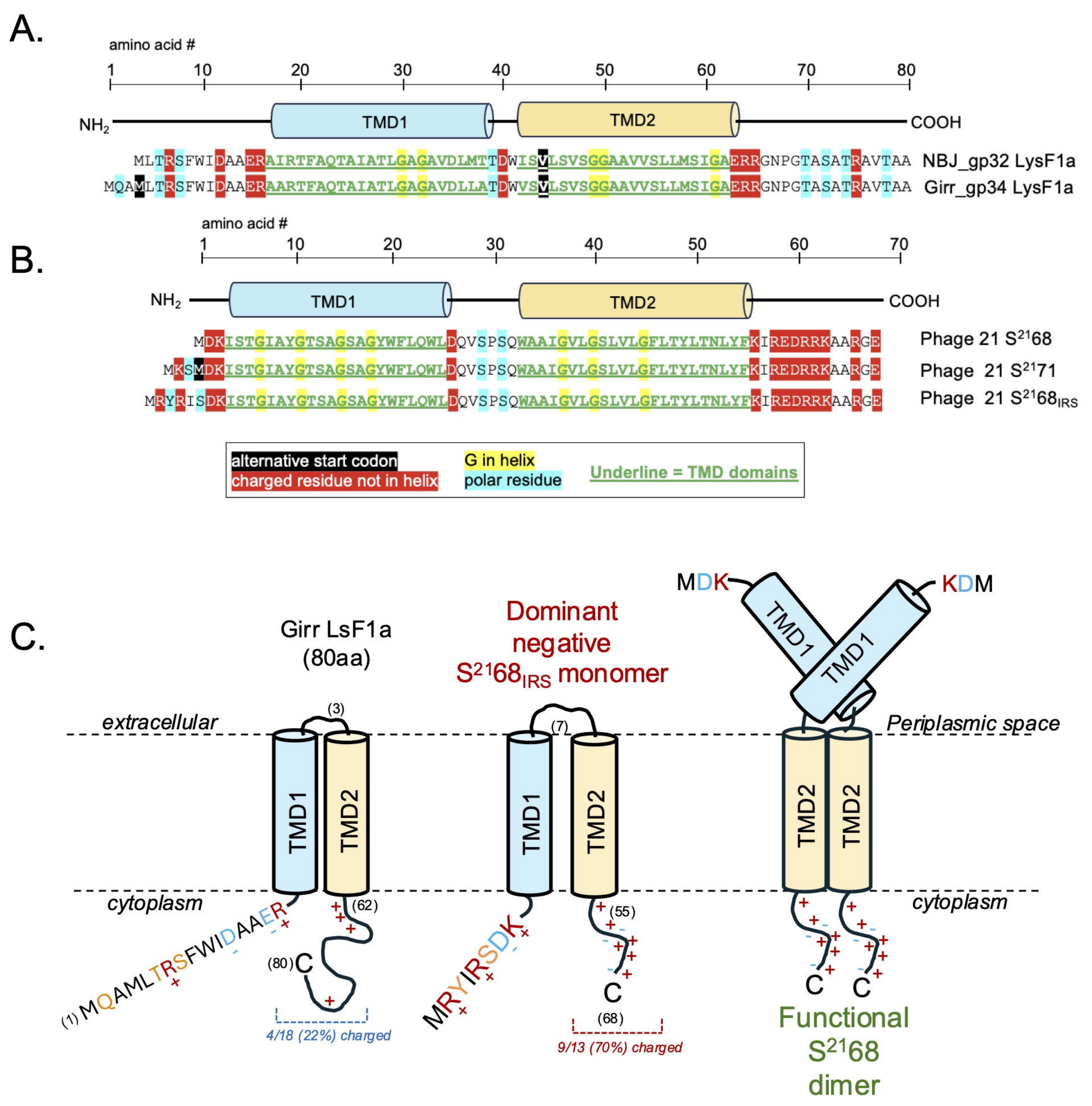
A.
amino acid #
1 10 20 30 40 50 60 70 80
NH2
TMD1
TMD2
COOH
MLTRSFWIDAAERAIRTFAQTAIATLGAGAVDLMTTDWISVLSVSGGAAVVSLLMSIGAERRGNPGTASATRAVTAA NBJ_gp32 LysF1a
MQAMLTRSFWIDAAERAARTFAQTAIATLGAGAVDLLATDWVSVLSVSGGAAVVSLLMSIGAERRGNPGTASATRAVTAA Girr_gp34 LysF1a
B.
amino acid #
1 10 20 30 40 50 60 70
NH2
TMD1
TMD2
COOH
MDKISTGIAYGTSAGSAGYWFLQWLDQVSPSQWAAIGVLGSLVLGFLTYLTNLYFKIREDRRKAARGE Phage 21 S21 68
MKSMDKISTGIAYGTSAGSAGYWFLQWLDQVSPSQWAAIGVLGSLVLGFLTYLTNLYFKIREDRRKAARGE Phage 21 S21 71
MRYRISDKISTGIAYGTSAGSAGYWFLQWLDQVSPSQWAAIGVLGSLVLGFLTYLTNLYFKIREDRRKAARGE Phage 21 S21 68IRS
alternative start codon
charged residue not in helix
G in helix
polar residue
Underline = TMD domains
C.
Girr LsF1a
(80aa)
Dominant
negative
S21 68IRS monomer
MDK
KDM
TMD1
TMD1
extracellular
Periplasmic space
(3)
(7)
TMD1
TMD2
TMD1
TMD2
TMD2
TMD2
cytoplasm
cytoplasm
(62)
(55)
(1) MQAMLTRSFWIDAAER
(80) C
MRYIRSDK
C
(68)
C C
4/18 (22%) charged
9/13 (70%) charged
Functional
S21 68
dimer

A.

1 10 20 30 40 50 60 70 80 90 100 110 120 # amino acids

MIWESVREAVDAAYQPDDGIDLIGLLIIGLPSTIAAIGTGIVGVLTVRGQRKGRERARQIDAKTDEIHEQTVNTHDTNMRDDLDEIRDLVRDGFKQIQRDIGGLREELRTERLERIEGDKRRD Girr gp35 LysF1b

MIWESVREAVDAAYQPDDGIDLIGLLIIGLPSTIAAIGTGIVGVLTVRGQRKGRERARRIDAKTYEIHEQTVNTHDTNMRDDLDEIRDLVRDGFKQIQRDIGGLREELRTERLERIEGDKRRD NBJ gp33 LysF1b

MTGSAVSALPSDWYGLAGLAVVNAAGLLALFMKARGTHKQVANSHSTNLRDDIDGLRDHIVELGRDIGGMRTDVGQLRGEVRDDRTHTHHRFRRIEDKLDELAGRGARESG Waterfoul gp32

MDLISVLALWPYLLPVVAGGAVWAMRRSFASTERVERLENRMTEMETRYASIPGTEDVHEMRLQIAELSGDIRVLSQRVQSFSHQLELLLENAVNRSNS Mu releasin

NH_2 — TMD1 — basic — KRHDE residues — COOH

Green = TMD domain | Basic region after TMD | + Charged | - Charged

B.

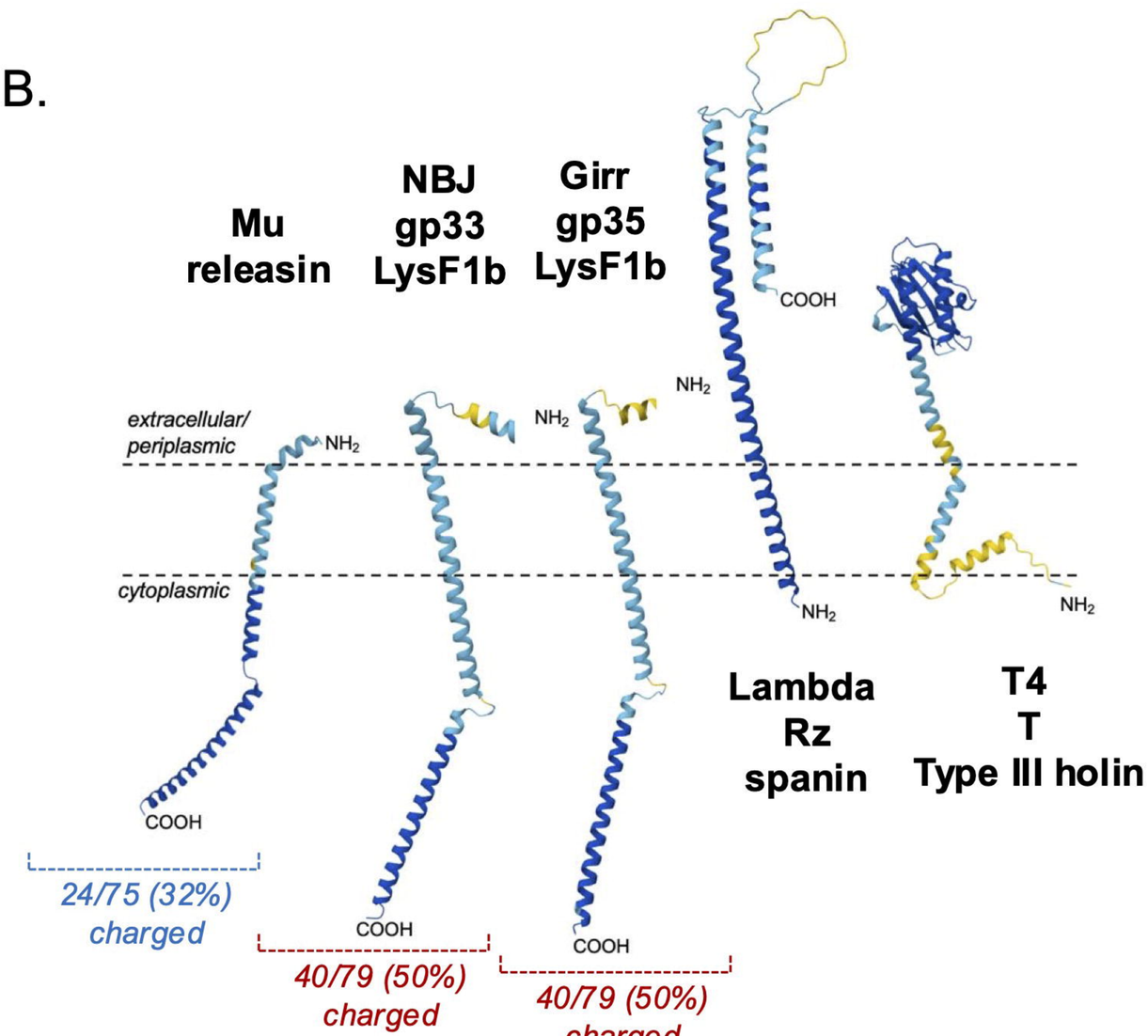

C.

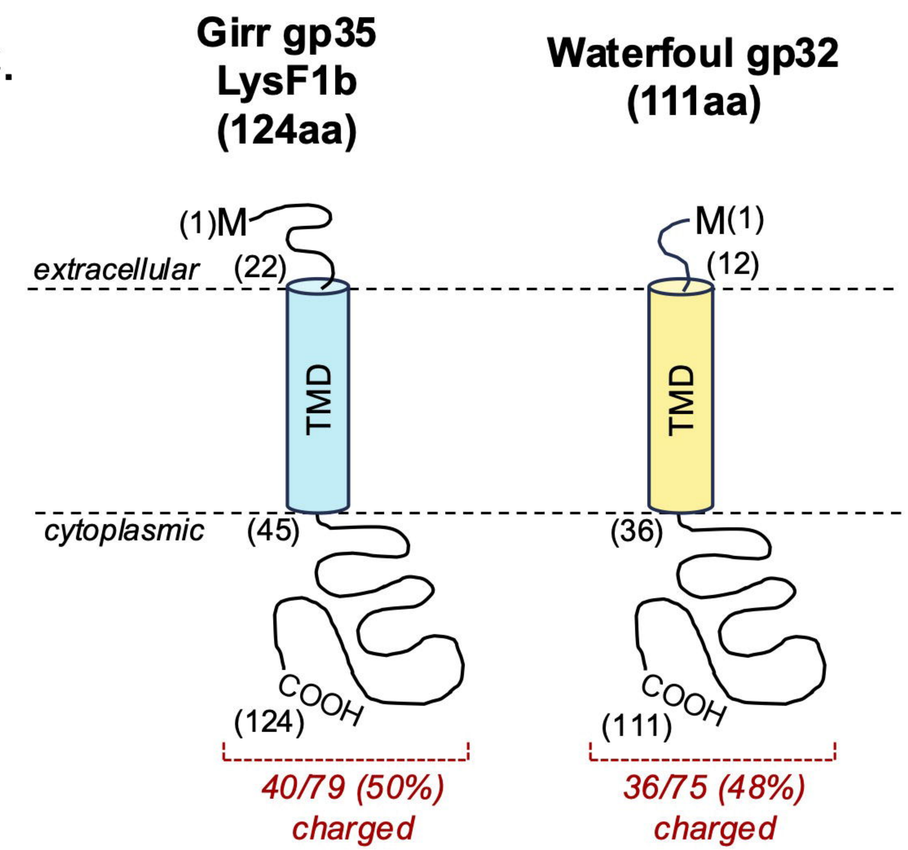

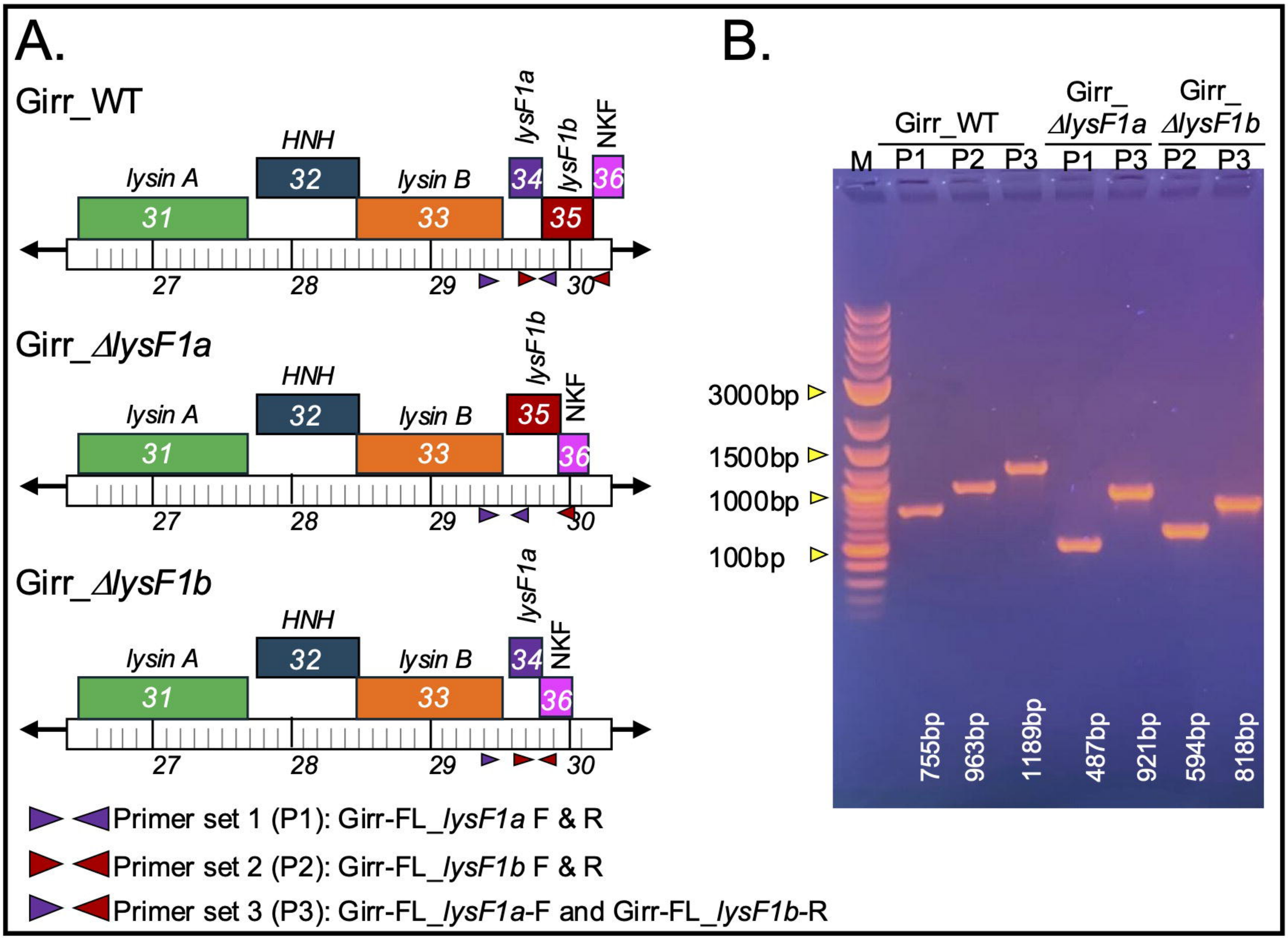
A.
Girr_WT
HNH
lysin A
lysin B
lysF1a
lysF1b
NKF
31
32
33
34
35
36
27
28
29
30
Girr_ΔlysF1a
HNH
lysin A
lysin B
lysF1b
NKF
31
32
33
35
36
27
28
29
30
Girr_ΔlysF1b
HNH
lysin A
lysin B
lysF1a
NKF
31
32
33
34
36
27
28
29
30
Primer set 1 (P1): Girr-FL_lysF1a F & R
Primer set 2 (P2): Girr-FL_lysF1b F & R
Primer set 3 (P3): Girr-FL_lysF1a-F and Girr-FL_lysF1b-R
B.
Girr_WT
Girr_ΔlysF1a
Girr_ΔlysF1b
M
P1
P2
P3
P1
P3
P2
P3
3000bp
1500bp
1000bp
100bp
755bp
963bp
1189bp
487bp
921bp
594bp
818bp

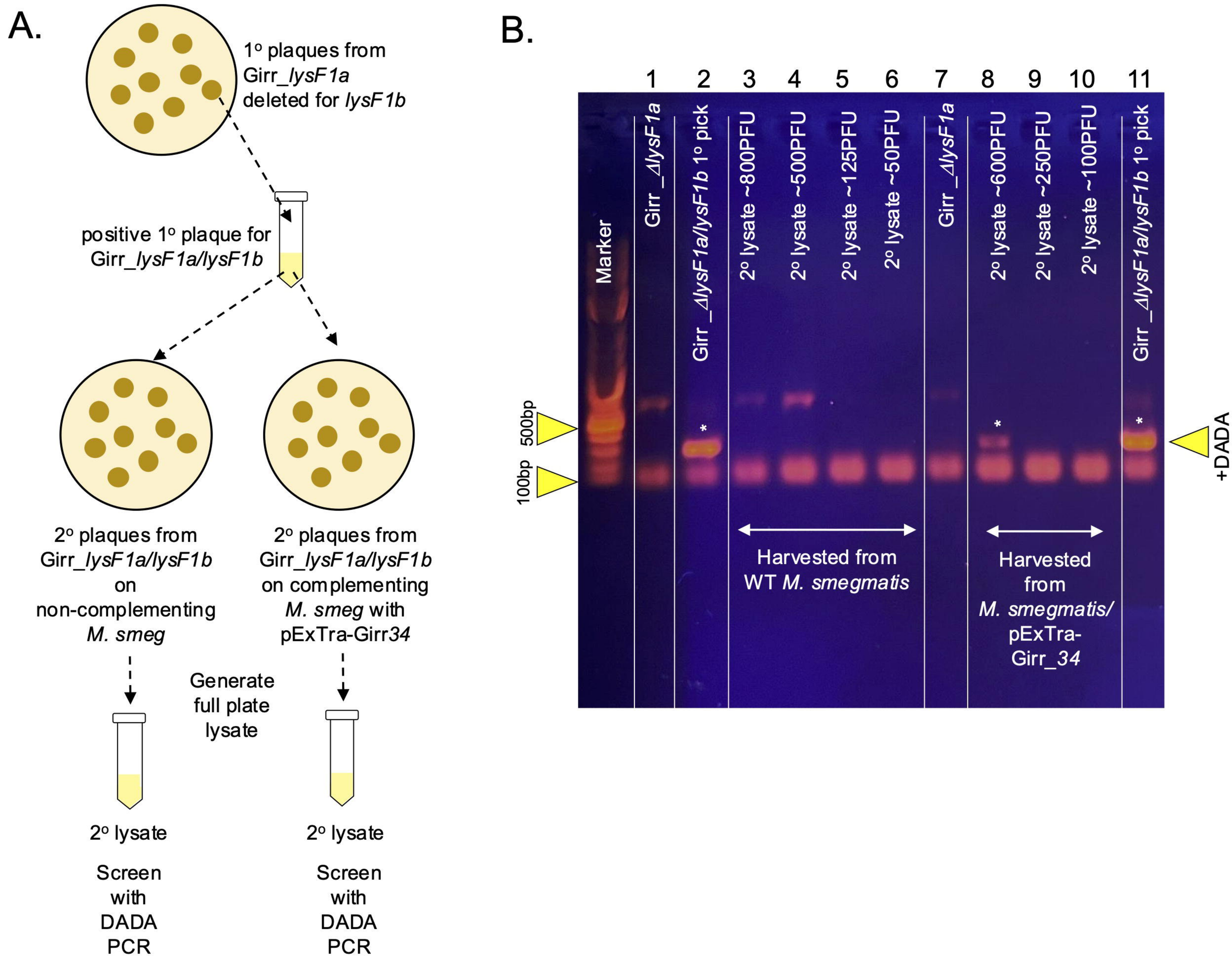
A.
1º plaques from Girr_lysF1a deleted for lysF1b
positive 1º plaque for Girr_lysF1a/lysF1b
2º plaques from Girr_lysF1a/lysF1b on non-complementing M. smeg
2º plaques from Girr_lysF1a/lysF1b on complementing M. smeg with pExTra-Girr34
Generate full plate lysate
2º lysate
2º lysate
Screen with DADA PCR
Screen with DADA PCR
B.
1 2 3 4 5 6 7 8 9 10 11
Marker
Girr _ΔlysF1a
Girr _ΔlysF1a/lysF1b 1º pick
2º lysate ~800PFU
2º lysate ~500PFU
2º lysate ~125PFU
2º lysate ~50PFU
Girr _ΔlysF1a
2º lysate ~600PFU
2º lysate ~250PFU
2º lysate ~100PFU
Girr _ΔlysF1a/lysF1b 1º pick
500bp
100bp
+DADA
Harvested from WT M. smegmatis
Harvested from M. smegmatis/ pExTra-Girr_34

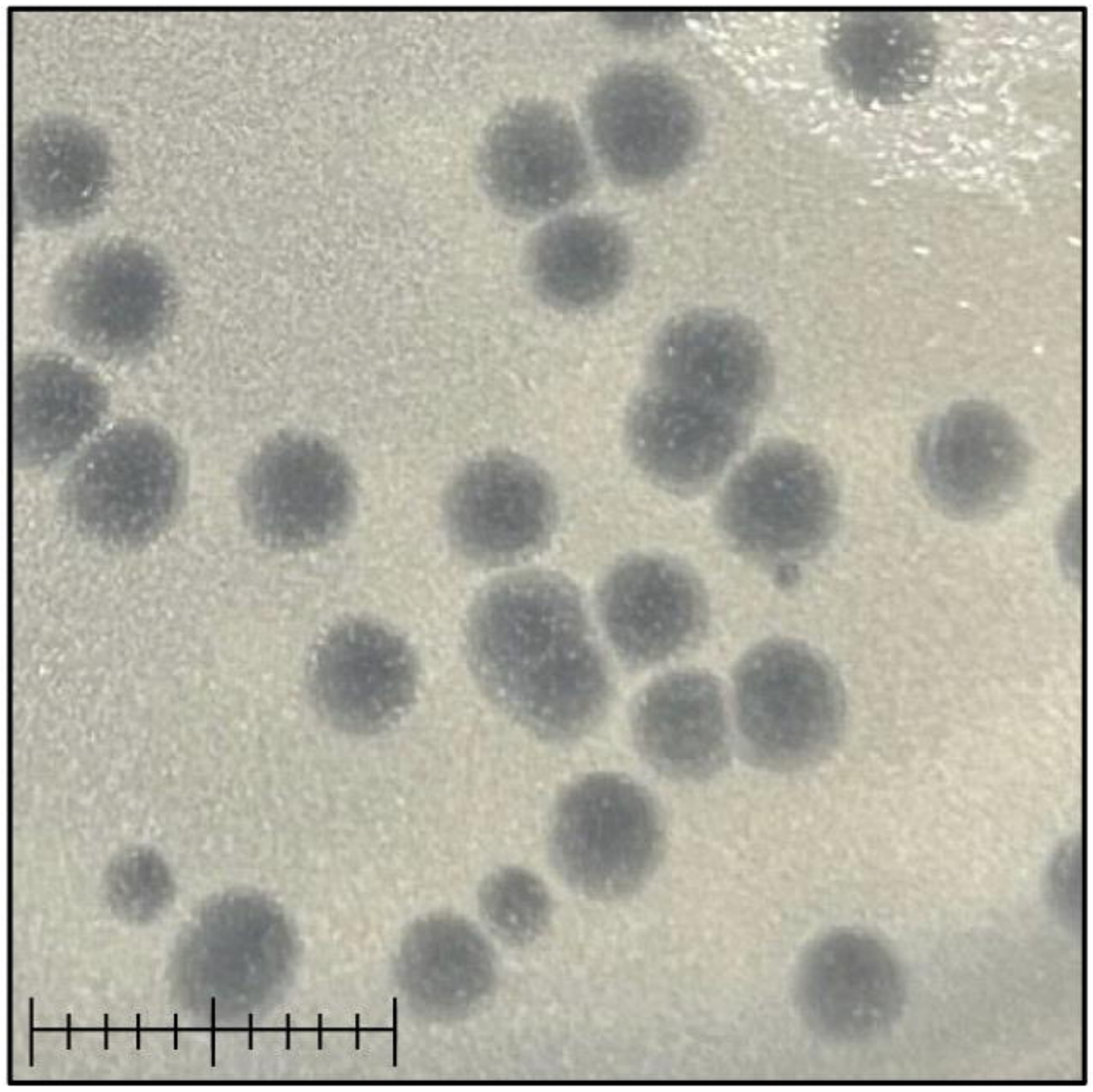

Girr_WT

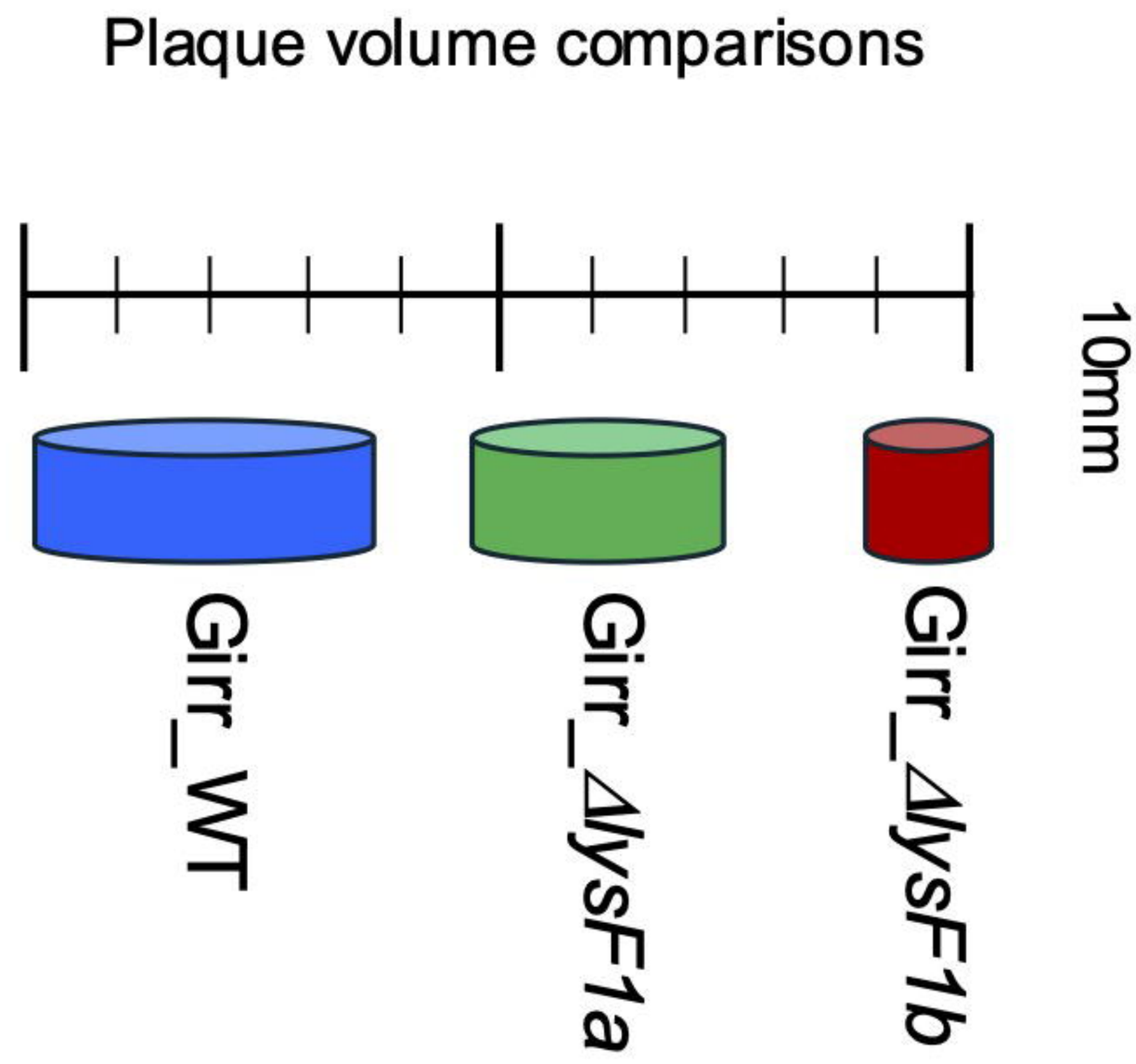

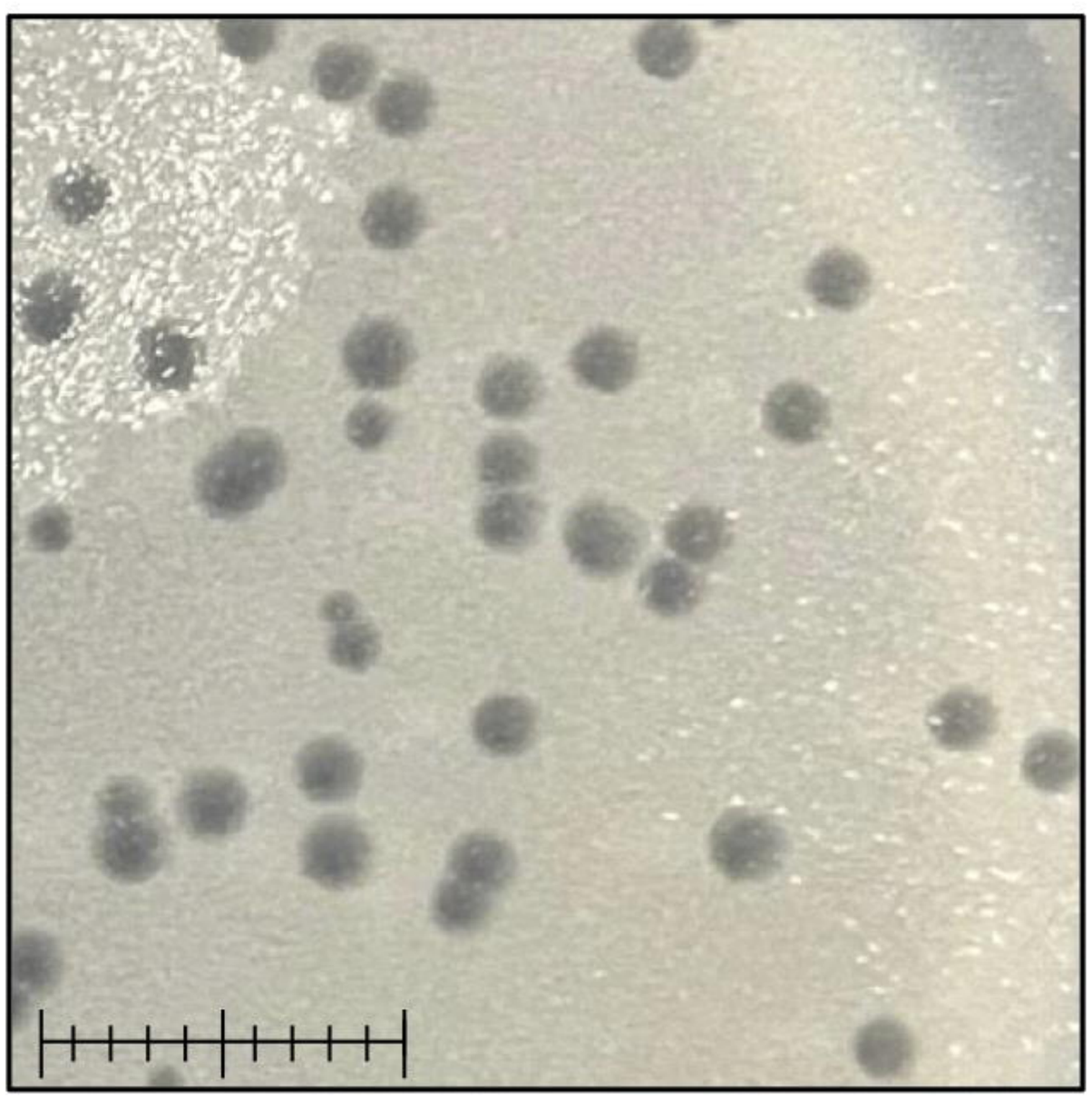

Girr_*ΔlysF1a*

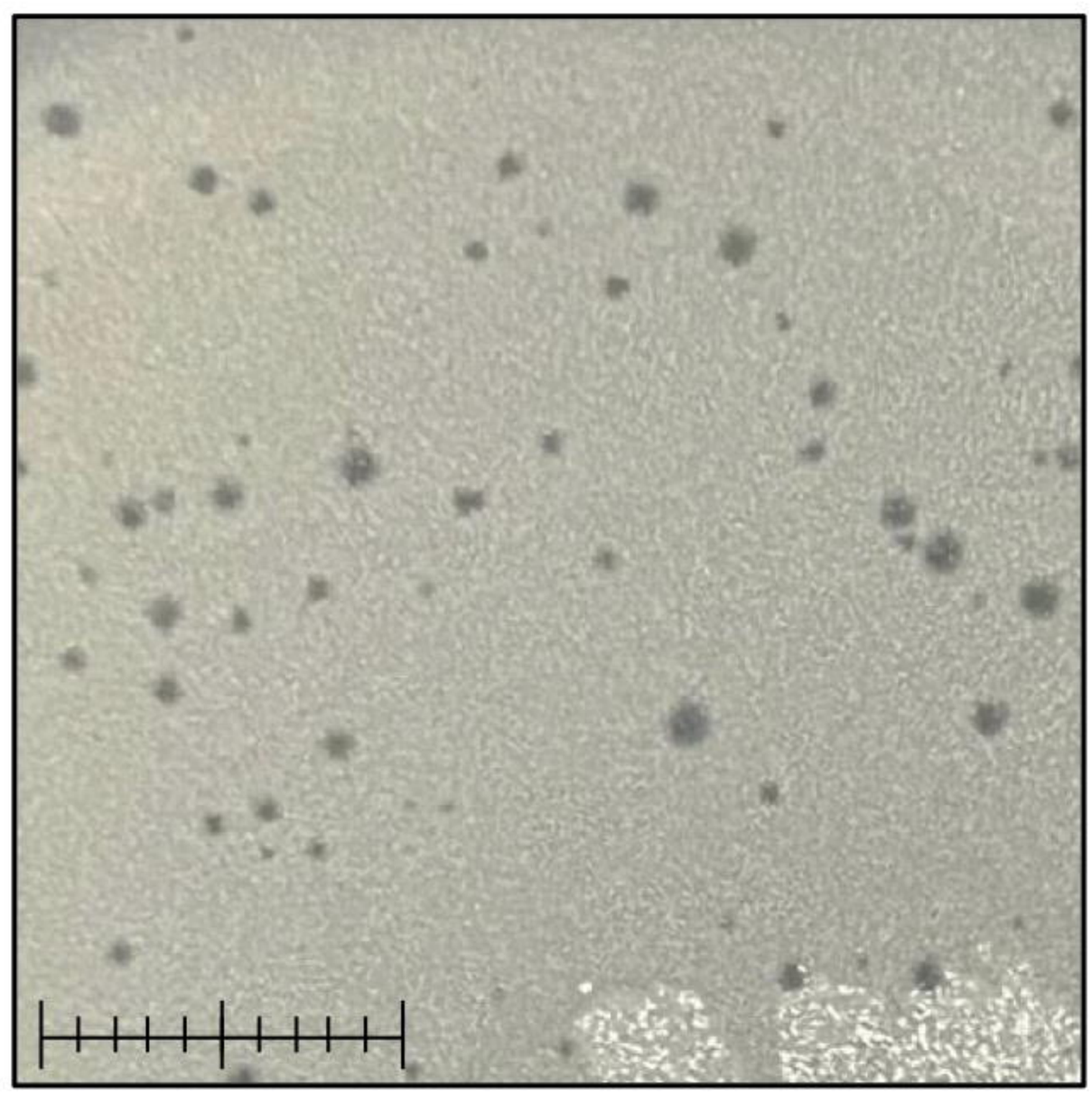

Girr_*ΔlysF1b*

A.

Girr_WT
M. Smegmatis
3.15 +/- 0.46 mm

Girr_*ΔlysF1b*
M. smegmatis
pExTra-Waterfoul_*32*
no aTc
0.85 +/- 0.25 mm

Girr_*ΔlysF1b*
M. smegmatis
pExTra-Waterfoul_*32Δ40C*
no aTc
0.89 +/- 0.30 mm

Girr_*ΔlysF1b*
M. smegmatis
pExTra-Waterfoul_*32ΔN*
no aTc
0.82 +/- 0.25 mm

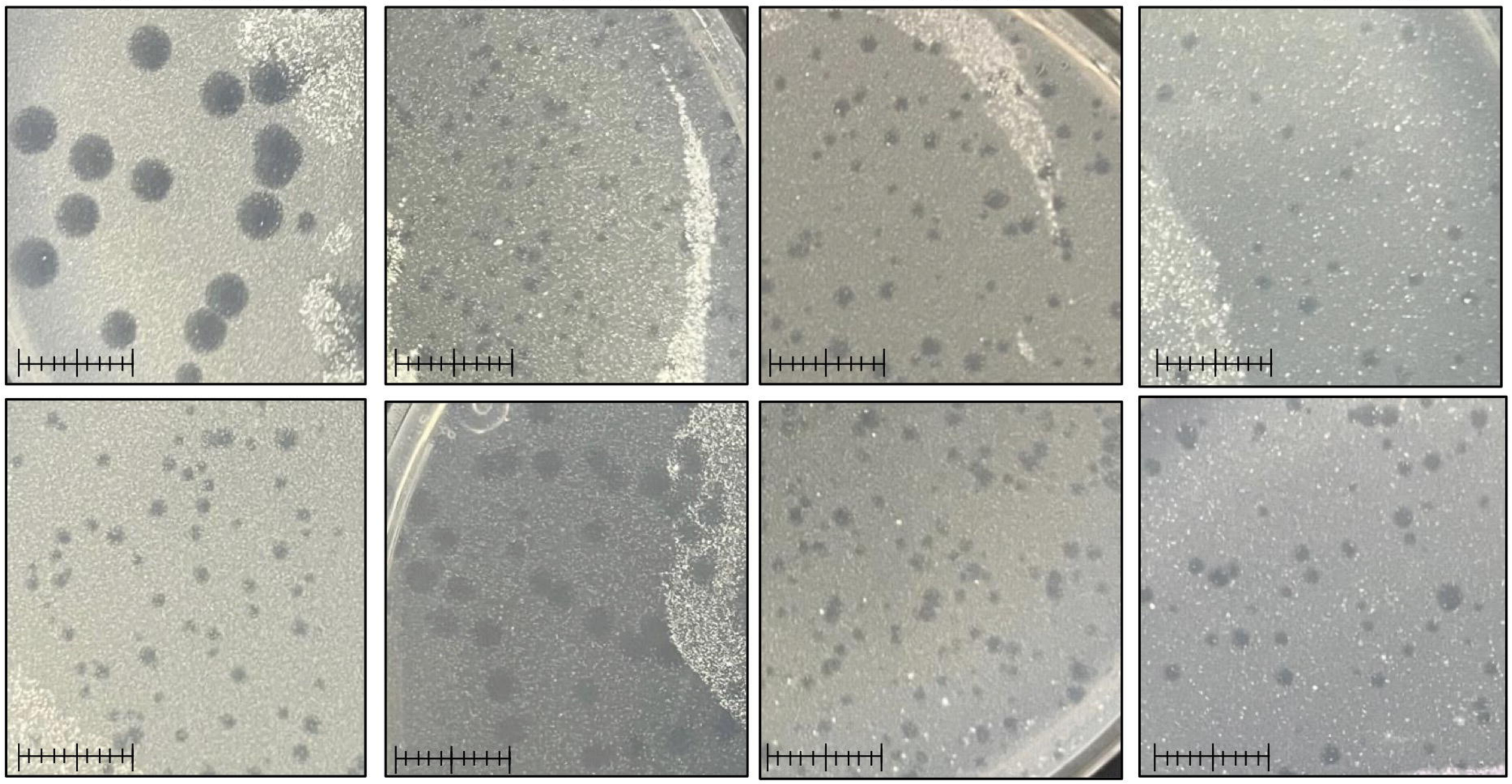

Girr_*ΔlysF1b*
M. Smegmatis
*0.79 +/- 0.20 mm

Girr_*ΔlysF1b*
M. smegmatis
pExTra-Waterfoul_*32*
+ aTc
**2.23 +/- 0.45 mm

Girr_*ΔlysF1b*
M. smegmatis
pExTra-Waterfoul_*32Δ40C*
+ aTc
0.88 +/- 0.29 mm

Girr_*ΔlysF1b*
M. smegmatis
pExTra-Waterfoul_*32ΔN*
+ aTc
0.84 +/- 0.31 mm

B.

Girr_WT
M. Smegmatis
4.15 +/- 0.65 mm

Girr_*ΔlysF1b*
M. Smegmatis
*0.95 +/- 0.36 mm

Girr_*ΔlysF1b*
M. Smegmatis
pExTra01
1.18 +/- 0.35 mm

Girr_*ΔlysF1b*
M. smegmatis/
pExTra-Girr_*35*
**2.33 +/- 0.367 mm

Girr_*ΔlysF1b*
M. Smegmatis
pExTra-NBJ_*33*
**2.19 +/- 0.298 mm

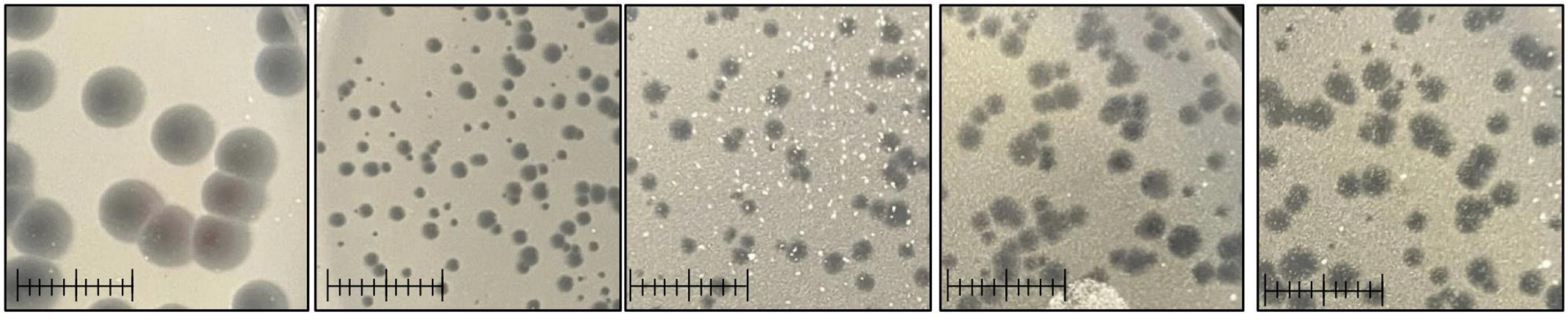

Girr_WT
M. Smegmatis
4.56 +/- 0.65 mm

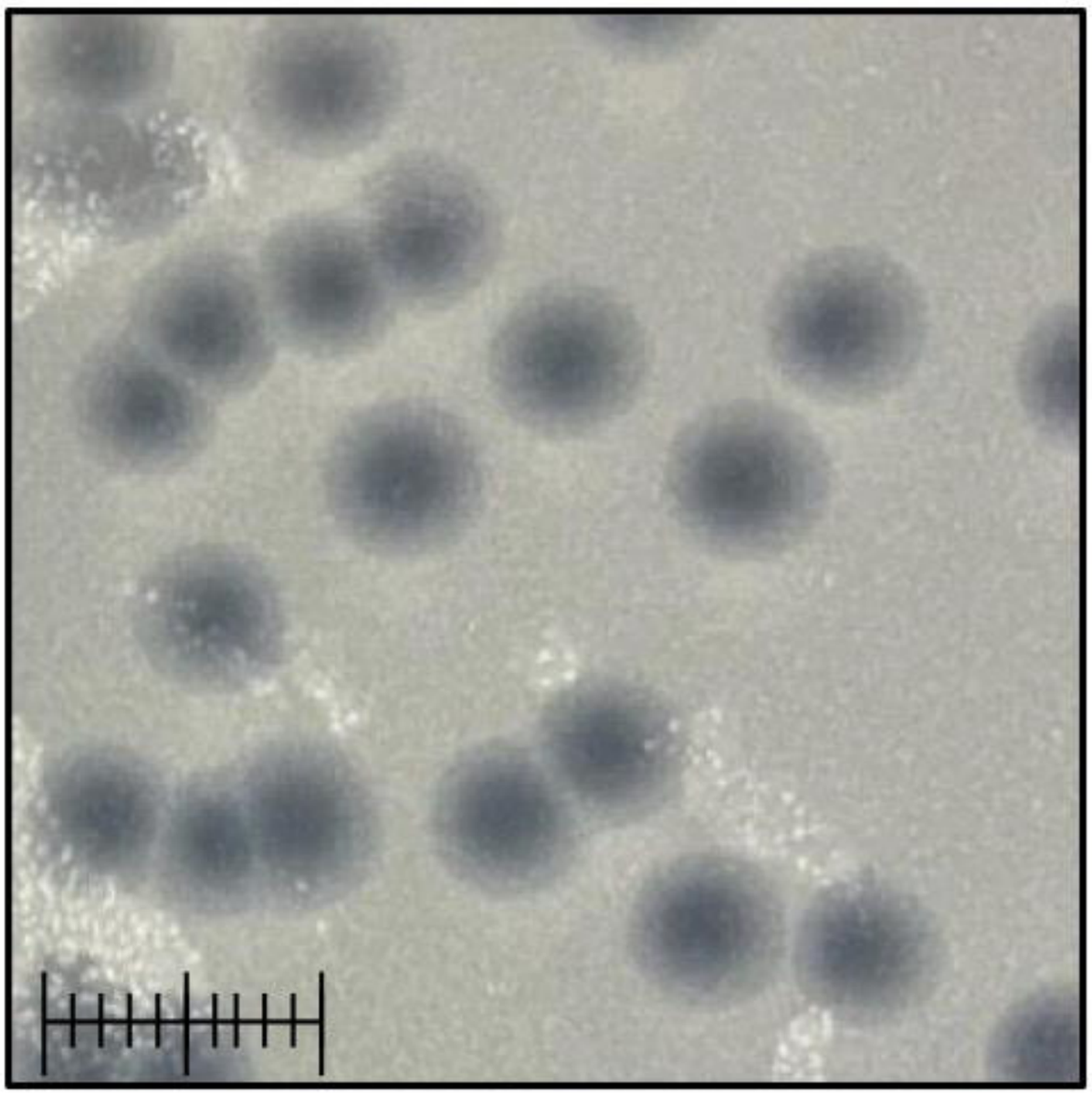

Girr_*ΔlysF1a*
M. Smegmatis
pExTra-Girr*34* + *aTc*
**4.15 +/- 0.55 mm

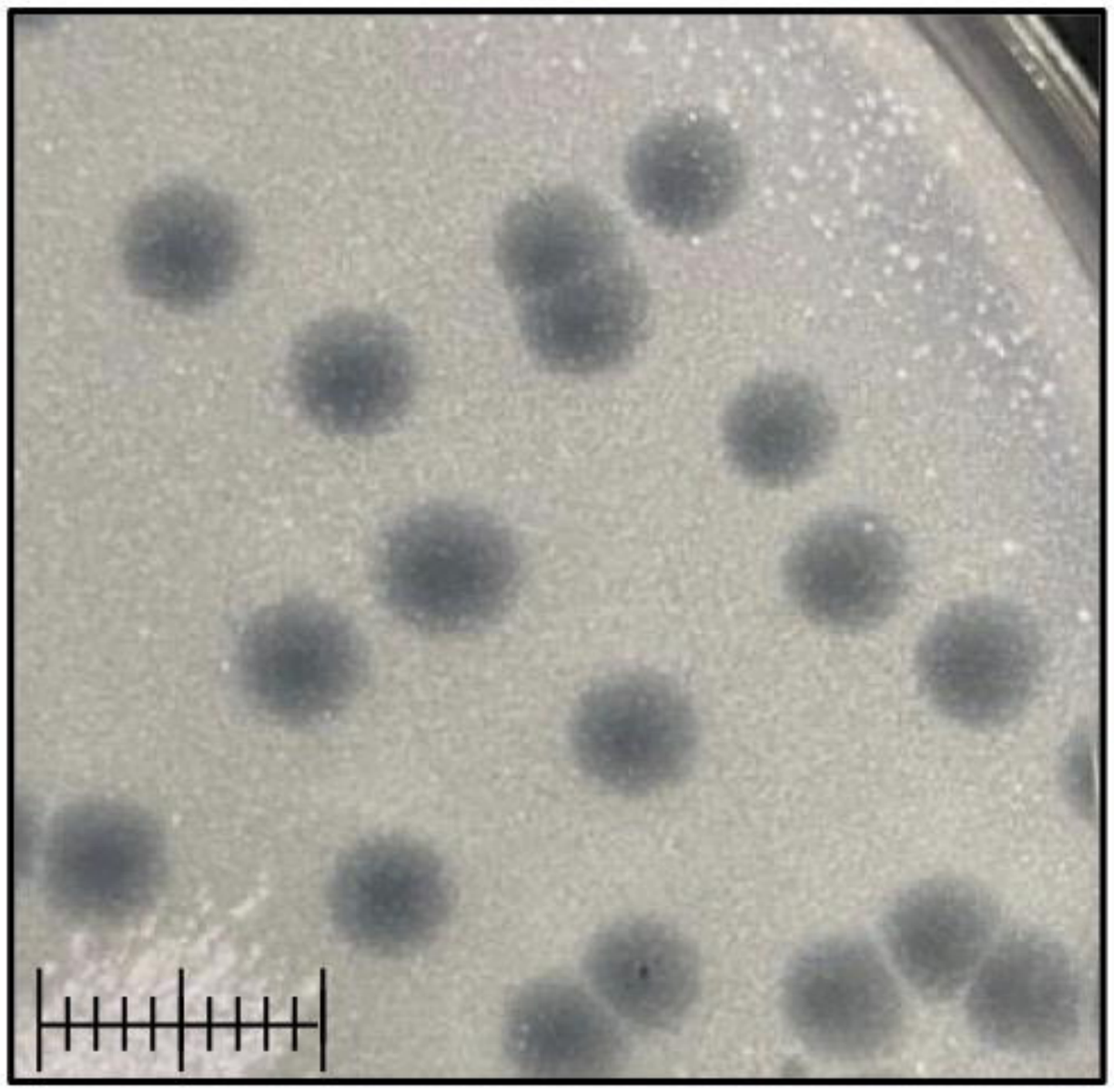

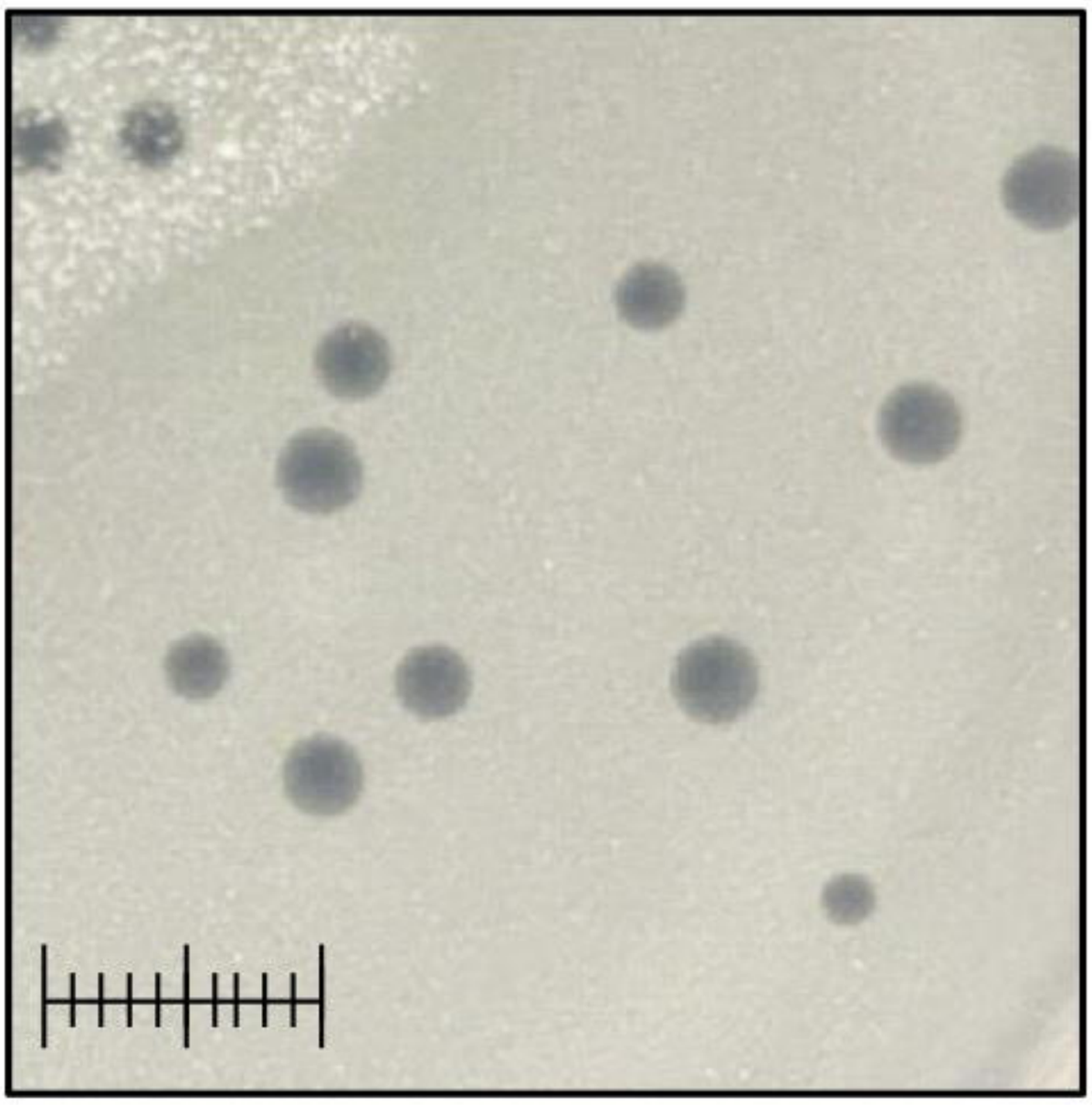

Girr_*ΔlysF1a*
M. Smegmatis
*2.79 +/- 0.55mm

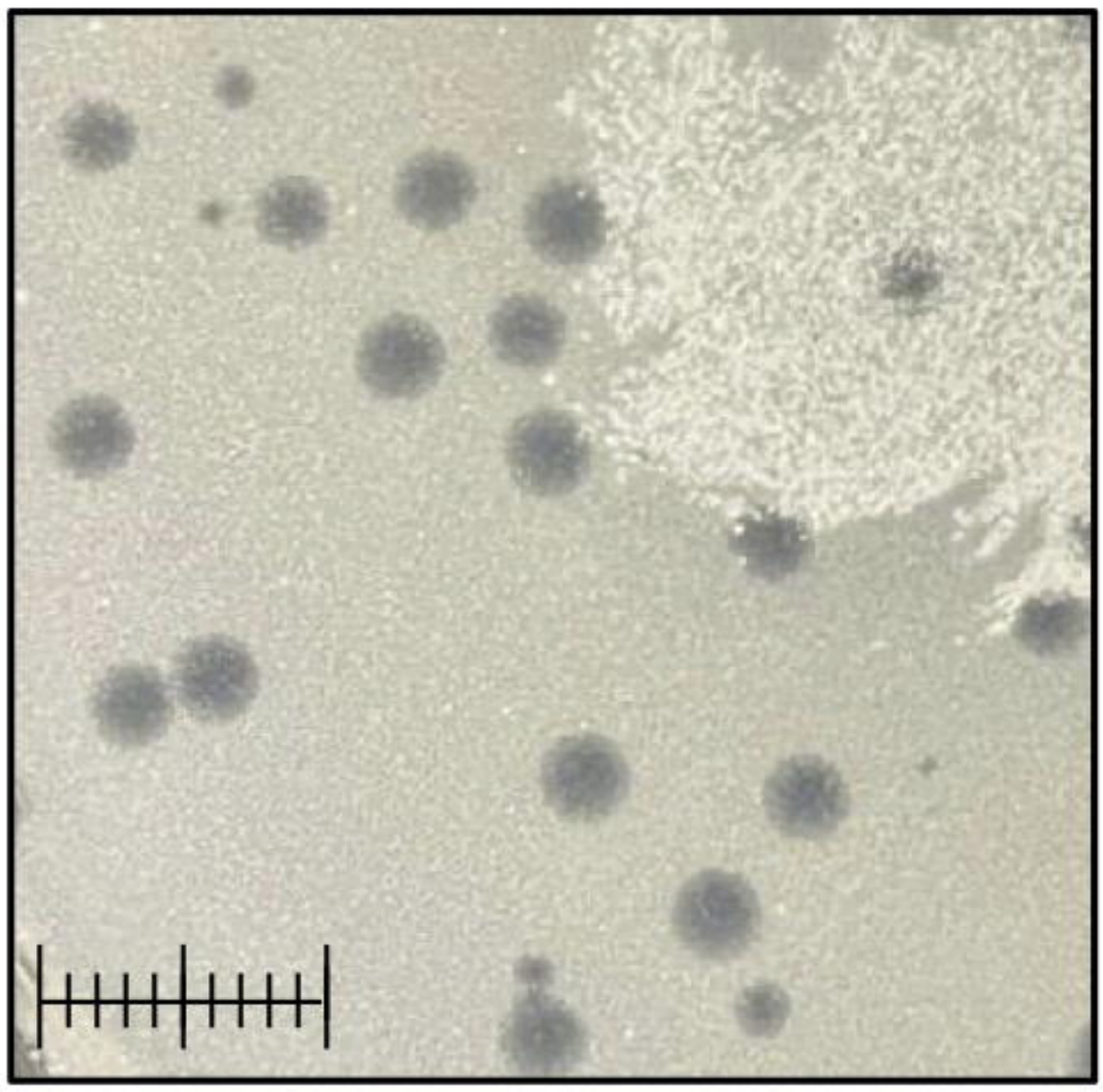

Girr_*ΔlysF1a*
M. Smegmatis
pExTra-Girr*34 no aTc*
2.83 +/- 0.353 mm

A.

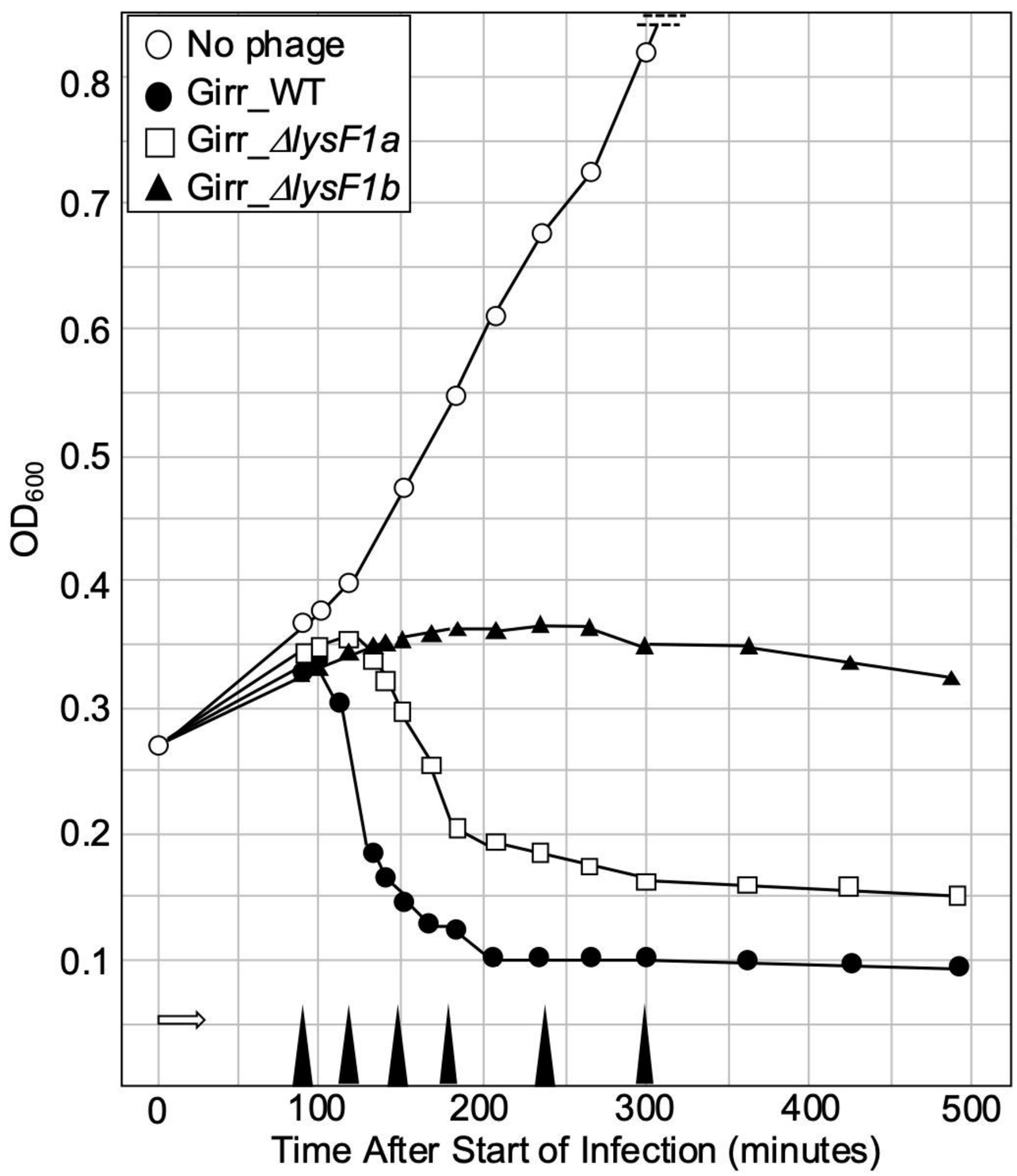
No phage
Girr_WT
Girr_ΔlysF1a
Girr_ΔlysF1b
OD600
0.8
0.7
0.6
0.5
0.4
0.3
0.2
0.1
0
100
200
300
400
500
Time After Start of Infection (minutes)

B.

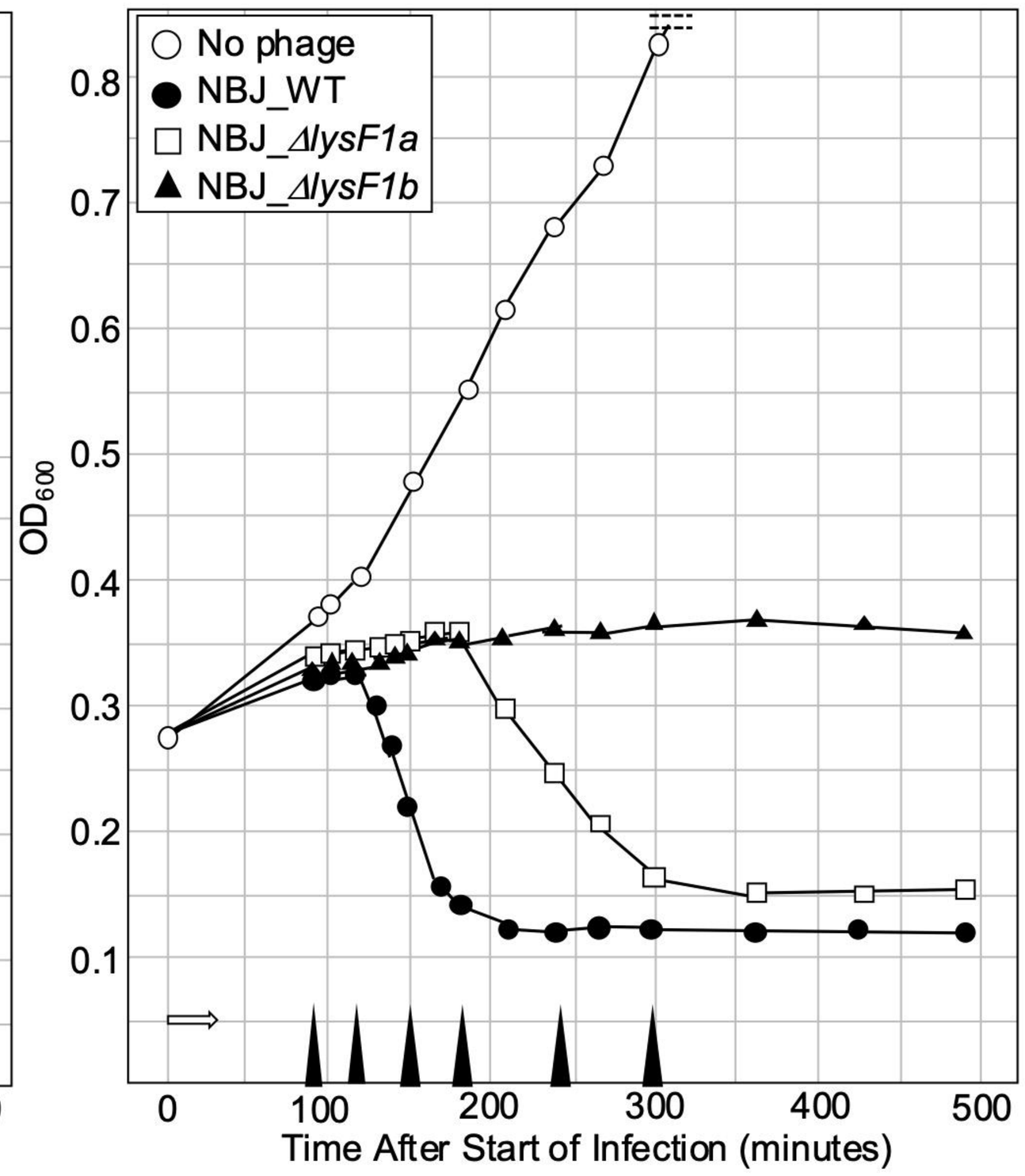
No phage
NBJ_WT
NBJ_ΔlysF1a
NBJ_ΔlysF1b
OD600
0.8
0.7
0.6
0.5
0.4
0.3
0.2
0.1
0
100
200
300
400
500
Time After Start of Infection (minutes)

C.

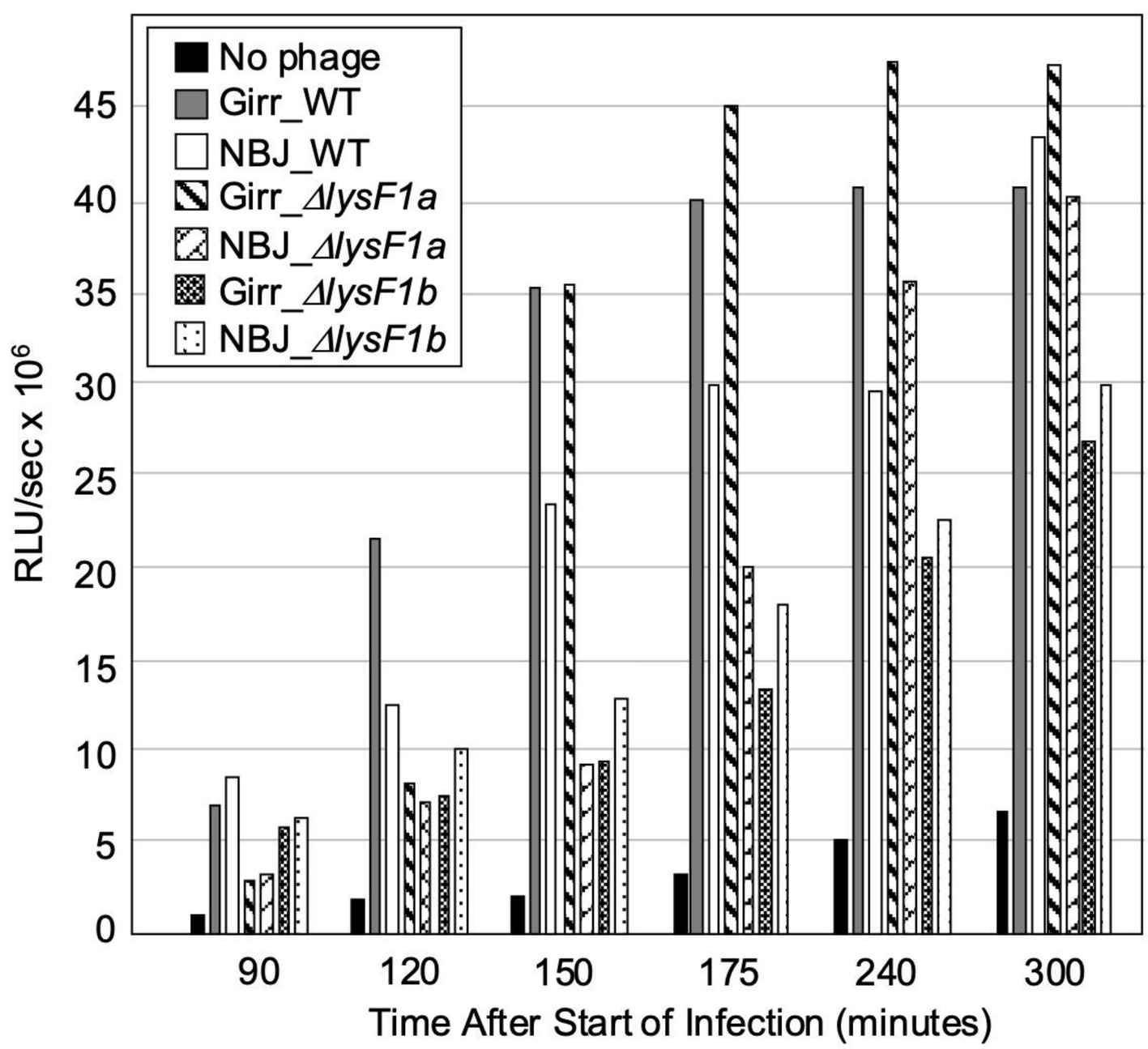
No phage
Girr_WT
NBJ_WT
Girr_ΔlysF1a
NBJ_ΔlysF1a
Girr_ΔlysF1b
NBJ_ΔlysF1b
RLU/sec x 10^6
45
40
35
30
25
20
15
10
5
0
90
120
150
175
240
300
Time After Start of Infection (minutes)

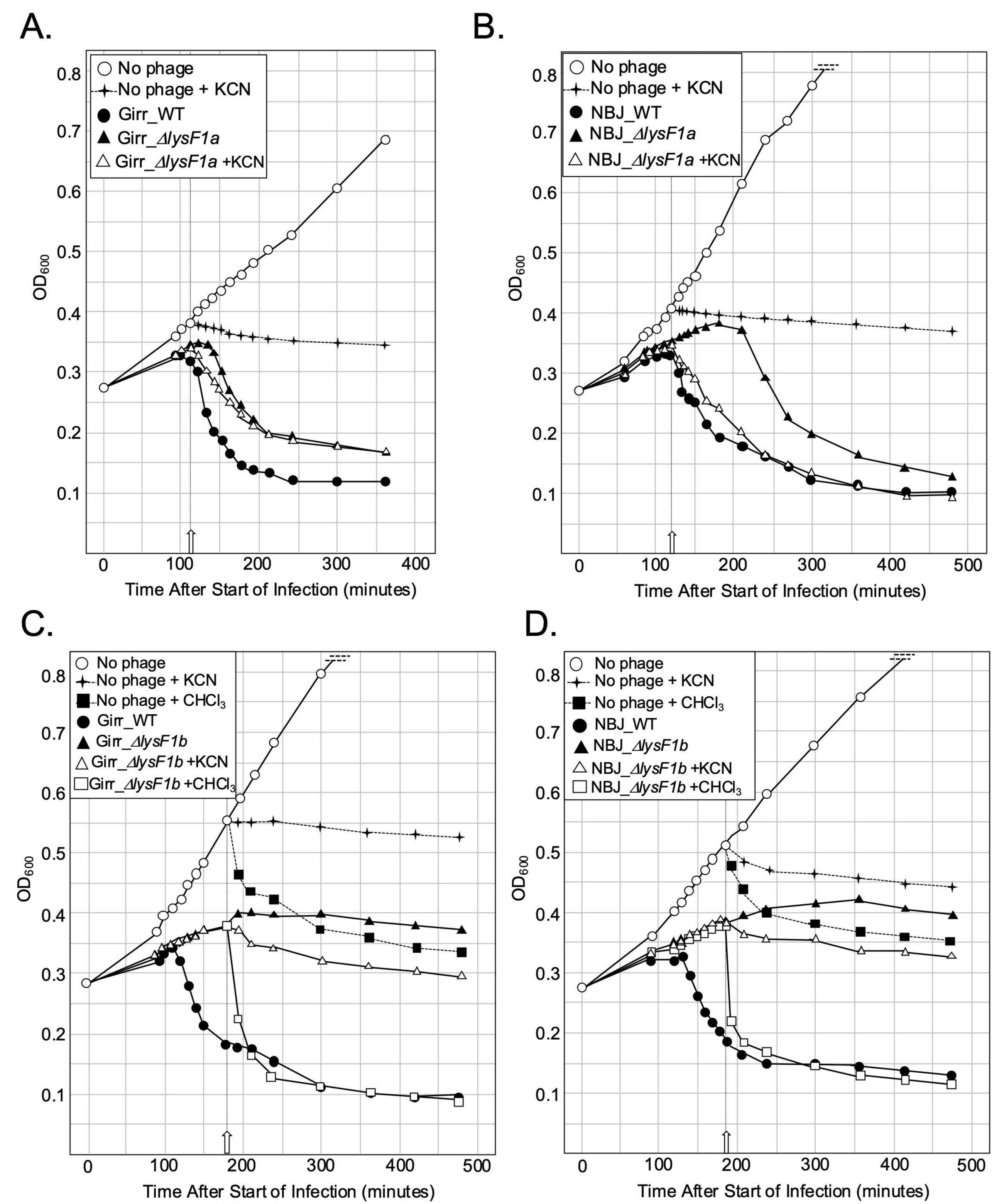
A.
No phage
No phage + KCN
Girr_WT
Girr_ΔlysF1a
Girr_ΔlysF1a +KCN
OD600
Time After Start of Infection (minutes)
B.
No phage
No phage + KCN
NBJ_WT
NBJ_ΔlysF1a
NBJ_ΔlysF1a +KCN
OD600
Time After Start of Infection (minutes)
C.
No phage
No phage + KCN
No phage + CHCl3
Girr_WT
Girr_ΔlysF1b
Girr_ΔlysF1b +KCN
Girr_ΔlysF1b +CHCl3
OD600
Time After Start of Infection (minutes)
D.
No phage
No phage + KCN
No phage + CHCl3
NBJ_WT
NBJ_ΔlysF1b
NBJ_ΔlysF1b +KCN
NBJ_ΔlysF1b +CHCl3
OD600
Time After Start of Infection (minutes)

A.

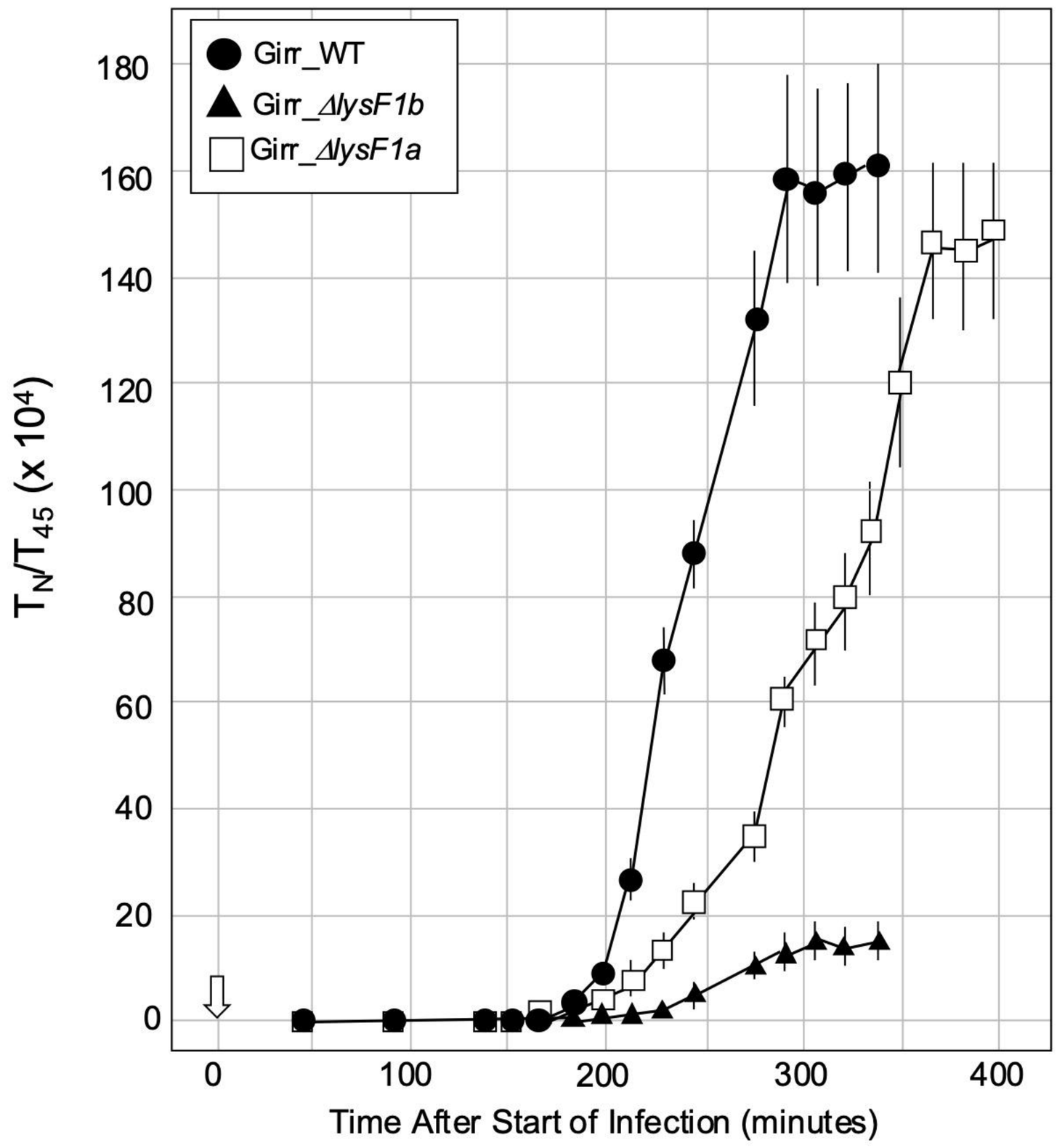

B.

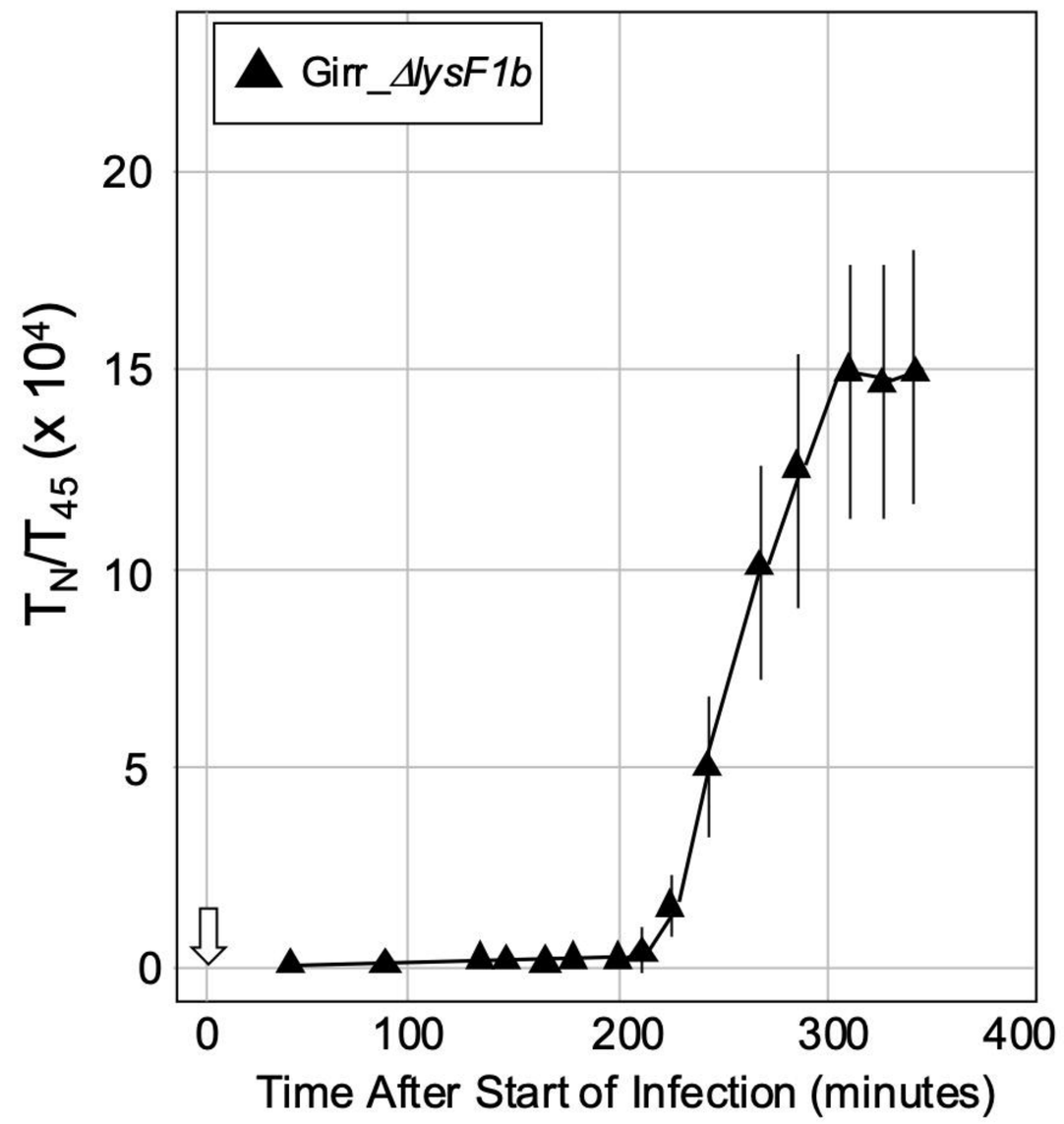

C.

phage	Burst Size PFU/cell
Girr_WT	277 +/- 81
Girr_*ΔlysF1a*	255 +/- 75
Girr_*ΔlysF1b*	*29.2 +/- 36

*statistically significant from WT phage *p<0.0001.*

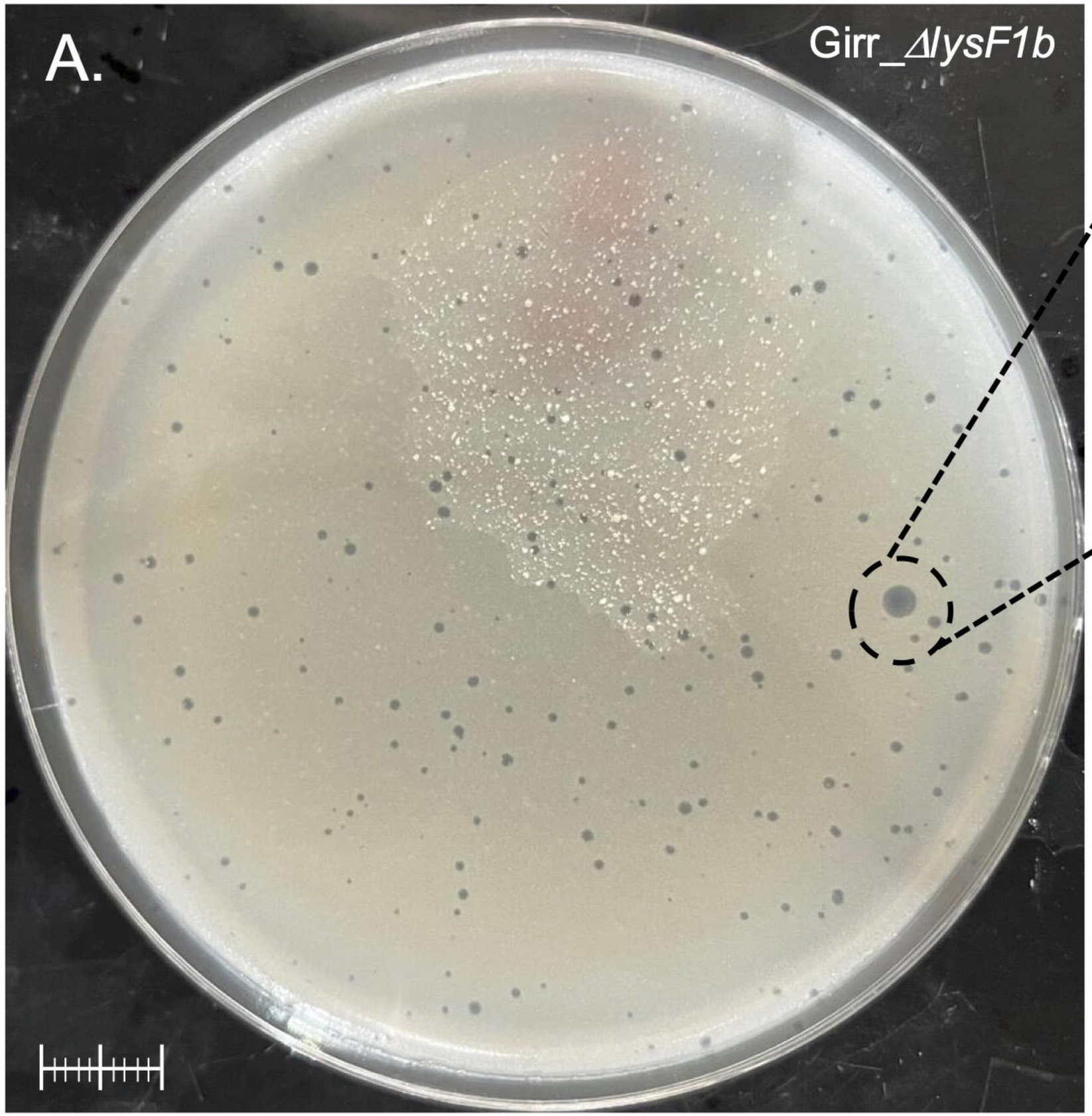

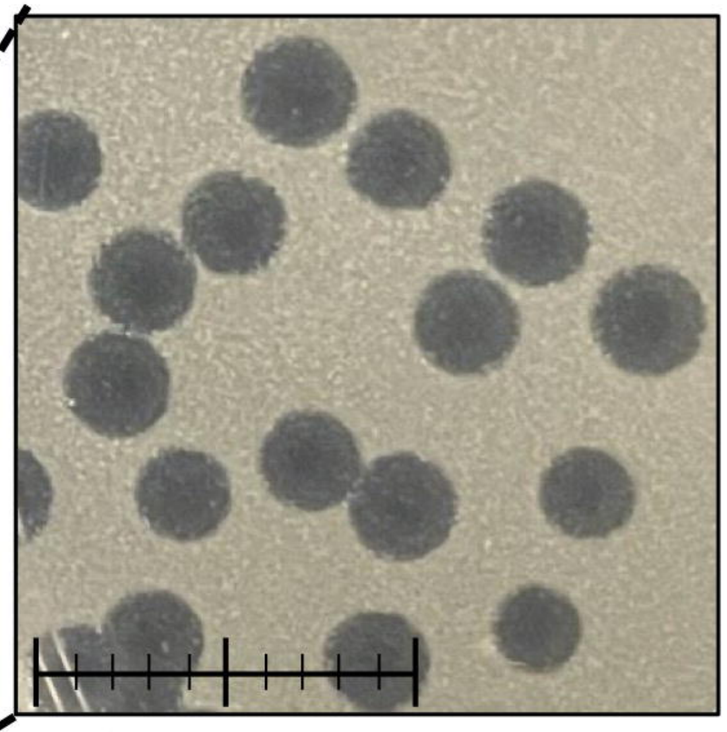

Girr_ΔlysF1b-LRM
3.01 +/- 0.26mm

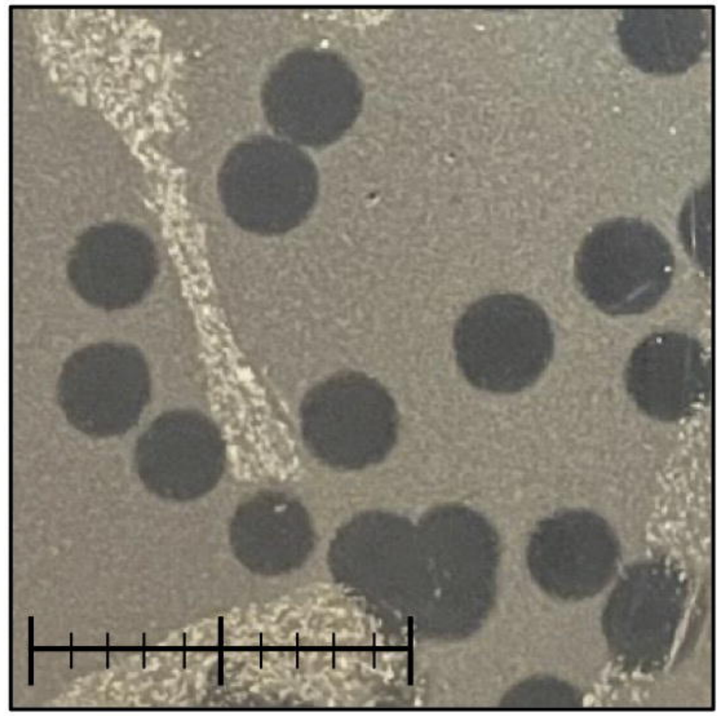

Girr_WT
2.94 +/- 0.25mm

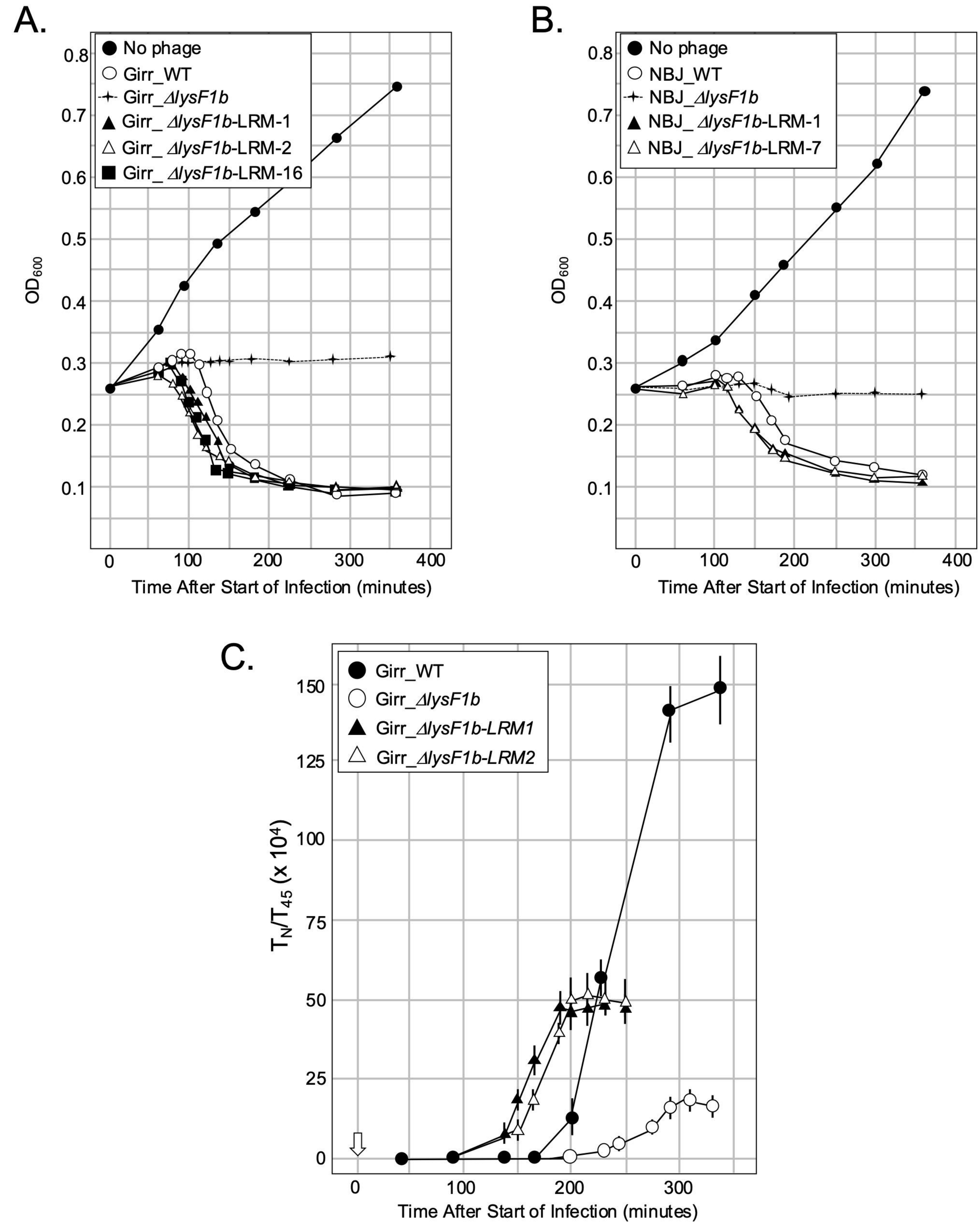
A.
No phage
Girr_WT
Girr_ΔlysF1b
Girr_ ΔlysF1b-LRM-1
Girr_ ΔlysF1b-LRM-2
Girr_ ΔlysF1b-LRM-16
OD600
Time After Start of Infection (minutes)
B.
No phage
NBJ_WT
NBJ_ΔlysF1b
NBJ_ ΔlysF1b-LRM-1
NBJ_ ΔlysF1b-LRM-7
OD600
Time After Start of Infection (minutes)
C.
Girr_WT
Girr_ΔlysF1b
Girr_ΔlysF1b-LRM1
Girr_ΔlysF1b-LRM2
TN/T45 (x 10^4)
Time After Start of Infection (minutes)

A.

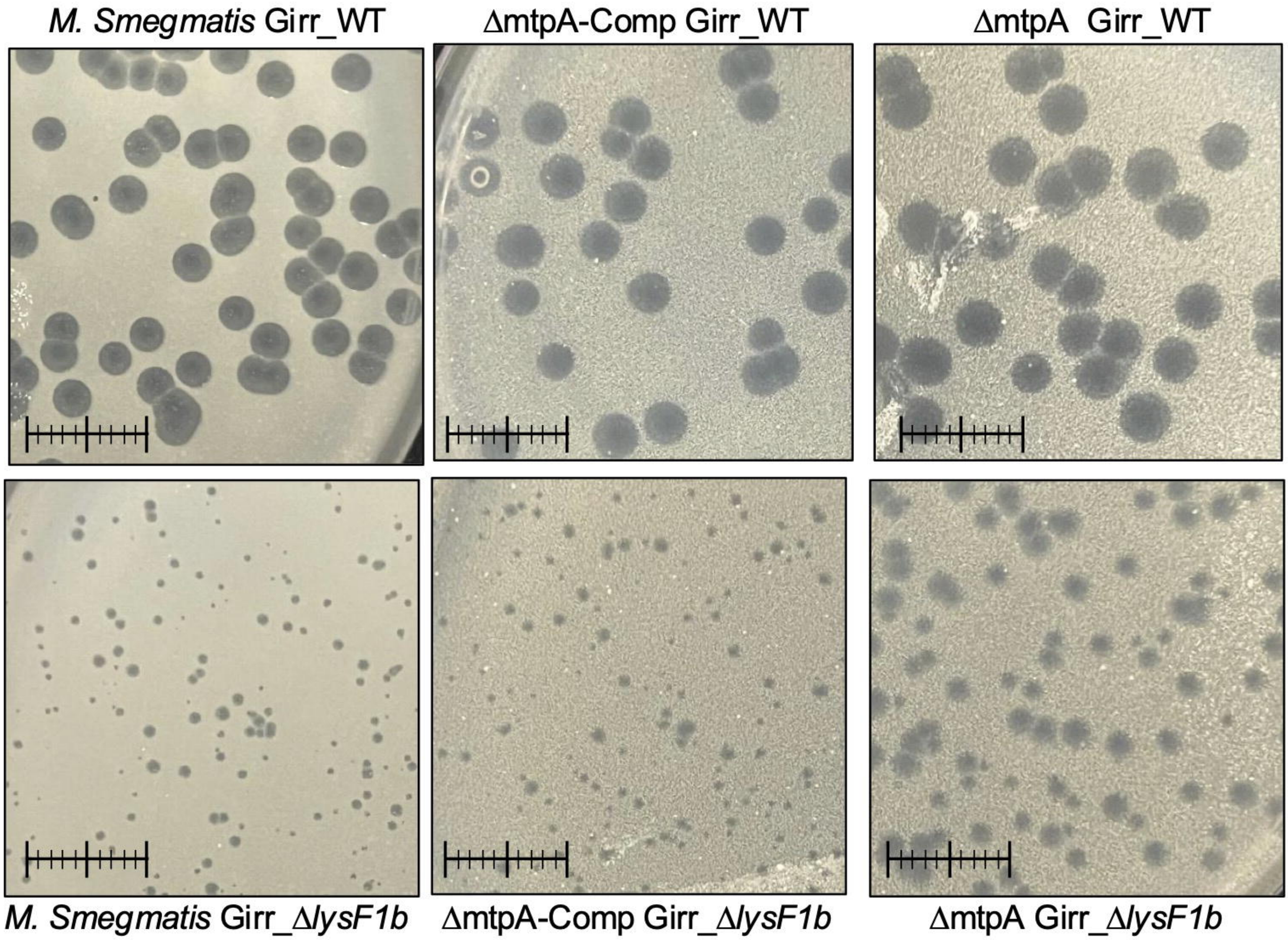
M. Smegmatis Girr_WT
ΔmtpA-Comp Girr_WT
ΔmtpA Girr_WT
M. Smegmatis Girr_ΔlysF1b
ΔmtpA-Comp Girr_ΔlysF1b
ΔmtpA Girr_ΔlysF1b

B.

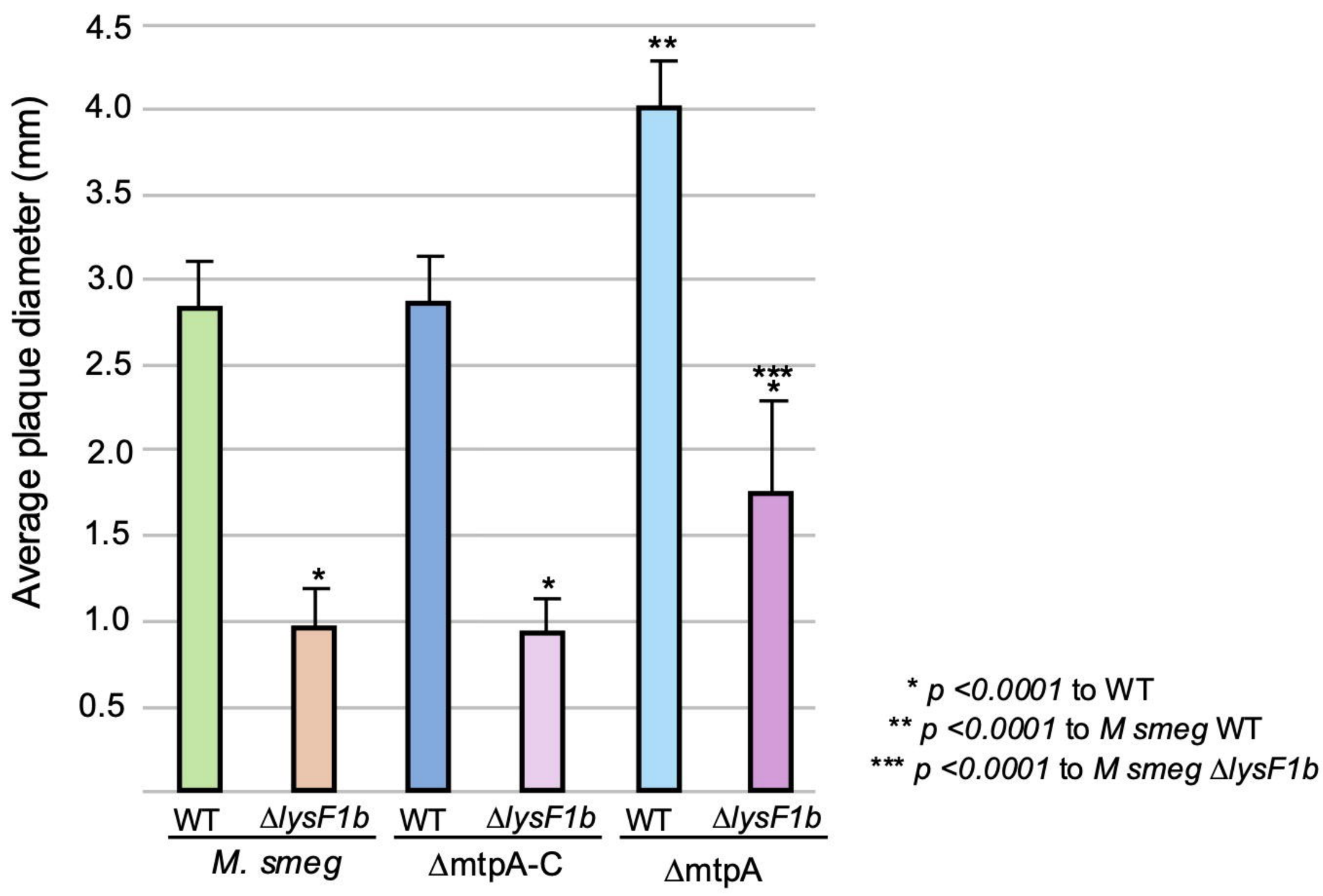
Average plaque diameter (mm)
4.5
4.0
3.5
3.0
2.5
2.0
1.5
1.0
0.5
**
***
*
*
*
WT
ΔlysF1b
WT
ΔlysF1b
WT
ΔlysF1b
M. smeg
ΔmtpA-C
ΔmtpA
* p <0.0001 to WT
** p <0.0001 to M smeg WT
*** p <0.0001 to M smeg ΔlysF1b

A.

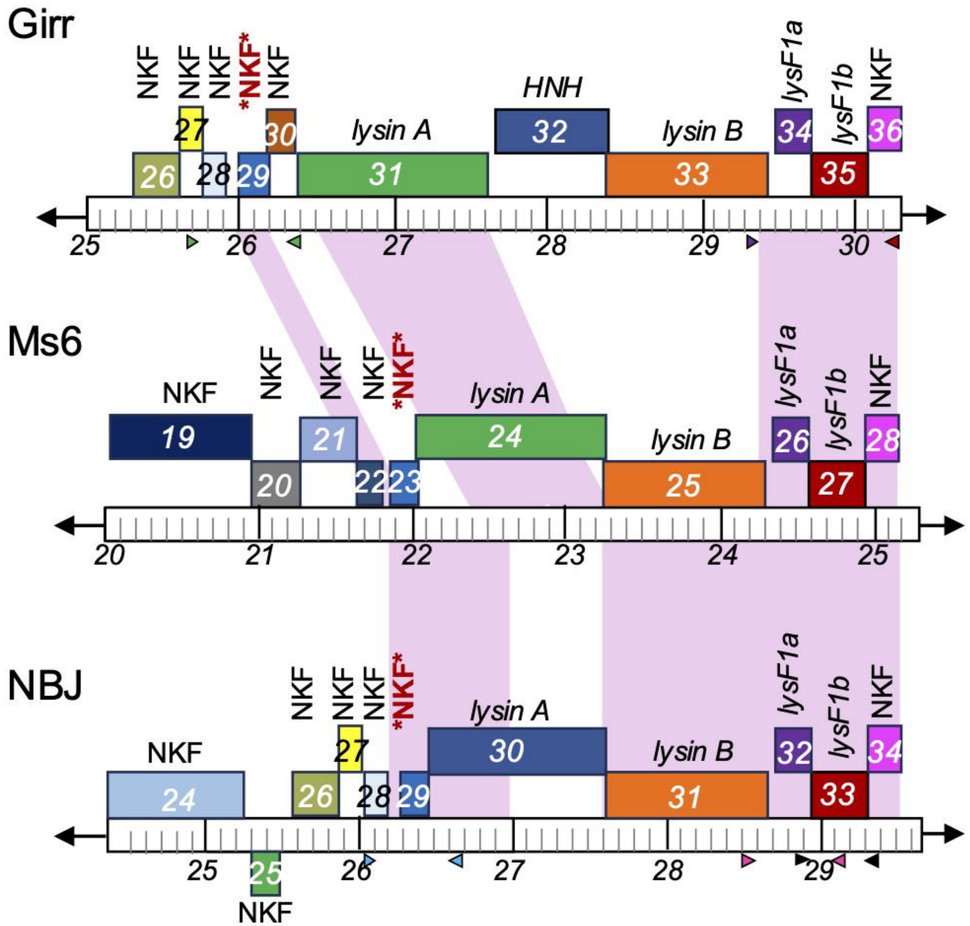

B.

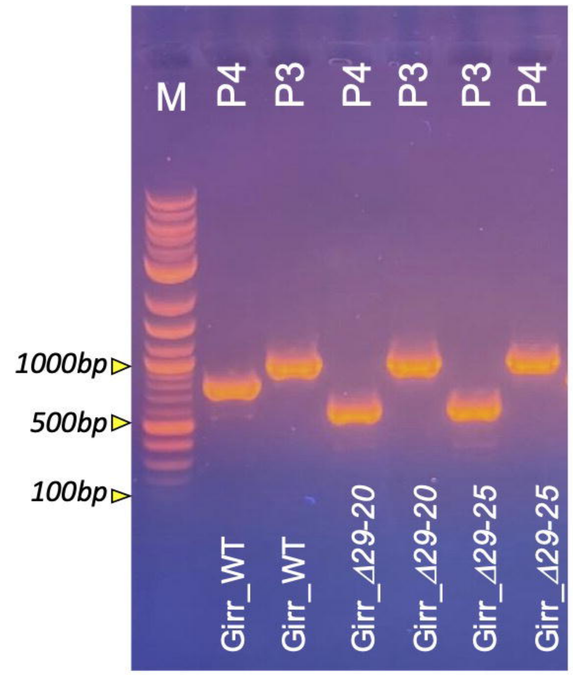

Primer set 3 (P3): Girr-FL_*lysF1a* F and Girr-FL_*lysF1b* R

Primer set 4 (P4): Girr-FL_*29* F & R

C.

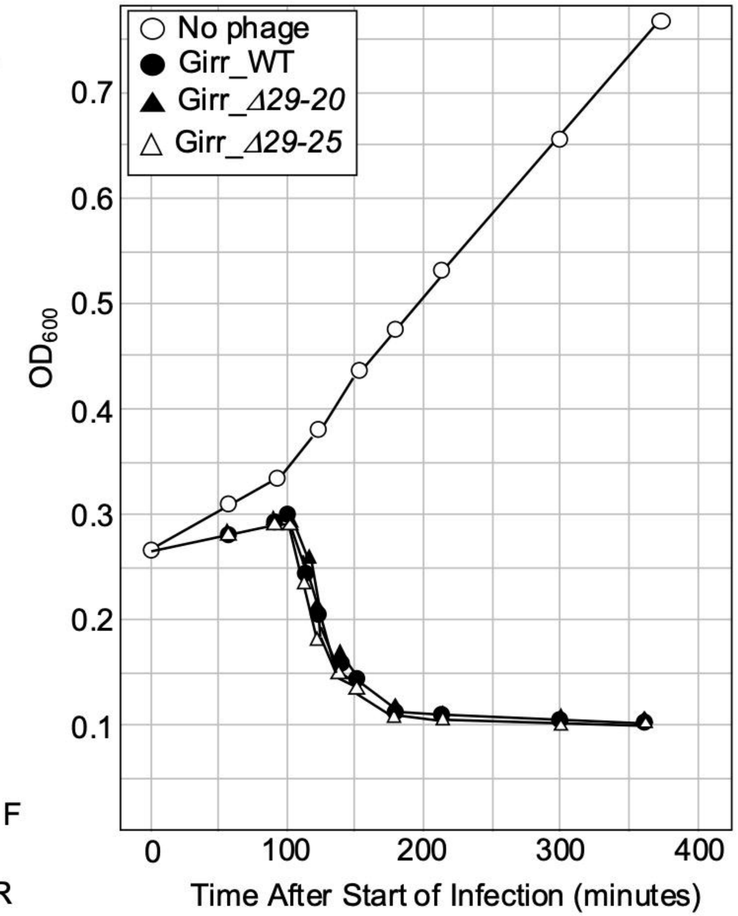

D.

```
Girr_29  MDRLGIILLKLLGPLADRIADRIADRITENLPDLSDLDDQIVAKLPDLTNLPEQVINIIGRLPRFPFLLGGKP
Ms6_23   MDRLGIVLLKLFGPLADRIADRIADRIAENLPDLSNLDDQIVAKLPDLTNLPAQVMDIIDSALRSIPVLGGILGSKR
NBJ_29   MDRLGIILLKLFGPLADRIADRIADRITENLPDLSNLDDQIVAKLPDLTNLPAQVMDIIDGALRSIPVLGGILGSKR
```

E.

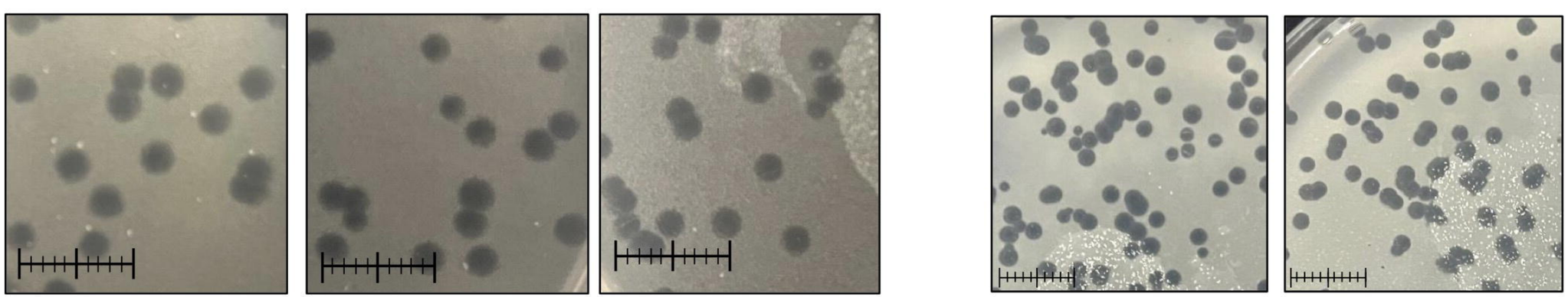

Girr_WT 3.11 +/- 0.12 nm

Girr_*Δ29-20* 2.98 +/- 0.16 nm

Girr_*Δ29-25* 3.02 +/- 0.14 nm

NBJ_WT 2.25 +/- 0.25 nm

NBJ_*Δ29* 2.15 +/- 0.09 nm